Investigation of Hydraulic Transmissions for Passenger Cars

Von der Fakultät für Maschinenwesen der Rheinisch-Westfälischen Technischen Hochschule Aachen zur Erlangung des akademischen Grades eines Doktors der Ingenieurwissenschaften genehmigte Dissertation

vorgelegt von

Mohamed Saber Ahmed Ibrahim

Berichter: Univ.-Prof. Dr.-Ing. Hubertus Murrenhoff
apl-Prof. Dr.-Ing. Jan-Welm Biermann

Tag der Mündlichen Prüfung: 01. Februar 2011

Diese Dissertation ist auf den Internetseiten der Hochschulbibliothek online verfügbar

Reihe Fluidtechnik

Band 56

Mohamed Saber Ahmed Ibrahim

Investigation of Hydraulic Transmissions for Passenger Cars

D 82 (Diss. RWTH Aachen University, 2011)

Shaker Verlag
Aachen 2011

Bibliographic information published by the Deutsche Nationalbibliothek
The Deutsche Nationalbibliothek lists this publication in the Deutsche Nationalbibliografie; detailed bibliographic data are available in the Internet at http://dnb.d-nb.de.

Zugl.: D 82 (Diss. RWTH Aachen University, 2011)

Printed in Germany.

ISBN 978-3-8322-9928-6
ISSN 1437-8434

Shaker Verlag GmbH • P.O. Box 101818 • D-52018 Aachen
Phone: 0049/2407/9596-0 • Telefax: 0049/2407/9596-9
Internet: www.shaker.de • e-mail: info@shaker.de

Dedicated to soul of my mother

Acknowledgment

This thesis evolved during my work as a guest scientific researcher at the Institute for Fluid Power Drives and Controls (IFAS) of RWTH Aachen University, Germany.

During my time at IFAS several people contributed to the work, all of whom I will acknowledge.

I would like to thank my supervisor Prof. Hubertus Murrenhoff the head of IFAS of RWTH Aachen University. His experience, generous support and valuable advice have made this work possible.

For the careful and internal review of this thesis my thanks go to Prof. Jan-Welm Biermann who agreed to act as the further referee, and also to Prof. Dieter Moormann for managing the doctoral examination procedure.

I would like to thank Dr. Achten, Dip.-Ing. Vael form Innas B.V., for allowing use of efficiency maps for the Innas hydraulic transformer and the floating cup pump and motors in the simulation of the Hy*d*rid drivetrain.

I express my sincere thanks to Dr. Torsten Kohmäscher for his assistance and guidance throughout my early work at IFAS. I would also like to thank my previous and present group leaders Kristof Schlemmer and Olivier Reinertz as well as chief engineers Marcel Meuser and David Prust respectively, for their support in reviewing the published papers during this work.

My deep thanks to Dr. Heinrich Theissen for his continuous support, translation of the abstract to German language and reviewing most of the chapters in the thesis. I also want to express my thanks to all members of IFAS for the wonderful working atmosphere. I am grateful to IFAS mates in work office Stefan Scharf, Stefan Fritz and Stefan Losse for their continuous advice and valuable comments in all day live at IFAS.

Above all, I thank God for his gift of faith, family and friends. Great thanks to my father who has supported me in various ways throughout this wonderful journey. A special gratitude goes to my wife Dina, who has always supported me in my scholastic ambitions. Her encouragement will never be forgotten. It is extended to my children Fatma, Ahmad, and Salma, without their innate warm love it would not have been possible.

Aachen, February 2010 ***Mohamed Ibrahim-Sokar***

Abstract

The rising use of vehicles and herewith the yearly decrease in available amount of crude oil left on the earth accompanied by a continuously increasing price puts high stress on the vehicle industry. Furthermore, Humans face a growing increase in the global environmental pollution concerns and tough emission standards constrain the maximum amount of vehicles emission to reduce air pollution. All of these factors force automobile and vehicle manufactures into never-ending effort to satisfy these requirements. Hence, the development of new vehicles to further reduce fuel consumption and emission is a mandatory.

The high power density of hydraulic pumps/motors and hydro-pneumatic accumulators make hydraulic technology look promising for vehicles' transmission and its integration in the automobile industry should be considered. Furthermore, a reasonable price, reliability and long life time of hydraulic units are good enough and required for this purpose. The recently developed hydrostatic units, that meet the increased requirements of high efficiency over a wide range of operation offer, new capability for hydrostatic drivelines in vehicle applications.

This thesis primarily addresses the potential of hydraulic transmission for use in automobiles. The analysis and simulations assume baseline vehicle specifications and components of a mid-sized passenger car. Three hydraulic drivetrain configurations were investigated. A continuously variable hydrostatic transmission integrated with an engine controlled to operate on the ideal fuel efficiency line is first introduced. Then, a secondary controlled hydrostatic transmission equipped with conventional hydrostatic units and an energy recovering system working under engine on/off control strategy is also investigated.

Alongside the above, an innovative series full hydraulic hybrid drivetrain, referred as “the Hy*d*rid” and its key components are researched in detail throughout the thesis. The general architecture of the Hy*d*rid was introduced by the Dutch organization Innas BV, replacing the mechanical transmission with a distinct series hydraulic transmission which includes innovative components such as a three port-plate hydraulic transformer, fixed displacement pump and in-wheel hydro-motors designed on the floating cup technology. A generic power management strategy of the system power flows is developed by rule based algorithm, and the most efficient power flow control for each driving pattern is established.

Results of the drivetrains performance, fuel consumption and CO_2 emissions during a standard driving cycle are presented to evaluate the potential of each configuration to be applied in passenger cars.

Kurzfassung

Der wachsende Einsatz von Fahrzeugen und hiermit die jährliche Abnahme der verfügbaren Rohölmenge, verbunden mit ständig steigenden Ölpreisen, stellen hohe Anforderungen an die Fahrzeugindustrie. Weiterhin sieht die Menschheit einem geschärften globalen Umweltbewusstsein und strengen Emissionsvorgaben entgegen, die den Maximalbetrag der Fahrzeugemissionen beschränken, um die Luftverschmutzung zu reduzieren. All diese Faktoren zwingen die Automobilbranche zu immer neuen Anstrengungen, um diese gegensätzlichen Anforderungen zu erfüllen. Infolgedessen ist die Entwicklung neuer Fahrzeuge zur Reduzierung des Treibstoffverbrauches und der Emissionen zwingend notwendig.

Die hohe Leistungsdichte hydraulischer Pumpen und Motoren und der hydraulischen Gasdruckspeicher lassen die Hydraulik vielversprechend für die Kraftübertragung in Fahrzeugen erscheinen, und ihre Integration sollte in der Autoindustrie überlegt werden. Kosten, Zuverlässigkeit und Lebensdauer der hydraulischen Einheiten sind darüber hinaus für diese Anwendung angemessen. Die in letzter Zeit entwickelten Hydraulikeinheiten, die die gestiegenen Anforderungen an hohem Wirkungsgrad über einen weiten Arbeitsbereich erfüllen, eröffnen neue Möglichkeiten für hydrostatische Antriebsstränge in Fahrzeugen.

Die vorliegende Arbeit beschäftigt sich in erster Linie mit dem Potential hydraulischer Kraftübertragung in Automobilen. Der Analyse und Simulation liegen Fahrzeugspezifikationen und Komponenten für einen Mittelklasse-PKW zugrunde. Es wurden drei hydraulische Antriebsstrang-konfigurationen untersucht. Als erstes wird eine stufenlos verstellbare hydrostatische Kraftübertragung vorgestellt, bei der der Verbrennungsmotor auf der Kurve des minimalen Kraftstoffverbrauchs geführt wird. Danach wird ein sekundär geregeltes hydrostatisches Getriebe mit konventionellen Einheiten und einem Energierückgewinnungssystem untersucht, wobei der Verbrennungsmotor nach einer Ein/Aus-Strategie gesteuert wird.

Schließlich wird durch die gesamte Arbeit ein innovativer serieller Antriebsstrang, der unter dem Namen "Hy*d*rid" bekannt ist, einschließlich seiner Komponenten im Detail erforscht. Die allgemeine Architektur des Hy*d*rid wurde durch die niederländische Firma Innas BV eingeführt, die damit die mechanische Kraftübertragung durch eine serielle hydraulische Übertragung ersetzt. Darin enthalten sind neuartige Komponenten wie der hydraulische Transformator mit drei Anschlüssen, eine Konstantpumpe und hydrostatische Radmotoren, die alle nach dem Floating-Cup-Prinzip aufgebaut sind. Mit regelbasierten Algorithmen wurde eine allgemeingültige Managementstrategie für die Energieflüsse im System aufgebaut. Die jeweils effizienteste Energieflusssteuerung für jedes Fahrtmuster wurde herausgearbeitet.

Die Leistung des Antriebsstrangs, der Kraftstoffverbrauch und die CO_2-Emissionen wurden über einen Standard-Fahrzyklus ermittelt und dargestellt, um das Potential der verschiedenen Konfigurationen beim Einsatz im PKW zu beurteilen.

Contents

Nomenclature

Latin letter

a	Distance from CG to front axle	m
A_f	Frontal area	m^2
a_F	Vehicle acceleration	m/s^2
b	Distance from Center of Gravity (CG) to rear axle	m
C_d	Air drag coefficient	-
F_a	Acceleration force	N
F_{Aer}	Aerodynamic drag	N
F_{ex}	Excess traction force	N
f_r	Rolling resistance coefficient (firm Asphalt)	-
F_R	Rolling resistance force	N
F_{St}	Road grade force	N
F_T	Traction force at the drive wheels	N
g_f	Final drive gear ratio	-
g_i	Gear ratio	-
h	Height of Center of Gravity of a vehicle	m
i_F	Final drive ratio	-
i_{HST}	Hydrostatic transmission ratio	-
i_P	Pump mount ratio	-
$i_{T,min,v}$	Minimum transmission ratio	-
$i_{T,min,v}$	Maximum transmission ratio	-
J_d	Rotational inertia of the driveshaft	$kg.m^2$
J_E	Rotational inertia of the engine	$kg.m^2$
$J_{g,i}$	Rotational inertia of a gear	$kg.m^2$
J_T	Rotational inertia of the transmission from engine side	$kg.m^2$
J_w	Rotational inertial of the wheels	$kg.m^2$
L	Distance between front and rear axle	m
$\dot{m}_f$	Mass flow rate of fuel	g/s

m_F	Vehicle curb weight	kg
M_{axle}	Torque on the axles	Nm
M_c	Torque on the clutch (input to the transmission)	Nm
M_d	Torque output to the driveshaft	Nm
M_{ICE}	Engine torque	Nm
M_M	Hydro-motor torque	Nm
m_p	Payload	kg
M_P	Pump torque	Nm
m_r	Equivalent mass of the rotating components	kg
m_T	Towing capacity	kg
M_w	Wheel torque	Nm
N	Normal load on the wheels	N
n_M	Hydromotor speed	rpm
n_p	Pump speed	rpm
n_w	Wheels speed	rpm
P_E	Engine power	kW
P_M	Hydromotor power	W
P_P	Pump power	W
P_T	Traction power required at the wheels	W
$Q_{Loss,p}$	Flow losses of the pump	l/min
$Q_{Loss,p}$	Flow losses of the motor	l/min
Q_M	Hydromotor flowrate	l/min
Q_P	Pump flowrate	l/min
r_w	Wheel radius	m
t	Time	s
v_F	Vehicle velocity	km/h
$v_{F,max}$	Maximum vehicle velocity	km/h
V_g	Displacement volume of a hydrostatic unit	cm^3
V_M	Hydromotor displacement	cm^3
V_P	Pump displacement	cm^3
W_g	Gross vehicle weight	N

Greek letter

α_{st}	Road inclination angle	*deg*
δ_{IHT}	Port plant angle of Innas hydraulic Transformer	*deg*
ε_{M}	Setting angle of hydro-motors	-
ε_{P}	Setting angle of pump	-
η_F	Mechanical efficiency of final Drive	-
η_{ICE}	Engine efficiency	-
η_{mech}	Mechanical efficiency	-
η_{hm}	Hydro-mechanical efficiency	-
$\eta_{o,M}$	Overall efficiency of the motor	-
$\eta_{v,IHT}$	Volumetric efficiency of IHT	-
$\eta_{v,M}$	Volumetric efficiency of the hydromotor	-
$\eta_{v,P}$	Volumetric efficiency of the pump	-
λ	Mass factor of rotating parts	-
μ_p	Tyre peak coefficient of road adhesion	-
ρ_a	Air density	kg/m^3
ω_{ICE}	Engine angular speed	*rad/s*
ω_w	Wheel speeds during braking	*rad/s*
$\dot{\omega}_d$	Rotational acceleration of the driveshaft	rad/s^2
$\dot{\omega}_w$	Rotational acceleration of the wheels	rad/s^2
Δp	Pressure difference	*bar*
ΔV	Change in accumulator volume	*liter*

Abbreviations

BSFC	Brake Specific Fuel Consumption
CBED	Cumulo Brake Energy Drive
CHD	Cumulo Hydrostatic Drive
CV-HST	Continuously Variable Hydrostatic Transmission
EEA	European Environmental Agency
EPA	American Environmental Protection Agency
EUDC	Extra-Urban Driving Cycle (Highway part of the NEDC)
FTP-75	Federal Test Procedure cycle
HEV	Hybrid Electric Vehicle
HHV	Hydraulic Hybrid Vehicle
HLA	Hydraulic Lunch Assist
HMT	Hydro-Mechanical Transmission
HRB	Hydraulic Regenerative Braking
HST	Hydrostatic Transmission
ICE	Internal Combustion Engine
IHT	Innas Hydraulic Transformer
IOL	Ideal Operating Line
IVT	Infinitely Variable Transmission
NEDC	New European Driving Cycle
ODI	Online Data Import
OICA	Organization of Motor Vehicle Manufacturers
OOP	Optimal Operating Points
PG	Planetary Gear
SC-HST	Secondary Controlled Hydrostatic Transmission
UDC	Urban Driving Cycle (City part of the NEDC)

Chapter 1

Introduction

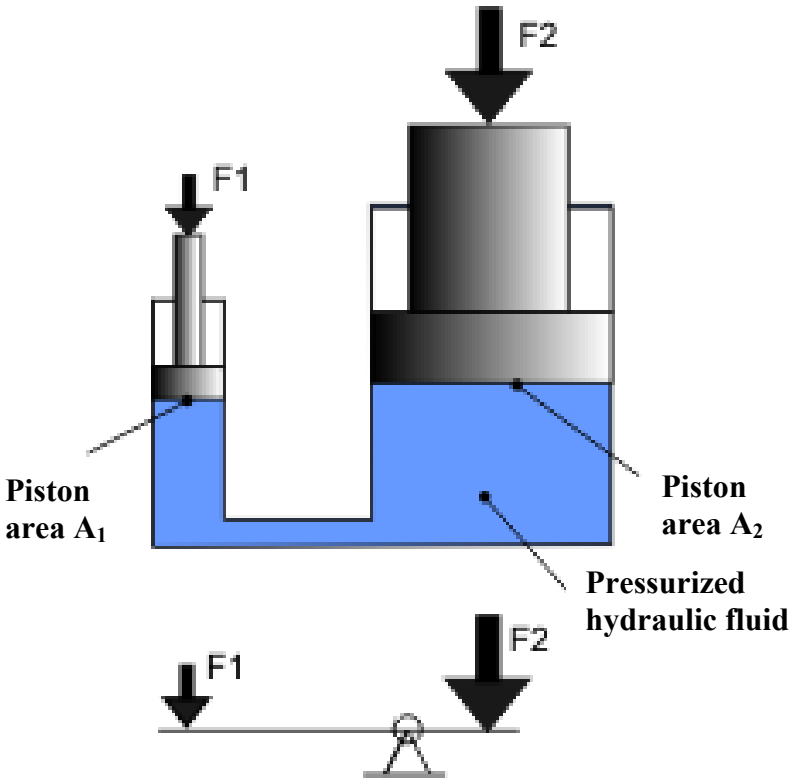

Mechanical analogy

1.1 General Aspects

Increased fuel economy and decreased hazard emissions such as CO_2 and NO_x are the two major demands for automobile manufacturers to produce more energy-efficient and environmentally friendly vehicles. Passenger and heavy duty vehicles consume a huge amount of fuel worldwide. This significant usage of fuel is the motivation for developing a vehicle that improves fuel economy.

In the current automotive industry, there is a strong emphasis being placed on the fuel efficiency of a vehicle. This demand for fuel efficiency is driven primarily by fluctuating fuel prices and a desire to reduce emissions. In response to this demand, during the past 30 years, enormous progress has been made in hybrid vehicle technology resulting in increased sales of these types. Hybrid vehicles have proven to be efficient because they draw their power from a primary power source, usually, an Internal Combustion Engine (ICE) coupled with an auxiliary power source capable of energy recovery. Currently, mass produced hybrid vehicles have been electric hybrids, facilitated by the recent advances in electronics.

Electric motors/generators still suffer from low power density compared to hydraulic motors as shown in Figure 1.1, which limit their ability for rapid acceleration or deceleration [1]. To overcome this shortcoming, hydraulic drivetrain needs to be investigated for use in vehicles.

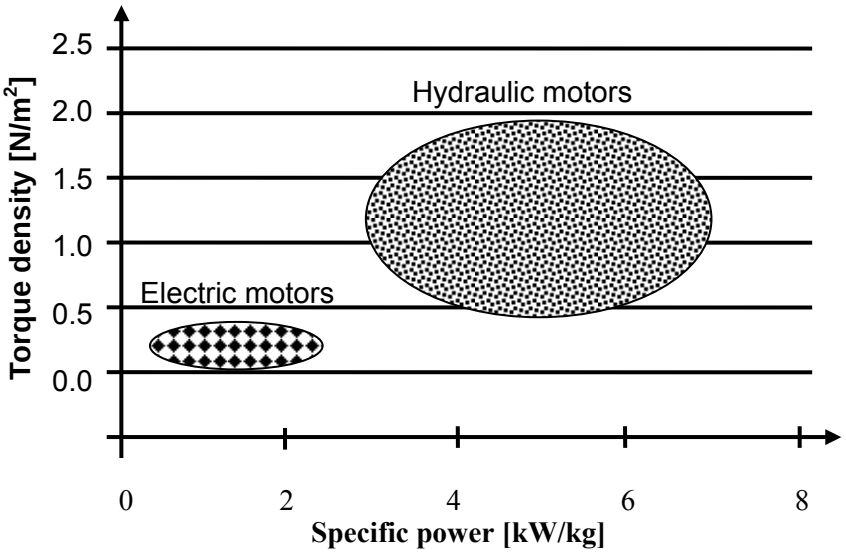

Figure 1.1: Specific power versus torque density of electric and hydraulic motors [1]

Looking at the whole powertrain, the fuel economy of passenger cars can be improved in various ways. Increasing the efficiency of the powertrain components, such as the engine and the transmission, is one way to do so. Another is to operate the engine in more fuel-optimal regions. Drivetrain hybridization, using mechanical flywheel, electric batteries and super-capacitors, or a hydro-pneumatic accumulator to restore the lost energy in braking is considered to be the best method.

1.2 Motivation for the Research of Hydraulic Transmissions

Hydraulic drives have, of course, been used on a number of stationary applications and off-road vehicles for decades. Hydraulic systems have proven to be very reliable and robust. They allow a flexible layout and easy control for the drive, including energy storage in accumulators. Interest in development of hydrostatic transmission components and its control has increased during the past few decades in response to increased concern about fuel consumption and environmental pollution.

The high power density of hydraulic pumps/motors and accumulators as well as the ease of control of hydraulic components make hydraulic technology look promising for vehicle transmission, especially for applications with frequent stop-and-go. Although hydro-pneumatic accumulators have an inferior energy density, they have an excellent power density, much higher than electric batteries. Moreover, cyclical charging and discharging at high power rates considerably reduces the service life of the state of the art batteries. Although electric hybrid powertrains and similar systems have proven to be more efficient than conventional vehicles, the overall efficiency of the system could be greatly improved by using an auxiliary power source, such as a hydro-pneumatic accumulator, with a much higher energy and power density.

A main reason for not yet considering hydrostatic drivetrains in passenger vehicles may lie in the conception that hydraulic components have inferior efficiency compared to mechanical drives. Current prototypes of hydraulic hybrid drivetrains show the potential to save 25 to 40 % which is still considered too low compared to requirements of current drivelines [2]. Since requirements are tougher, there is a need for new and more efficient components. Therefore, the traditional configurations of hydraulic transmission need to be replaced with new ones that involve the integration

of transmission and power source to obtain the optimum operation from the vehicle. The recently developed hydraulic units that permit operation at higher system pressure and higher speeds with high efficiency may provide a chance for hydraulic drivelines to be used in passenger vehicles.

In automotive technology, adding a secondary power source to the primary power source, i.e. combustion engine, forms a hybridized vehicle. Generally, using hybrid drivetrains is widely considered a key technology strategy in improving fuel efficiency and reducing emissions. Energy can be saved by using an accumulator because it is able to recover energy during deceleration.

Hydraulic Hybrid Vehicles (HHVs) are one of several new energy saving automotive technologies being developed by some vehicle-manufacturers and are still under development in universities and research centers. The present prototype models of HHVs being in use such as urban delivery trucks, city busses and refuse trucks involve frequent stop-and-go driving have demonstrated their ability to significantly reduce fuel consumption and CO_2 emissions. One major benefit of a hydraulic hybrid vehicle is the ability to capture a large percentage of the energy normally lost in vehicle braking. Efficiency of the ICE of a vehicle can be significantly increased by series hydraulic hybrids rather than parallel configurations. This is a result of controlling the accumulator pressure range between upper and lower limits avoiding operation of the engine under partial loads.

Energy consumption and exhaust emissions of hybrid vehicles strongly depend on their configuration, efficiency of the components and applied control strategy. A high efficiency transmission can be designed using new developed hydraulic units arranged in distinct configuration as introduced in this thesis to reduce fuel consumption and emissions. Therefore, an extensive analysis is included for an innovative configuration of series hydraulic hybrid drivetrain designated here by “the Hy*d*rid”. The analysis assumes base vehicle specifications and components similar to a mid-sized Sedan like a 2007 Volkswagen Passat.

1.3 Aim of the Work

Studying the potential of three different configurations of hydraulic transmission integrated with a diesel engine for use in cars through simulation.

Optimizing performance using powerful simulation models is relatively inexpensive compared to hardware design and development. Furthermore, competing designs can be evaluated and compared before hardware decision need to be made.

Another objective is to develop appropriate control strategies that can be used for each concept. Investigating the effectiveness of these strategies on performance will be considered.

A comparison of fuel consumption and CO_2 emissions during a standard driving cycle for a continuously variable hydrostatic transmission and a secondary controlled transmission as well as the innovative series hydraulic hybrid drivetrain known as the "Hy*d*rid" to the mechanical transmission of the baseline vehicle will be made.

There will also be an exploration of the new configuration of Hy*d*rid drivetrain as well as developing an energy management strategy to obtain the highest overall efficiency will be focused on.

1.4 Scope of the Work

The scope of the thesis is conducted in an effort to explore the potential and feasibility of hydraulic hybrid transmission represented by the innovative distinct configuration of the series hydraulic hybrid drivetrain referred to as the Hy*d*rid to use in passenger cars. Thereby it will also be focused on the new technologies used, such as the three ports hydraulic transformer and the floating cup design applied to the hydrostatic units.

1.5 Outline of the Thesis

The structure of the thesis begins with a general introduction for the thesis in *chapter 1* followed by a literature survey, description and discussion of the state of the art hydraulic hybrid vehicles technologies that can be found in *chapter 2*. The next two chapters deal with the baseline vehicle. To be more specific, *chapter 3* contains all of the common factors and geometrical parameters describing the benchmark vehicle such as ICE characteristics, vehicle dynamics, as well as properties of the driving cycle that will be used as assessment criterion to evaluate performance, fuel economy and emissions for each drivetrain of the introduced hydraulic transmissions. In *chapter 4* the gear-shift mechanical transmission of the baseline vehicle is studied and

simulated to assure that operating conditions and all common geometrical parameters of the vehicle such as rolling friction coefficient and frontal area and drag coefficient, which will be used in the other proposed hydraulic transmissions, will lead to the same manufacturer data.

In *chapter 5* analysis and simulation of a continuously variable hydrostatic transmission integrated with a controlled diesel engine to operate along the points of minimum fuel consumption on the engine map is introduced. The control strategy aims to feed the vehicle with optimum power and proper transmission ratio.

A secondary control pressure coupled hydrostatic transmission simulation study using state of the art hydraulic units is represented in *chapter 6*. This transmission aims to study the effect of recuperating braking energy on the vehicle performance.

Chapter 7 describes in some depth the key design feature and components of the innovative series hydraulic hybrid vehicle, referred to as the Hy*d*rid, being modeled and evaluated in the thesis. A rule based energy management strategy for improvements in fuel economy over the base vehicle can be gained by applying the proposed strategy. Conclusions and opportunities for future research work and outlook are proposed in *chapter 8*.

Chapter 2

State of the Art

with

Reference to Hydraulic Transmission

2.1 Introduction

While the automotive transmission has undergone many changes and improvements within the lifetime of the automobile industry, the established methods of power transmission have remained basically the same for most of that period. Even though systems such as Continuously Variable Transmissions (CVTs), electric, and hybrid-electric drivetrains have made inroads into the automobile marketplace at different times over the past century, the gearbox with discrete shifting gear ratios has still been the standard by which other systems are judged and evaluated. Even though the basic transmission designs have been around for most of the past century, continued refinement and research has improved conventional transmissions to the point where they will be accepted as the standard until a truly cost effective and efficient piece of technology can replace them [3].

Today, energy efficiency of transmission systems for automobiles and trucks has become one of the most important topics in vehicle design, mainly due to increased fuel costs, environmental issues and emission regulations. Over the years, many different concepts have been developed that aim to improve fuel economy and reduce emissions.

The specific properties of hydraulic drive systems such as high power density, which offer important advantages such as continuously variable transmission, continuous power transmission, infinitely variable transmission and high transmission ratios have opened up broad fields of applications for such units [4].

Hydraulic drivetrains have reached a technology level that permits a large-scale introduction even in the class of full-sized passenger cars. The conventional form of a continuously variable hydrostatic transmission can be integrated with an appropriate control means for efficient operation of the engine would make it suitable for urban use. Also the known form of secondary controlled hydrostatic transmission can be applied in the vehicle drivetrain. Different hydraulic hybrid drivetrain configurations and prototypes were introduced by the American Environmental protection Agency (EPA) and most of them are still in the first stages of examination.

The goal of this chapter is to present appropriate reviews on the state of the art in previously conducted work available in the literature as well as development and

techniques in the field of hydrostatic and or hydraulic hybrid transmission used in automotive application, so far.

2.2 Background

The first hybrid vehicle in the world shown in Figure 2.1 was developed by engineer Ferdinand Porsche in 1900 and called Lohnerporsche. It is considered a series type Hybrid Electric Vehicle (HEV) which used a hybrid of gasoline engine and electric motor and battery.

Figure 2.1: The 'Lohnerporsche' [5]

The hybrid-electric vehicle did not become widely available until the release of the Toyota Prius in Japan in 1997, followed by the Honda Insight in 1999. While initially perceived as unnecessary due to the low cost of gasoline, worldwide increases in the price of petroleum caused many automakers to release hybrids in the late 2000s; they are now perceived as a core segment of the automotive market of the future [5].

In 1648 a Frenchman, Blaise Pascal showed that the pressure in a fluid at rest is transmitted equally in all directions. Nearly 150 years elapsed before Englishman Joseph Bramah exploited this principle. In 1795 Bramah was granted a patent for a hydraulic press to transmit and amplify force by using a hand pump to pressurize a column of fluid. In 1906 the electric system for elevating and training guns in the battleship U.S.S. Virginia was replaced by a variable speed hydrostatic transmission system to maneuver the guns. The subsequent development of a range of components has widened the field of application of fluid power technology, which is concerned with the transfer, storage and control of energy by means of a pressurized fluid. For

example, the design of hydrostatic transmission systems by axial piston pump and motor to produce rotary motion was a major development. Interest in fluid power servomechanisms was boosted in 40s by the demand for automatic fire control systems and military aircraft controls [6, 7, 8]. In 1962 the principle of Secondary-Control was first patented in England by the engineers Pearson and Burret. The idea was also born in the Army University of Hamburg independent of the earlier patent in 1977. Cooperation with Mannesmann Rexroth made it possible to initiate tests and eventually simulate different concepts of secondary-controlled systems. The cooperation ended in 1986, but at that time several orders had already been booked from the industry. During this time, secondary-control became more common in industry [9].

In last decades many hybrid vehicle concepts have been developed. Hydraulic hybrid drivetrains have been a core focus of the American Environmental protection Agency (EPA) under the EPA's Clean Automotive Technology Program since the mid-1990s. Much of EPA's early research focused on the design of individual hydraulic hybrid components optimized for passenger vehicle applications (i.e., smaller, lighter, and more efficient), but more recently EPA has been working with their cooperative partners to demonstrate complete hydraulic hybrid drivetrains in specific vehicle applications. EPA has developed two types of hydraulic hybrid vehicles –mild hydraulic hybrids and full hydraulic hybrids. It built a mild hydraulic hybrid urban delivery vehicle that competed in the Michelin Bibendum Challenge in September 2003 and won a gold medal for fuel efficiency and a silver medal for acceleration performance. EPA is currently building a full hydraulic series hybrid urban delivery truck that will have further fuel economy and performance improvements [10].

2.3 Review of Relevant Literature and Technical Publications

Hydrostatic transmissions have been widely used in mobile machines and off-road vehicles such as wheel loaders, graders or tractors. In [11,12,13,14] various application can be found, such as earth moving machines, building and construction machines using different configurations of hydrostatic transmissions. The hydraulic transmission can be used to perform transmission of power from the engine to the vehicle wheel or in other design can be combined to work in parallel with the existing

mechanical gearbox. Much research was done in the area of applying hydraulic circuit as alternative transmission to mechanical gears. Since the major research efforts concern different forms and designs of hydrostatic transmissions, the focus of the following survey concentrates on mobile applications and road vehicles. A description of different hydraulic transmission systems applied and utilized in the automotive industry is also included.

2.3.1 Non regenerative Hydrostatic and Hydro-mechanical Transmissions

Individual and compound hydraulic drivetrains are reviewed here, not including any storing energy element. Those drivetrains are represented by conventional hydrostatic transmission and hydrostatic-mechanical systems or Hydro-Mechanical Transmissions (HMTs) which are composed of a hydrostatic transmission connected in parallel with mechanical transmission by planetary gears. The later system is generally known as power split drivetrain.

2.3.1.1 Conventional hydrostatic transmission drivetrain

A number of investigations of hydrostatic transmissions using different open and closed-loop concepts, which are not specified for on-road vehicle drivetrains were conducted in 1790's and 1980. In the early 80's Rydberg [15] investigated performance optimization of vehicle drivetrains with hydrostatic transmission. He used a simulation model considering leakage flow losses and indicates the importance of digital control in mobile applications. Research projects in the 90's suggested a way to increase the efficiency of hydrostatic transmissions used in drivetrains such as J. Lennevi, et al. 1994 [16] who proposed a gain scheduling law based on PID-control to guarantee the desired closed-loop behavior for the whole operating range, while M. Sanelius, 1999 [17] showed that adaptive control concepts using variable displacement pumps and fixed displacement motors improve vehicle operation. Sanelius suggested the application of two hydraulic motors in parallel, where one of them can be disconnected from the driveline and controlled to zero displacement in order to increase total efficiency of the HST from low to high vehicle speed.

To investigate the steady state and dynamic characteristics of hydrostatic transmission, Huhtala 1996 [18] developed nonlinear models with steady loss models both of a pump and a motor. He used command generator displacement to determine

the desired set values of the transmission input speed and the vehicle speed. Based on PI-fuzzy controller, Huhtala suggested an adaptive control strategy to achieve a high efficiency hydrostatic transmission.

Several studies concerning the steady and dynamic performance of the continuously variable transmission using different modeling and control concepts can be found in [19, 20, 21, 22, 23, 24, 25, 26, 27].

Ossyra J.C 2005 [28] analyzed and proposed in simulation and experimental work different control concepts based on cascade displacement setting for the displacement of the pump and the motor for off-road vehicles with hydrostatic transmission. The results show a reduction of fuel consumption from 12 ~ 20 %.

Macor and Tramontan 2007 [29] presented a hydrostatic transmission connected to a hybrid propulsion system consisting of ICE and an electric motor connected to an energy storing battery to absorb or supply energy according to the traction. The system is applied to a transportation bus with maximum speed of 60 km/h. Using HST allows the engine to work at a fixed point and sized for average power which in turn results in a fuel and emission reduction.

2.3.1.2 Non-regenerative hydro-mechanical transmission

A typical hydro-mechanical transmission (HMT) consists of mechanical transmission parts, planetary gears, clutches and a hydrostatic transmission (HST). HMTs transmit the power by two paths, the hydrostatic path and the mechanical path [30]. HMT combine the benefits of continuous variable transmission and high efficiency of mechanical transmission.

Berger 1986 [31] and Blumenthal 1989 [32] investigated the suitability of applying hydro-mechanical power split transmission in medium sized cars. Berger built a simulation model for the combined HMT drivetrain including losses for system elements. The obtained steady and cycle based results from the developed simulation model show 18 % saving in fuel consumption compared to a mechanical transmission.

Carl et al. 2006 [33] made a detailed study to apply power split in vehicle drivetrains. Carl investigated four architectures of power split transmission illustrating the advantages and disadvantages of each type with regards to energy consumption, efficiency, system complexity, compactness and control effort for on-road and off-road

vehicles. It was concluded that the output-coupled system shown in Figure 2.2 is advantageous for lower power type systems or systems that desire very simple control effort such as wheel loaders as well as in smaller passenger vehicles. For higher power applications such as busses, refuse vehicles, semi-trucks, and other high speed vehicles with high tractive forces compound-coupled or dual-stage input-coupled drives are suitable.

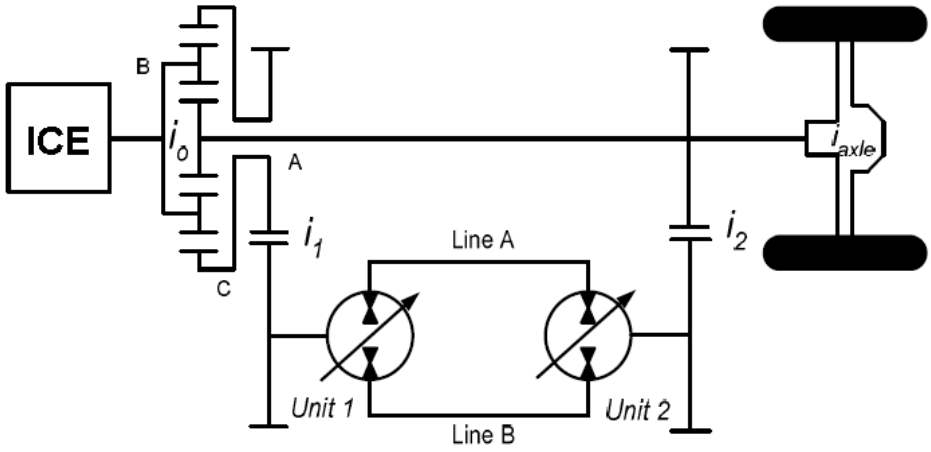

Figure 2.2: Output-coupled power-split transmission [33]

Kohmäscher 2008 [34] provides a detailed analysis for six possible combinations of input-coupled and output coupled HMTs as well as one selected Compound HMT. A simulation approach for hydro-mechanical power split transmissions was introduced for use in a wheel loader equipped with a 120 kW engine. He focuses on building loss models for hydraulic units and compound planetary gears which are an essential component for HMTs. It was found from the simulation results that the fuel consumption can be reduced by 25 % for the proposed duty cycle.

2.3.2 Regenerative hydrostatic transmission drivetrains

Mobile machines and vehicles that store wasted braking energy in a hydraulic-pneumatic accumulator for reuse it during acceleration or cruise mode is presented here. They can be divided into three categories, parallel, series and a combination of both i.e. series-parallel drivetrain.

Work showing a comparison of parallel, series, and regenerative power split configurations of hydraulic hybrid vehicles has been done by Stelson [35] and Meyer [36] in 2008. It was found that parallel configuration obtains the best fuel economy

with regenerative power split being the least efficient. But the pumps and motors used are oversized to apply in passenger vehicles and therefore operate at low efficiency.

2.3.2.1 Parallel hydraulic hybrid

A parallel hybrid vehicle involves adding the hydraulic power and the conventional mechanical power together. It can be found in literature under several names and is not limited to Mild hydraulic hybrid vehicle by EPA, Hydraulic Lunch Assist (HLA) by Eaton Corporation, Hydraulic Regenerative Braking (HRB) system by Bosch, Hydraulic power assist by Ford Motor Company, or in general parallel hydraulic hybrid drivetrain.

It has an internal combustion engine coupled to mechanical transmission and a hydraulic pump/motor connected to storage device that captures and stores a large fraction of the energy normally wasted in vehicle braking. The stored energy will be used to help engine in propelling the vehicle during the next vehicle acceleration. Parallel HHV can be viewed as an add-on to a conventional drivetrain.

In the early 1980's the Comulo Division of Volvo Flygmotor (now a part of Parker Hannifin) in close cooperation with AB VOAC Hydraulics Trollhättan AB in Sweden, developed a highly efficient over-center variable displacement bent axis type connected to a hydro-pneumatic accumulator to work in parallel with mechanical transmission as shown in Figure 2.3. Development started 1983 and it has been used in ordinary city buses on Stockholm roads from 1985. The developed drivetrain, called Cumulo Brake Energy Drive (CBED), considered the first on-road parallel hydraulic hybrid vehicles launched for the market. A reduction of fuel consumption and gas emissions by 16 to 25 % has been demonstrated [37].

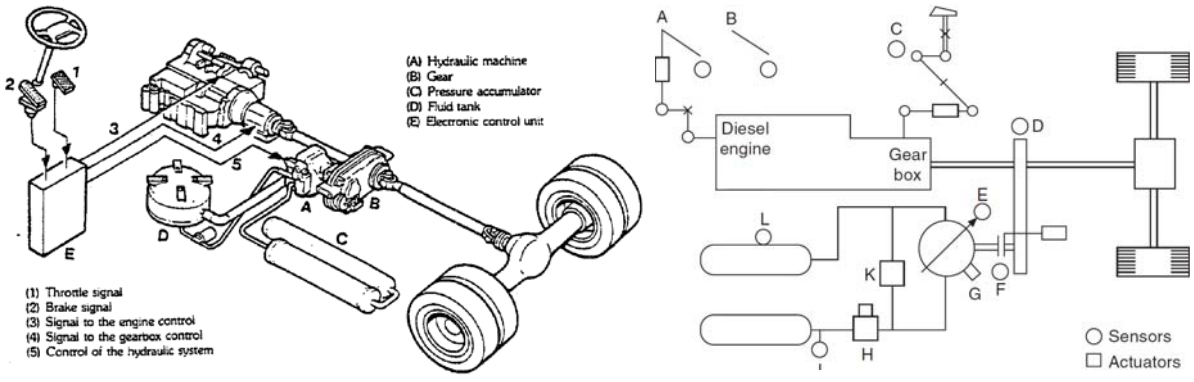

Figure 2.3: Cumulo Brake energy Drive (CBED) [37]

Optimal power management strategy of a parallel hydraulic hybrid system applied in medium delivery truck vehicle is presented by [38]. A dynamic programming strategy has been proposed which results in a fuel economy increase from 28 ~ 48 % in comparison to the conventional vehicle.

Research at Purdue University done by [39] applied optimal power management strategy on regenerative power-split transmissions. They found that the introduced concept has a significant potential for improving fuel economy in vehicle applications.

In January 2002, Eaton Corporation, a major automotive component supplier, unveiled its HLA and stated that the HLA system could be ready for commercial introduction by mid-decade [10, 40]. Eaton Corp. designed HLA for use in specific vehicle applications shown in Figure 2.4.

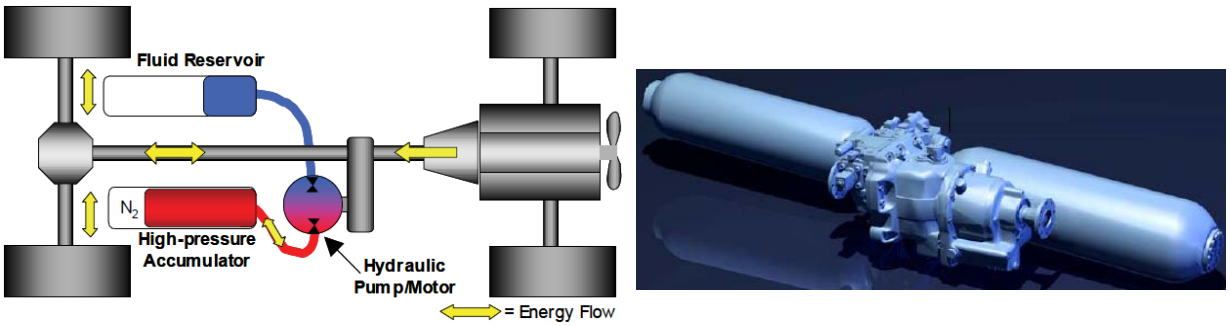

Figure 2.4: Eaton HLA drivetrain [41]

The technical advantages of applying parallel hydraulic hybrid in heavy duty vehicles such as refuse trucks was discussed in [41]. It was concluded that the parallel HHV can improve fuel economy by up to 30 %.

Another research work on parallel hydraulic hybrid for use in passenger cars was conducted at IFAS of RWTH Aachen University in [42] and is shown in Figure 2.5. It introduced a test vehicle called IFASter to demonstrate the ease of integrating a hydraulic component in a conventional vehicle to build simple parallel hydraulic hybrid configuration.

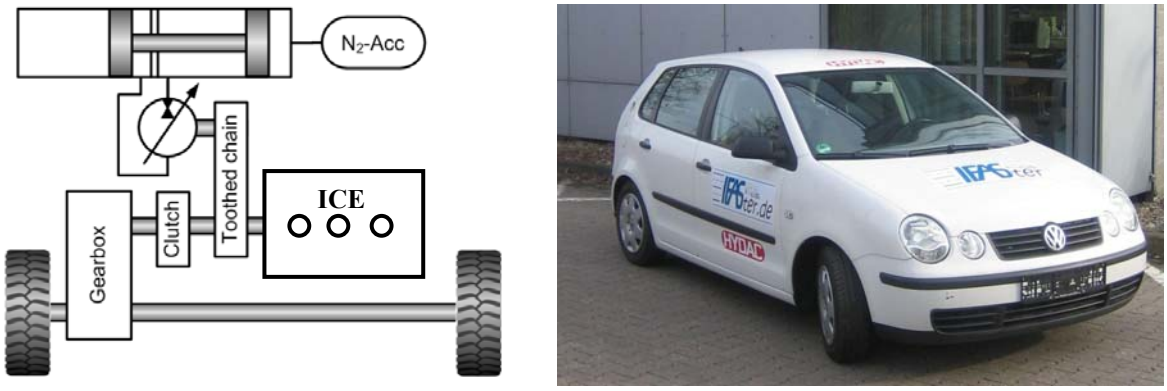

Figure 2.5: Proposed configuration of the parallel HHV [42]

2.3.2.2 Regenerative power-split drivetrains

A hydro-mechanical transmission (HMT) drivetrain with regeneration and independent wheel torque control of a hydraulic hybrid passenger vehicle was presented by [43, 44]. The shown drivetrain in Figure 2.6 exhibits the benefits of both the parallel and series architectures but is based on a complex case which requires a comprehensive control strategy. A little saving in fuel consumption is achieved by this configuration.

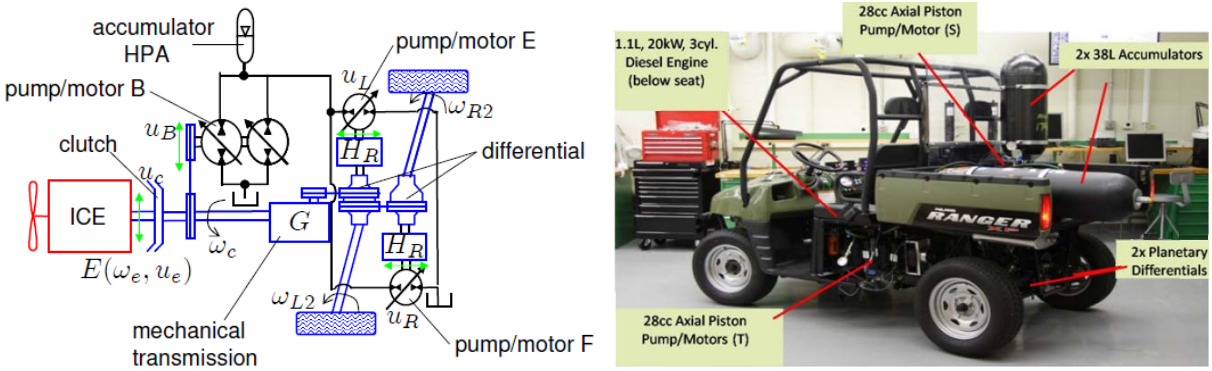

Figure 2.6: Proposed HMT drive train with independent wheel torque control of a passenger vehicle system [43, 44]

2.3.2.3 Series Hydraulic hybrid drivetrains

The traditional secondary controlled hydrostatic transmission is considered one form of series hydraulic hybrid vehicles. Within this configuration the mechanical transmission is removed completely. The internal combustion engine is disconnected from the road load applied on of the vehicle wheels. The vehicle is propelled by the controlled power supplied by a hydrostatic transmission.

As stated before, the idea of secondary controlled drives appeared in the 70s. Wassenberg at 1982 [45] introduced a comparison study between primary and

secondary controlled hydrostatic transmission for use in prototype field vehicle weights 4.5 ton with maximum speed about 41 km/h. It was indicated that the secondary controlled drive is more powerful for use in this application especially from the energy consumption point of view. On the same prototype vehicle [46] made a detailed study indicating that the maximum speed range can be increased to 60 km/h by using the secondary controlled system.

Different control methods, modeling and simulation to improve the dynamic behavior of the secondary controlled system are treated in [47, 48]. Investigations concerning the effect of accumulator volume on the performance of the transmission can be found in [49, 50].

Further development was done on the aforementioned CBED parallel hybrid vehicle in 1991 to replace the mechanical transmission with a complete series hydraulic system called Cumulo Hydrostatic Drive (CHD), shown in Figure 2.7, including two independent control units for primary and secondary sides [37]. It aims for use in refuse trucks which mainly operate with frequent speed variations and moderate average speeds. Tests indicate that about 20 ~ 40 % fuel consumption can be obtained [2].

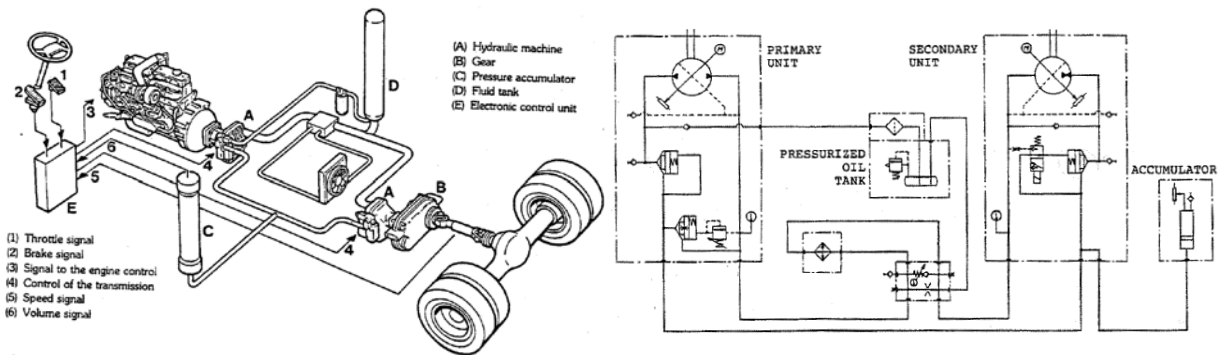

Figure 2.7: Cumulo Hydrostatic drive (CHD) [37]

Some years ago, Parker Hannifin launched “the RunWise” project, which would become the largest project undertaken by the Industrial Group of Parker Hannifin. The goal was to develop an energy recovery hydraulic hybrid transmission for refuse trucks. Although many of the fundamental theories from the Cumulo project were adopted, a completely new system was developed [51].

EPA unveiled the world’s first full hydraulic hybrid SUV at the 2004 Society of Automotive Engineers (SAE) World Congress in Detroit, Michigan. This vehicle had

outstanding performance in the laboratory. Dynamometer tests showed that the full hydraulic hybrid SUV depicted in Figure 2.8 offered an estimated 35 ~ 55 % fuel economy improvement in comparison to a comparable, commercially available SUV. The increase in fuel economy consequently results in a reduction of carbon dioxide (CO_2) emitted from the engine [52].

Figure 2.8: A complete view of full hydraulic hybrid SUV at SAE Congress [52]

In June 2006, EPA with a partnership arrangement with United Parcel Service (UPS), Eaton Corporation, and the U.S. Army's National Automotive Center introduced the world's first full series hydraulic hybrid delivery truck shown in figure 2.9 to a crowd of auto industry representatives, environmentalists, and reporters in Washington, DC. Laboratory tests show that this EPA patented technology can increase fuel efficiency by 60 to 70 % in urban driving conditions and reduce carbon CO_2 compared to conventional UPS diesel delivery trucks [52].

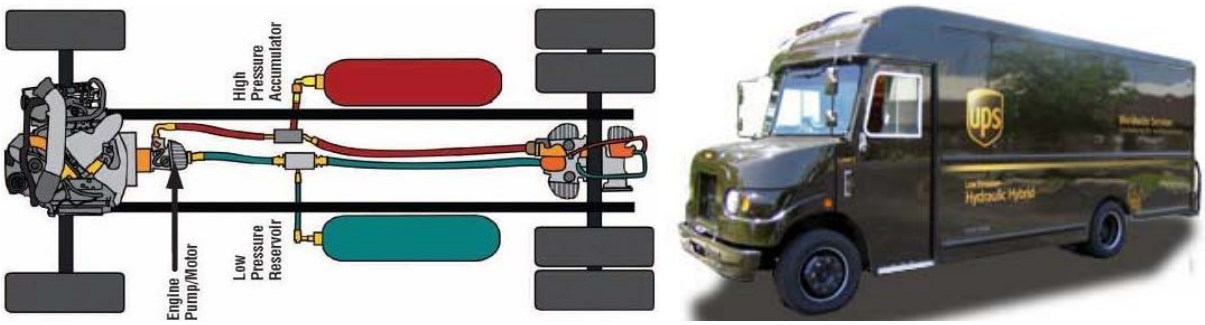

Figure 2.9: UPS full hydraulic hybrid drivetrain [52]

Ivantysynova et al. 2006 [53] studied and modeled with a software tool two different hydrostatic transmission for application in refuse trucks. One transmission

was developed by Parker Hannifin, which uses two secondary controlled motors supplied from a constant pressure net of a pressure controlled pump as shown in Figure 2.10. The second is based on a simple output-coupled power split drive design. It has been shown that the secondary controlled drives consumes less fuel than the proposed power split drive.

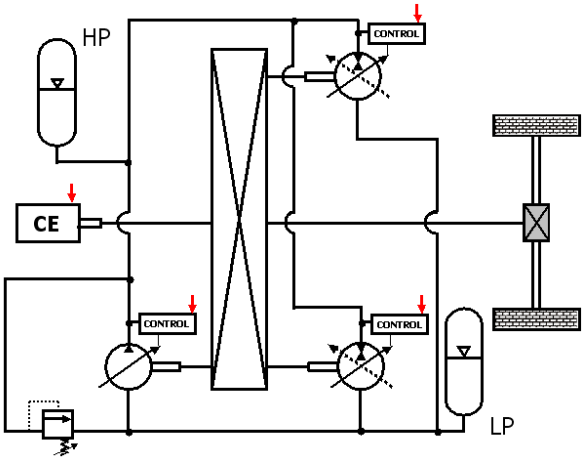

Figure 2.10: Secondary controlled Hydrostatic transmission setup [53]

Freightliner Custom Chassis Corporation (FCCC) [54], a subsidiary of Daimler Trucks North America, has made an initial 20 unit commercial commitment for a series hydraulic drives system from Parker Hannifin Corporation which introduced its pilot hydraulic hybrid on display in March 2009 in The Work Truck Show Hybrid Pavilion at Chicago. Preliminary testing indicated that the hydraulic hybrid improves fuel economy between 50 ~ 70 % over traditional diesel-powered vehicles with automatic transmissions in stop-and-go applications.

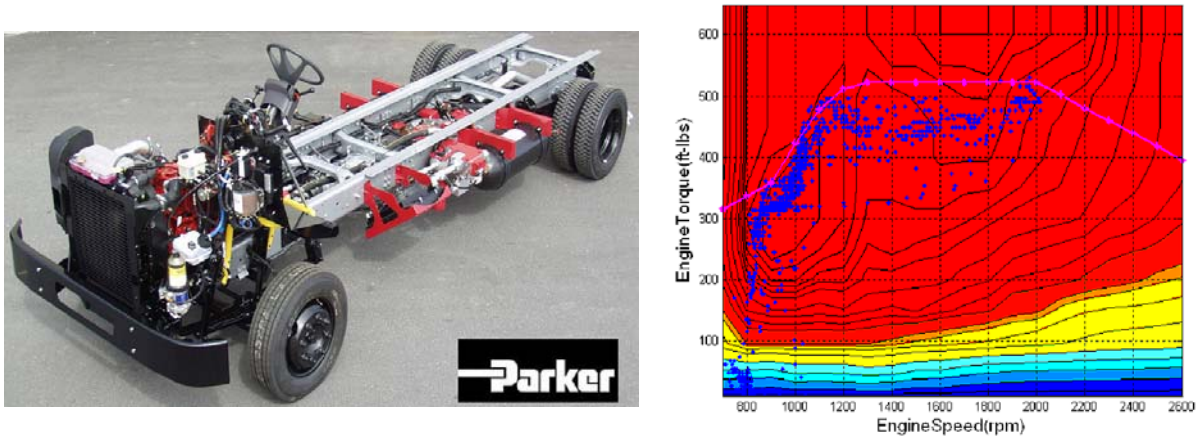

Figure 2.11: Parker Series HHV and its Engine operating point's [54]

The Scottish company Artemis Intelligent Power Ltd, has for the first time publicly revealed in Edinburgh, UK May 2008 [55], a new type of hybrid car and truck

transmission based on its novel Digital Displacement® technology which was developed in Scotland. The demonstrated prototype car is a BMW-530i equipped with a Digital Displacement® Hybrid Transmission and has achieved 50 % reduction of fuel consumption for city driving compared with the same car equipped with a manual transmission. The two prototypes of Artemis are shown in Figure 2.12.

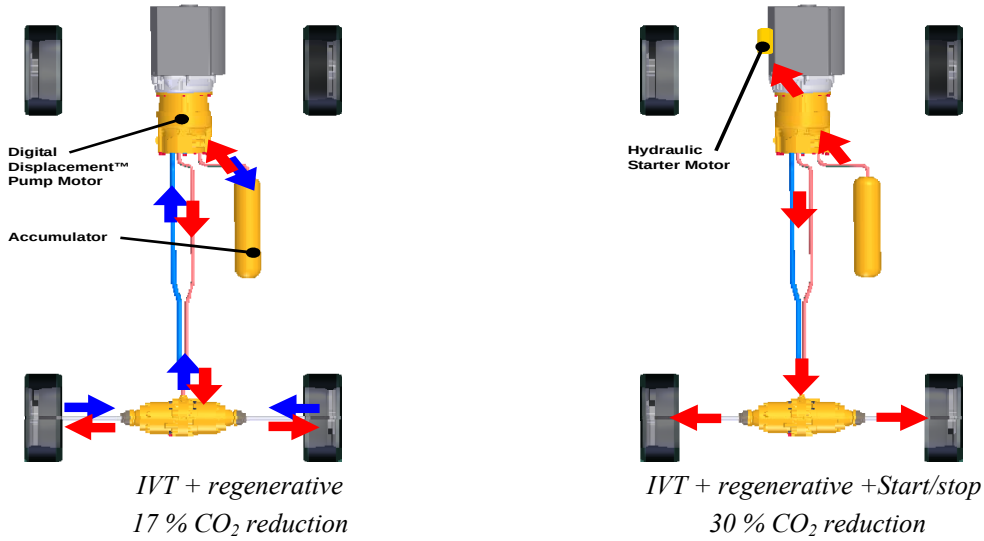

Figure 2.12: Artemis's Digital Displacement® Hybrid Transmission prototypes [55]

The heart of the system is a six piston radial digital displacement hydraulic pump/motor unit shown in Figure 2.13. This hydraulic unit replaces the port plates and swash plates in conventional hydraulic machines with computer controlled high-speed solenoid valves driven by a microprocessor. These solenoids actively control poppet valves that rectify the flow into and out of each cylinder. The hydraulic pump connected to a conventional combustion engine replacing the gearbox. It is hydraulically connected to Digital Displacement Motors coupled to the wheels.

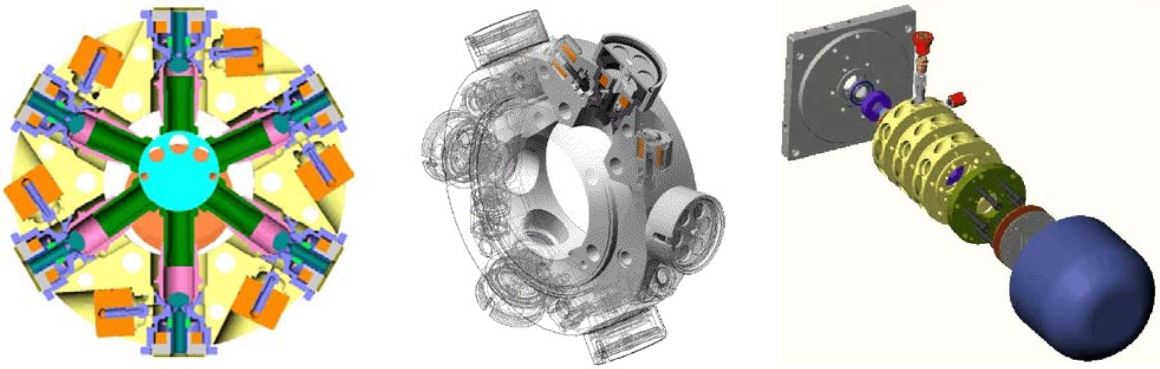

Figure 2.13: Artemis modular digital displacement six piston radial machine [56, 57]

Peter Achten from Dutch engineering organization Innas B.V developed a new concept of hydraulic transformer, referred to as the Innas Hydraulic Transformer

(IHT). The IHT as indicated in Figure 2.14 is designed with three ports [58]. It has been built and tested in a forklift [59, 60]. Achten also developed floating cup technology for use in hydrostatic pumps, motors and transformers. This development is shifting towards applying such technology for hydraulic hybrid vehicles.

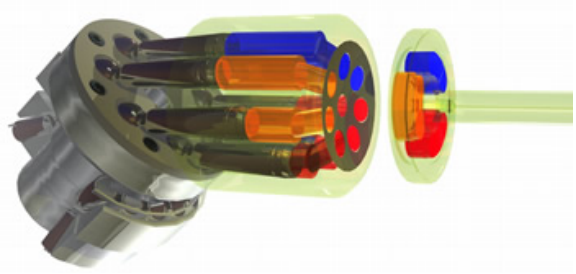

Figure 2.14: The Innas Hydraulic transformer [60]

Achten [61, 62] proposed a layout for an all-wheel full hydrostatic transmission, shown in Figure 2.15, for automobile use, as opposed to mechanical transmission. The proposed transmission is called "The Hy*d*rid". A simulation on the proposed Hy*d*rid using an internal combustion engine and all-wheel hydromotors is carried out at IFAS of RWTH Aachen University and will also be treated in this thesis.

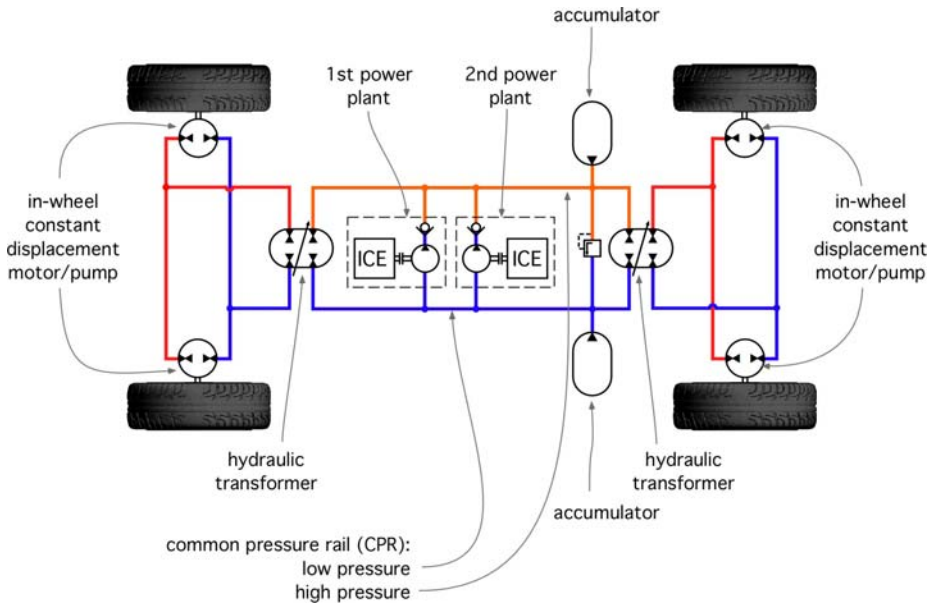

Figure 2.15: Hydraulic layout of the Hydrid with two drive engines [62]

2.4 Summary

The surveyed literature shows that a small amount of work has been done on hydraulic hybrid drivetrains. So far some research has focused on the field of hydraulic hybrid vehicles from concepts to prototypes of its three convenient types, parallel, series and parallel-series.

It becomes evident from the aforementioned literature review that applying hydraulic hybrid technology did not address the area of passenger cars. Generally, it is applied and tested in a special vehicle application such as refuse trucks and city buses characterized by frequent start stop operation. Adding a hydraulic system to the vehicle's mechanical transmission as in parallel hydraulic hybrid will add weight, while regenerative power split systems are heavy, often complex to control and therefore difficult to realize in small to medium sized vehicles. This adds to the weight of the vehicle, thus offsetting some of the gains with regards to fuel economy making it unsuitable for use in passenger cars. A gap still exists in applying this technology to cars with the current state of the art hydrostatic pumps and motors. One reason is the limitation of maximum pressure and maximum speed of current hydrostatic pumps and motors especially variable displacement units. Furthermore, the efficiency of the current hydrostatic pumps and motors deteriorate rapidly if working under extreme conditions of high pressure and or speed. Variable displacement pumps and motors exhibit high weight and high noise levels during operations acceptable for industrial use, which need to be addressed for passenger car use.

Currently, the situation stands to be altered by the development of hydraulic units e.g. the new digital displacement machines and the floating cup principle hydrostatic units. A small constant displacement pump and motors with low weight and low noise together with the state of the art IHT installed in the Hy*d*rid allow for an increase in transmission efficiency. The ability to store braking energy can be achieved by using a medium sized accumulator. A real-time or on line simulation modeling of the Hy*d*rid is needed to explain and investigate its operation under a proposed energy management strategy. Realization of the operation and performance of the introduced Hy*d*rid drivetrain in various cycles that include an aggressive and smooth driving pattern is required and will be treated later on. Given the above, the approach in this thesis will be to explore the efficiency of the Hy*d*rid drivetrain for use in passenger cars, using detailed simulations to study its performance.

Chapter 3

Basics and Standards for the Evaluation

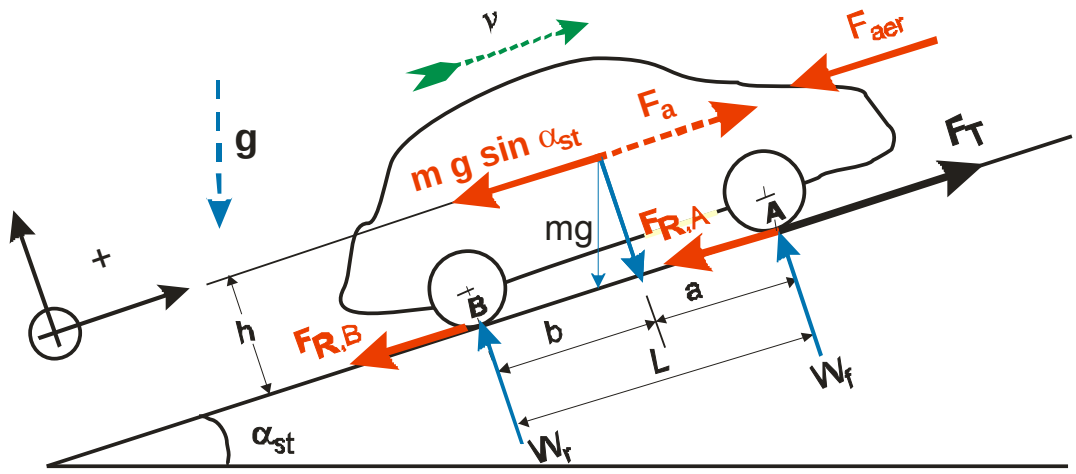

3.1 Introduction

The current study deals with different types of drivetrains, that include common parts such as the Internal Combustion Engine (ICE) and the vehicle body as well as the driving cycle used in simulation. All of the common parameters and factors such as ICE characteristics, vehicle dynamics, as well as driving cycle properties need to be discussed. The selected driving cycle is considered as assessment criterion to evaluate the performance of the introduced transmissions.

The baseline conventional vehicle used in this study is a mid-sized passenger car similar to Volkswagen Passat equipped with a six gear transmission. A Mercedes Benz turbocharged diesel engine (maximum torque 370 N m @ 1800 rpm - 2800 rpm, maximum power 120 kW @ 4200 rpm) is applied as the baseline internal combustion engine because the engine data was readily available.

The aims of describing the benchmark vehicle and engine model are to assure that the drive conditions, vehicle parameters and primary power source are the same for all simulation models built.

3.2 Simulation Approach

Throughout this research work, DSH*plus* 3.6.1 software was used to build different drivetrain simulation models. DSHplus software can be used for a variety of systems and industrial applications, having tools for modelling and simulating the hydraulic and mechanical parts of driveline systems. These tools include different technical libraries such as hydraulic, pneumatic, thermo-hydraulic, mechanical, control or electric components. DSH software is optimized for ease of use and speed of calculation for different systems building. It is integrated with source codes and code generation products, which enables the design and testing of controllers in real-time. DSH*plus* models can be converted to C++ code with real-time operation, to enable testing of embedded controllers using hardware-in-loop (HIL) tests instead of hardware prototypes. In all built drivetrain simulation models, components loss data and efficiency maps are loaded to each component element.

3.3 Internal Combustion Engine

Energy is needed to propel an automobile. This requirement for energy is in most cases covered by the conversion of chemical energy from fossil fuels to mechanical energy. Usually, an Internal Combustion Engine (ICE) is used in the vehicle; therefore, it is necessary to know the properties of the engine when developing the introduced drivetrains and their control. The significant steady-state characteristics of the diesel engine are the torque and power behaviours as a function of its rotational speed.

The common prime mover used in the simulation models is a direct injection diesel engine. The engine efficiency map is derived from the data of the OM 639 diesel engine of the Mercedes Benz A-class [63]. The maximum engine power is 120 kW at 4200 rpm and the maximum engine torque of 370 Nm is available over a wide range from 1800 to 2800 rpm. Engine fuel consumption map and engine characteristics are shown in Figure 3.1. The Wide Open Throttle line (WOT) represents the maximum torque at a wide open throttle for every engine speed.

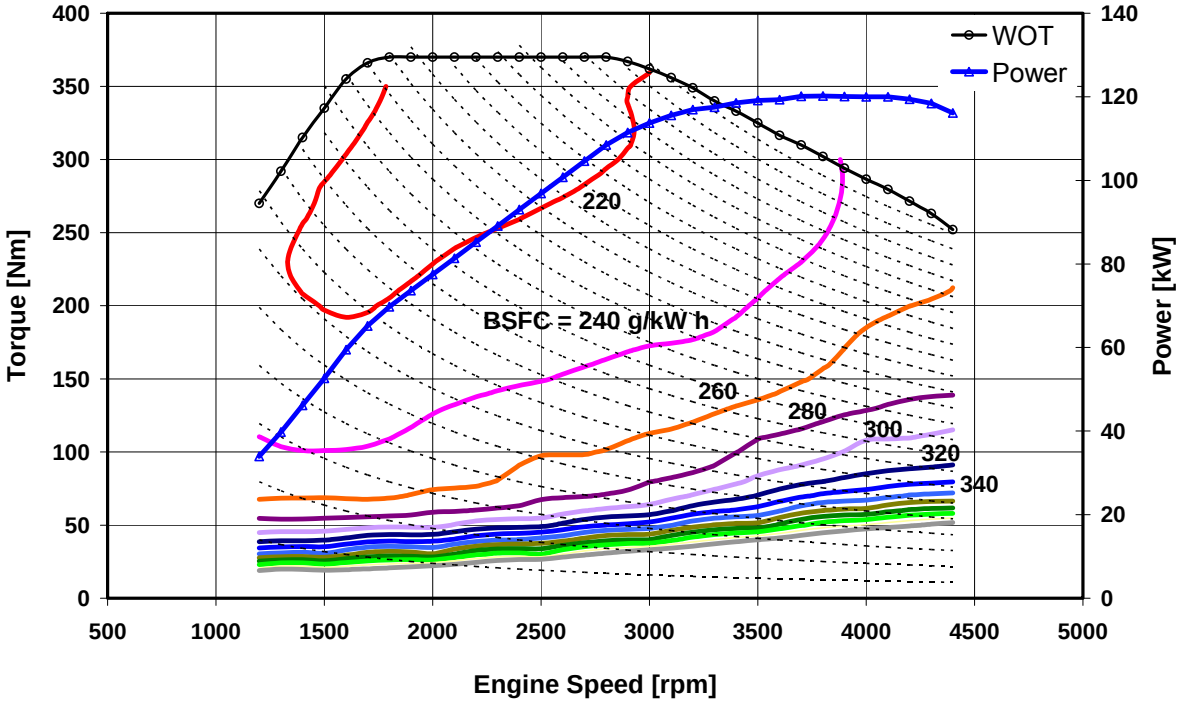

Figure 3.1: ICE Fuel consumption map, torque and power characterizes.

The dashed curves of hyperbolas in the diagram stand for the lines of constant power. They are spaced apart by a step of 5 kW. The shell curves represent the lines of

constant brake specific fuel consumption. Important points in the indicated diagram are the maximum torque and power.

An engine achieves maximum efficiency when the intake of air is widely opened and the engine is running near its peak torque. Any engine will have different Brake Specific Fuel Consumption (BSFC) values at different speeds and loads. BSFC is a measure of fuel efficiency at the engine shaft. It is generally expressed in g/kW-h unit. The relation between the fuel consumption rate, BSFC, shaft brake power, and engine efficiency can be expressed as follows;

$$P_{ICE}\ [kW] = M_{ICE}\ [Nm].\omega_{ICE}\,[rad/s]/1000 \tag{3-1}$$

$$BSFC\ [g/kW\,h] = \frac{\dot{m}_f\,[g/s].\ 3600}{P_{ICE}\ [kW]} \tag{3-2}$$

$$\eta_E = \frac{P_{ICE}}{Q_f} = \frac{P_{ICE}}{\dot{m}_f\ .\ LHV_f} = \frac{3600}{BSFC\,[g/kWh].\ LHV_f\ [J/g]} \tag{3-3}$$

The Lower Heating Value (LHV_f) of the diesel fuel is 44000 *J/g* which represents the net calorific value of the burned fuel.

3.3.1 Engine Parameters und Variables

The DSH*plus* model of the engine as any other component includes some fixed parameters and variables. It includes the following parameters; engine moment of inertia, minimum and maximum speed as well as engine maximum torque, engine drag and specific fuel consumption look-up tables.

The engine model variables are the amount of fuel throttle corresponding to the pedal position as the input command denoted by [alpha] in the model. It represents the amount of fuel consumed from a fuel tank to develop engine propulsion power. The delivered engine torque depends on the throttle position and is a fraction between 0.0 and 1.0 of its maximum. The engine speed and brake torque at the engine shaft which is represented by the -*Mech*- connection shown in Figure 3.2, are considered as the engine output. The figure shows also the possible measured signals from the engine model such as engine speed (n_ICE), power and fuel consumption.

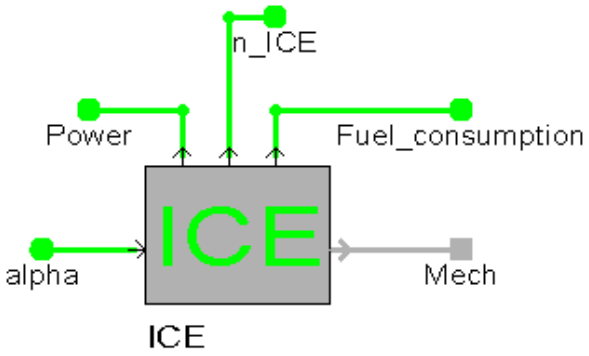

Figure 3.2: Engine model in DSHplus

3.4 Driving Cycle

Due to the increasing use of automobiles and increasing environmental pollutions, many governments in the seventies and the eighties forced the automobile manufacturers to develop vehicles with higher efficiency and lower emissions, which the establishment of emission laws. Connected with these laws the need for test procedures arose to compare several automobiles by a standard driving cycle.

A driving cycle represents certain driving patterns and is described by means of a velocity-time table. The track that is to be covered is divided in small time-steps, mostly seconds. The acceleration during a time-step is assumed to be constant. As a result the velocity during a time-step is a linear function of time. Because velocity and acceleration are known for each point of time, the required power as a function of time can be determined analytically.

The standard test cycle used in the simulation models is the NEDC. It is mostly used by the European countries for the certification of passenger cars and light trucks, as it is supposed to represent the typical usage of a car in Europe. The cycle consists of two main parts, Urban Driving Cycle (UDC) and Extra-Urban Driving Cycle (EUDC). UDC and EUDC were designed to represent city and highway driving conditions respectively. As shown in *Figures 3.3*, the total cycle duration is 1180 seconds, in which 780 seconds of 4.052 km urban trip at an average speed of 33.6 km/h and at a maximum speed of 50 km/h. The UDC includes four equal urban segments called ECE-15 to obtain an adequate driving distance and temperature. The EUDC cycle illustrates the aggressive pattern and high speed driving of the cycle on a flat road. It

takes 400 seconds for 6.955 km in highway drive with an average speed of 62.6 km/h and maximum speed of 120 km/h [64].

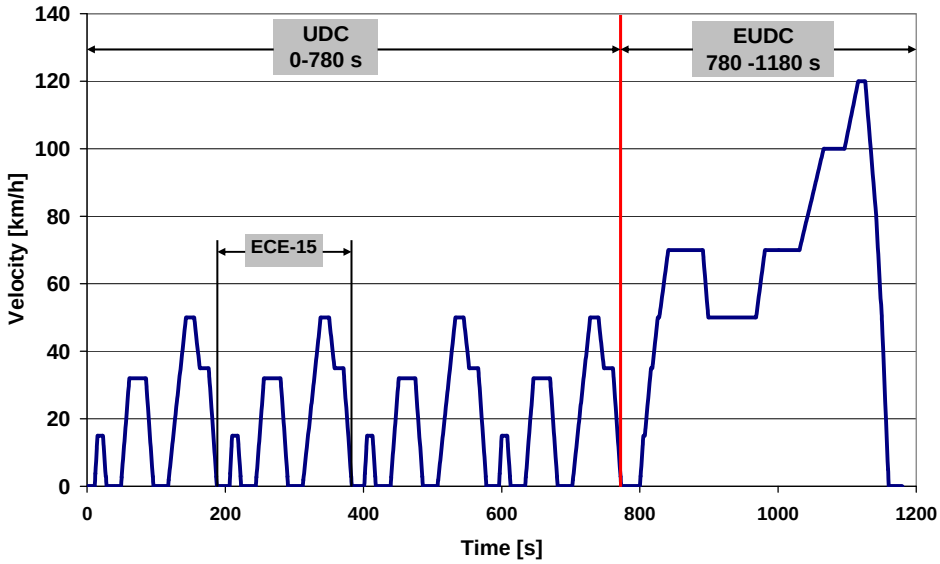

Figure 3.3: Profile and velocity patterns of the NEDC [64]

The driving cycle will be used in the simulations to define driver requirements and is also considered as an assessment criterion to evaluate the drivetrain fuel consumption and CO_2 emissions. The driver model uses the difference between test cycle velocity and the actual vehicle velocity to develop the appropriate error signal fed to the controller.

It can be concluded that applied test cycles differ significantly in terms of relative amount of the energy available for regenerative braking, average velocity, and magnitude of the segments featuring steady-state operation of the powertrains.

3.5 Vehicle Performance Requirements

The requirements of the drivetrain components such as engine and transmission are based upon vehicle requirements. In order to choose the components size and speed ratios, the demands of the drive vehicle must be specified. The performance requirements are acceleration and maximum speed, which result in a traction of the drivetrain.

3.5.1 Baseline vehicle specifications

To be able to determine the drivetrain components which fulfil performance requirements, the vehicle must be specified in terms of vehicle geometrical parameters and engine characteristics, which are summarized in *Table 3-1*.

***Table 3-1**: Baseline vehicle and engine parameters*

Parameter		**symbol**	**Value**	**Unit**
Curb mass		m_F	1554	*kg*
Payload		m_p	650	*kg*
Towing capacity	Braked	m_T	1800	*kg*
	Un-braked		750	*kg*
Height of Center of Gravity (CG)		*h*	0,65	*m*
Distance from CG to front and rear axle		*a, b*	1.2 , 1.3	*m*
Frontal area		A_f	2.26	m^2
Air drag coefficient		C_d	0.28	-
Rolling resistance coefficient (firm Asphalt)		f_r	0.008	-
Wheel radius		r_w	0.315	*m*
Maximum vehicle velocity		$v_{F,max}$	220	*km/h*

All of the initial conditions and input data such as vehicle parameters and command velocity from the driving cycle will be the same for simulation models of the introduced transmissions in the thesis.

Comparison of the data for the various models of the baseline vehicle is represented in *Table 3.2*. It indicates that automatic transmissions and all-wheel drive options increase the specific fuel consumption and the CO_2 emission of the vehicle. This is foremost due to the reduced efficiency of the 4WD-transmission compared to the manual. Furthermore, the increased weight of especially all-wheel drive option further deteriorates the fuel economy and the CO_2 emissions.

***Table 3.2**: Influence of transmission options on vehicle's fuel consumption* [62]

Fuel	**Transmission type** Automatic Transmission (AT) vs Manual transmission (MT)	**Additional weight**	**% of fuel consumption and CO_2-emissions**
Petrol	AT compared to MT	+ 34 kg	+ 3 to 7 %
	4WD compared to 2WD	+103 kg	+ 7 %
Diesel	AT compared to MT	+24 kg	+ 7 to 12 %
	4WD compared to 2WD	+100 kg	+ 14 %

3.5.2 Longitudinal vehicle dynamics

When a vehicle is in motion, different forces are acting upon it. To initiate and maintain vehicle motion, a thrust force is required at the tires. This force is usually referred to as the tractive force, which is required to overcome resisting forces during vehicle motion.

The major components of the resisting forces to be overcome by the tire traction force are comprised of aerodynamic drag, rolling resistance, inertia force, and grade force as shown in the free body diagram of Figure 3.4. The vehicle dynamics are adapted here as a lumped mass model.

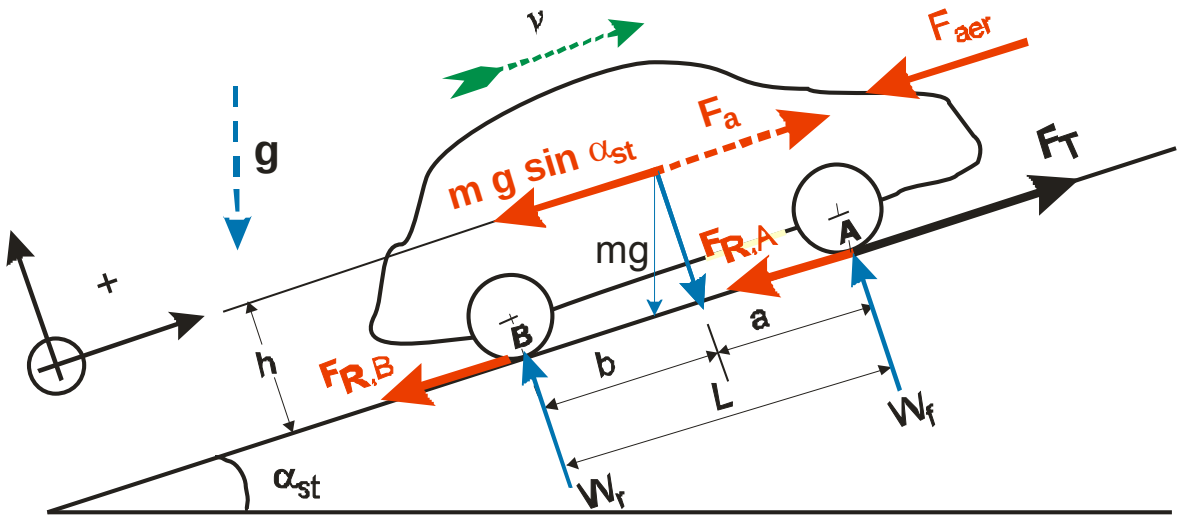

Figure 3.4: Free body diagram of the longitudinal dynamic forces acting on a vehicle

The analysis considers only the major forces that occur in the direction of vehicle motion, and do not take into account perpendicular forces on traveling surface. The traction force F_T required at the drive wheels is made up of the driving resistance forces [65], and is defined as

$$F_T = F_{Aer} + F_R + F_{Gr} + F_a \tag{3-4}$$

The aerodynamic drag on the vehicle is a function of vehicle velocity squared, air density, vehicle frontal area, and coefficient of drag. The rolling resistance force is a function of vehicle weight, rolling resistance coefficient. The Grade force is a function of vehicle weight and grade angle. While the inertia force is equal to effective vehicle mass multiplied by the vehicle acceleration, then:

$$F_T = \frac{M_T}{r_R} = \frac{1}{2}\,\rho_L\, c_d\ A_f\ v_F{}^2 + m_g\ g\ (f_R\ \cos\alpha_{St} + \sin\alpha_{St}) + \lambda\ m_g\ a \qquad (3\text{-}5)$$

The air drag force is the dominant at intermediate and high speeds because the required power to overcome the air drag force is proportional to the car velocity raised to power three.

It is known that a point exists beyond which, no matter how much torque an engine can provide to the vehicle's wheels, there will be no effect on performance. At this point the developed force only results in spinning of tires and does not overcome resistance nor accelerate the vehicle. For a 4WD vehicle, the gross vehicle weight (W_g) equals the normal load force (N).

The ability of a vehicle to develop traction depends on the weight on the drive wheels and coefficient of friction between wheels and road surface. Force required to spin the tyres (wheels begin to slip) known as the maximum tractive effort is given by,

$$F_{T,\max} = \mu_p\,.N\ =\ \mu_p\,.W_g\ .\cos\alpha_{st} \qquad (3\text{-}6)$$

Pushing fuel pedal down further than to get more force, the wheels will start spinning and lose grip and the traction force drops below the maximum amount. So, for maximum acceleration the traction force must be just below the friction threshold. Since installed engine capacity is limited, the propulsion capability of a vehicle is constrained.

Hence, the road performance can be expressed as follows,

$$m_g\ \lambda\ \dot{v} = F_{T,\max} - W_g\, f_R \cos\alpha_{St} - W_g \sin\alpha_{St} - \frac{\rho_a}{2}\ c_d\ A_f\ v_F{}^2 \qquad (3\text{-}7)$$

The power required at the wheel's axles is,

$$P_T = F_T\ .\ v_F$$

$$P_T = \left(\frac{\rho_L}{2}\ c_d\ A_f\ v_F{}^2 + W_g\,(f_R\ \cos\alpha_{St} + \sin\alpha_{St}) + m_F\ \lambda\ a\right).v_F \qquad (3\text{-}8)$$

DSH*plus* simulation model, shown in Figure 3.5, was built to calculate the demand load and power at the vehicle wheel during the NEDC cycle.

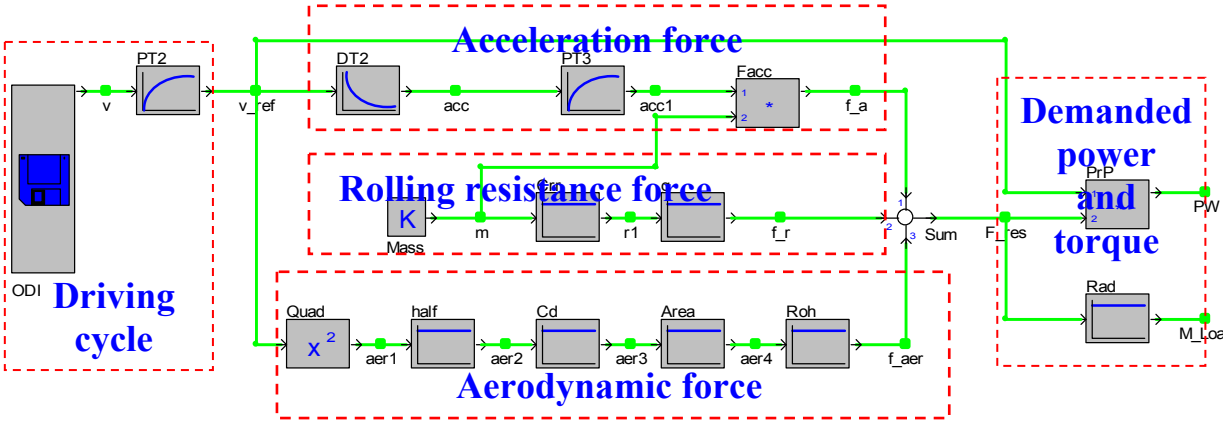

Figure 2.5: Longitudinal vehicle dynamics simulation model of the baseline vehicle

Load forces as well as the demand power that was required to overcome the resistance forces are shown in Figure 3.6. The load force curve is a parabolic curve, this because the load force is proportional to the velocity square. At maximum speed of 220 km/hr, power required at the wheels is about 105 kW as shown in the figure.

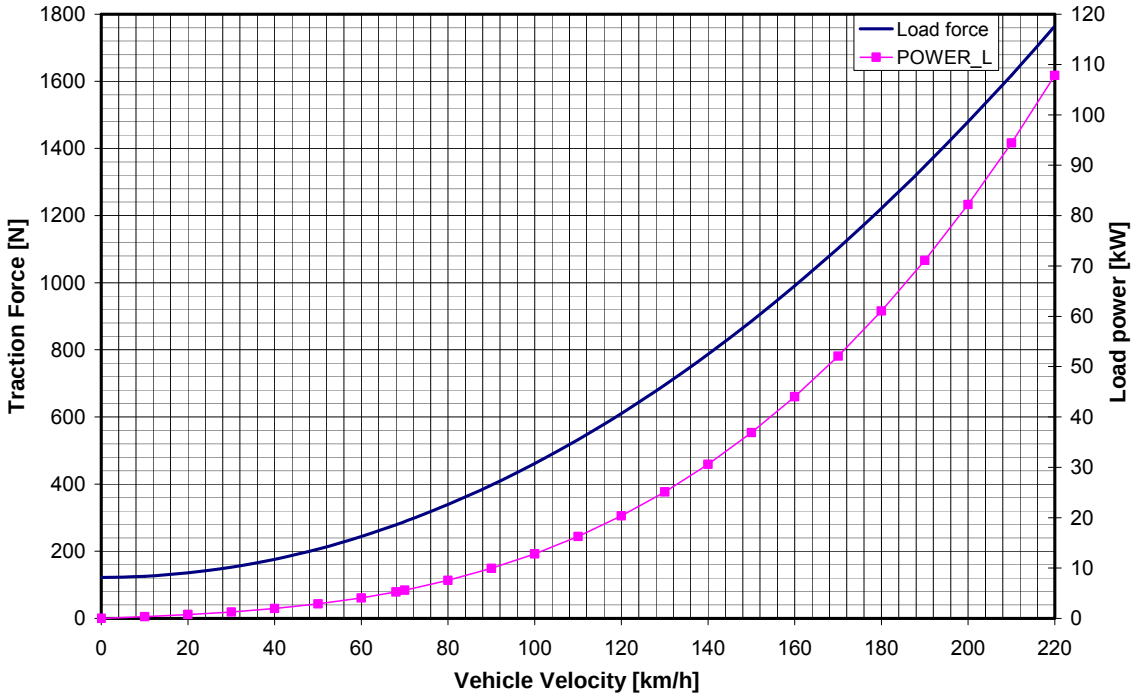

Figure 3.6: Road load force and power at the vehicle speed range

Simulation results of the longitudinal vehicle dynamics model including load force and load torque as well as the load power required at wheels to overcome the resistance forces along the NEDC cycle are shown in Figure 3.7. Positive load power occurs during acceleration and constant driving speed. It will be negative in deceleration phases, and then considered as lost power during braking mode.

The figure reveals that, the wheel torque ranges between -657 Nm and +557 Nm during of the NEDC. This is much lower than the maximum torque (4000 Nm at slope 38 %) for which the drivetrain must designed.

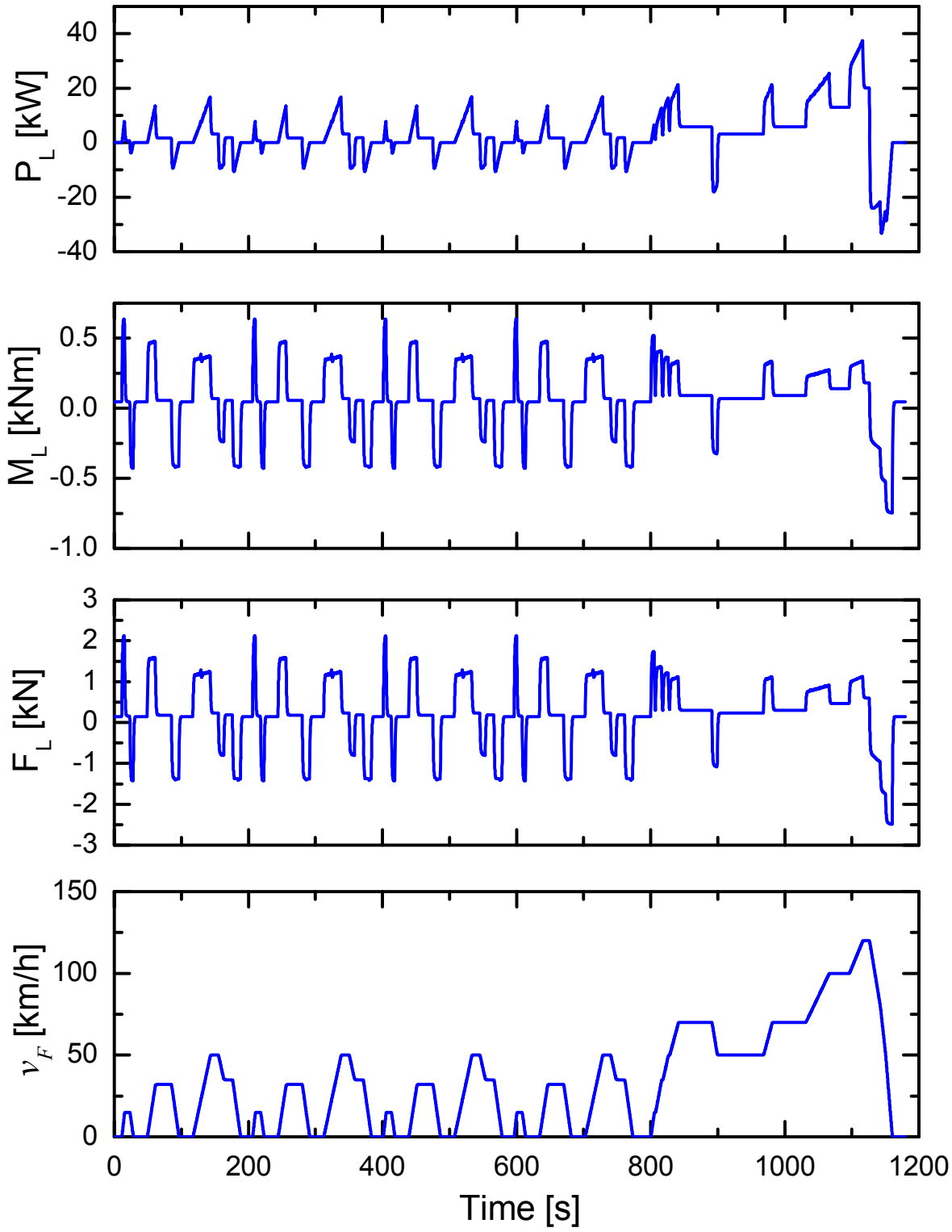

Figure 3.7: Load force, moment and power of the baseline vehicle during the NEDC cycle

3.5.3 Acceleration performance

The baseline vehicle can pull away from standstill, climbing up a hill with a 12 % slope being fully loaded vehicle and including the maximum allowable trailer load. Equation (3.4) can be rewritten in the form of Riccati's differential equation as follows;

$$dv = \left[\left(\frac{F_{T,\max} - W_g \left(f_R \cos\alpha_{St} - \sin\alpha_{St} \right)}{\lambda m_g} \right) - \left(\frac{\rho_{L\ c_W\ A}}{2\lambda m_g} \right) v_F{}^2 \right] dt \tag{3-9}$$

On integration of equation (3.9) the theoretical time or the velocity at any instant can be expressed as follows,

$$t = \frac{1}{\omega} \ln \left(\frac{\sqrt{\frac{F_{T,\max} - W_g . \left(f_R \cos\alpha_{st} - \sin\alpha_{st} \right)}{\lambda . m_g}} + \sqrt{\frac{\rho . c_w . A_f}{2\ \lambda m_g}} .\ v_F}{\sqrt{\frac{F_{T,\max} - W_g . \left(f_R \cos\alpha_{st} - \sin\alpha_{st} \right)}{\lambda . m_g}} - \sqrt{\frac{\rho . c_w . A_f}{2\ \lambda . m_g}} .\ v_F} \right) \tag{3.10}$$

$$\text{Where, } \omega = 2 \sqrt{\frac{\rho . c_w . A_f . \left(F_{T,\max} - W_g . \left(f_R \cos\alpha_{st} - \sin\alpha_{st} \right) \right)}{2 \left(\lambda . m_g \right)^2}} \tag{3-11}$$

$$\text{And, } v = \sqrt{\frac{F_{T,\max} - W_g . \left(f_R \cos\alpha_{st} - \sin\alpha_{st} \right)}{\frac{1}{2} \rho . c_w . A_f}} . \tanh \left(\frac{\omega}{\lambda . m_g} t \right) \tag{3-12}$$

With the parameters mentioned in *Table 3-1*, and assuming flat road. The vehicle will take 9.7 seconds to accelerate from 0 to 100 km/h (27.8 m/s).

Chapter 4

Mechanical Drivetrain

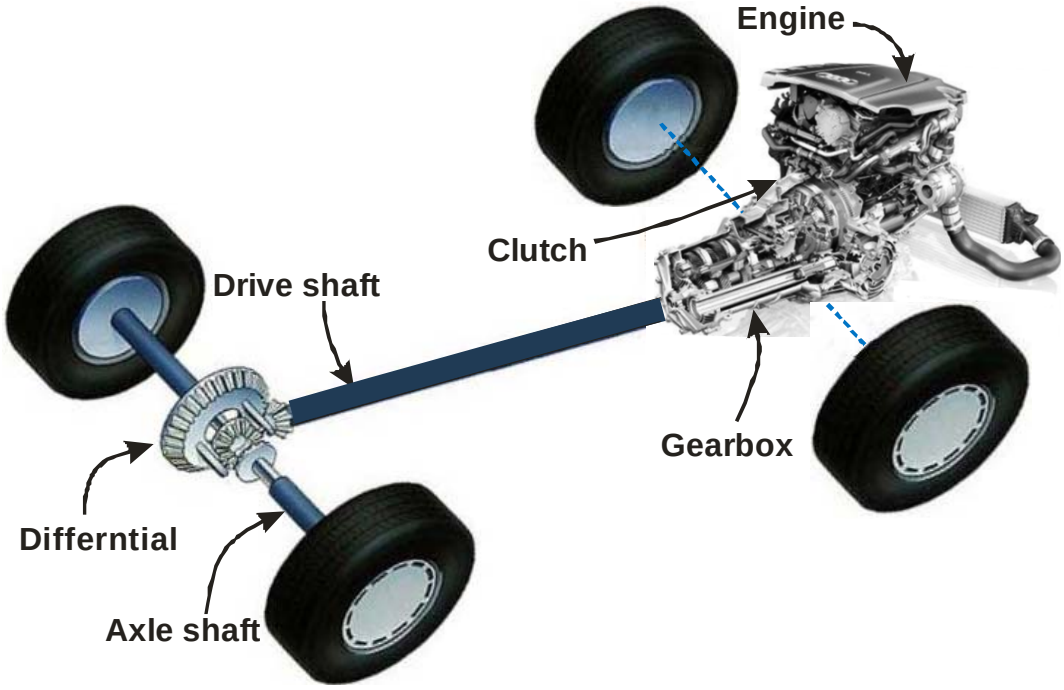

4.1 Introduction

The mechanical drivetrain is the oldest transmission used in automobiles. The first cars powered by internal combustion engines running on fuel appeared in 1806, which led to the introduction of the modern gasoline or petrol-fueled internal combustion engine in 1885 [66].

The transmission introduced in this chapter is a standard 6-speed semi-automatically shifted transmission as used in the VW mid-sized Passat. It is based on manual transmissions which include automatic clutches in order to synchronize, connect or disconnect the engine from the transmission gearbox automatically while the driver selects the proper gears.

The mechanical transmission installed in the mid-sized baseline vehicle is considered as the reference transmission for this study. The aim of this chapter is to build a simulation model to assure that all common circumstances, vehicle parameters and operating conditions will lead to the same data of fuel consumption and CO_2 emissions values announced by the manufacturer. The published data by the manufacturer is based on the New European Driving cycle (NEDC). The resulting fuel consumption values and CO_2 emissions from the simulation in two driving schemes i.e. the city (UCD) and highway driving (EUCD) cycles will be used in comparison with the introduced different hydraulic drivetrains in this work.

In this chapter, the basic dynamic relations for the mechanical drivetrain transmission are introduced. The velocity range that can be obtained for each gear over the engine speed range of the geared transmission is also explained. The performance of the baseline vehicle with regards to the maximum traction force and power of the mechanical transmission against the road load resistance is calculated and presented. Simulation model for the whole drivetrain including driver model and controller, followed by simulation results and comparison with the manufacturer's data is introduced.

4.2 Drivetrain Components

The standard mechanical drivetrain consists basically of mechanical clutch, gearbox, drive shaft (propeller shaft), final drive and wheel axle shafts to transfer the

engine torque to the vehicle wheels as shown in Figure 4.1. In a manual transmission, the driver disconnects the engine from the transmission input with the clutch pedal while selecting the gear via the gear lever or while braking and synchronizes, or connects the engine back to the transmission during propulsion. The torque from the engine is converted via the gearbox and the differential before applying it to the vehicle's wheels.

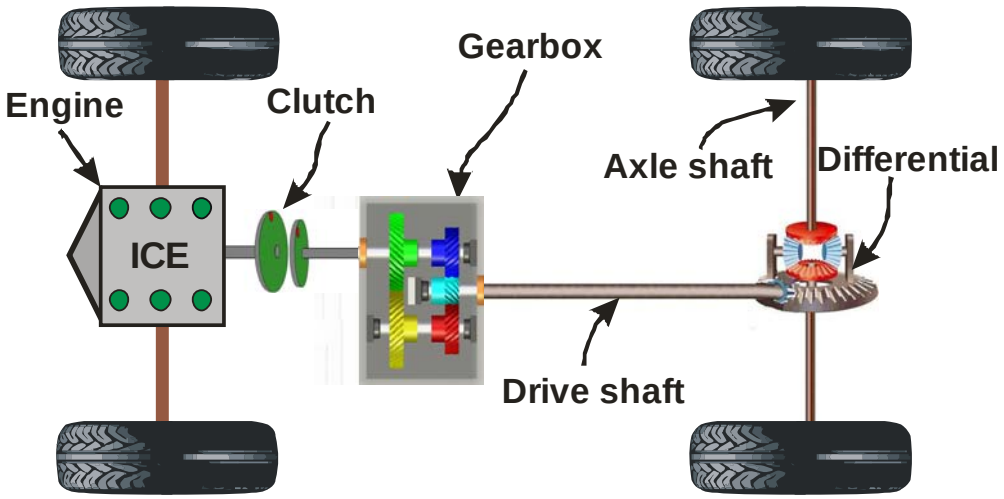

Figure 4.1: Mechanical drivetrain components layout

The all-wheel drive versions of the mid-sized Passat described here have six forward speeds and one reverse gear. The gear-shift ratios as well as moment of inertia and mechanical efficiencies for each gear are listed in *Table 4-1* [67].

***Table 4-1**: Gear ratios of the mid-sized baseline vehicle*

Gear	**Gear ratio**	***Inertia* [kg.m^2]**	***Efficiency***
1st	3.46	0.145	0.966
2nd	2.05	0.102	0.967
3rd	1.30	0.079	0.972
4th	0.91	0.057	0.973
5th	0.90	0.034	0.97
6th	0.76	0.03	0.98
Final drive - 1/4 Final drive - 5/6	4.12 3.33	0.135	0.98
Reverse	3.98	0.135	0.98

The largest gear (6th gear) is generally designed to attain the maximum vehicle velocity. While the minimum gear (1st gear) is designed to sustain the maximum traction required at the wheels e.g. for climbing ability and the smallest possible driving speed with an engaged clutch [68].

The forward velocity v_F of the vehicle is proportional to the angular velocity of the engine, and can be expressed in terms of transmission gear ratios and wheel radius as follows;

$$v_F = \frac{2\pi n_{ICE} . r_w}{g_i g_f} \tag{4-1}$$

Generally, the internal combustion engine cannot operate below a minimum engine speed n_{min}. Consequently the vehicle cannot move slower than a minimum speed v_{min} while the engine is connected to the drive wheels. At starting and stopping stages of motion, the vehicle needs to have speed less than v_{min}. So, a clutch or torque converter must be used for starting, stopping, and gear shifting.

A gear-speed plot can be drawn by using equation (4-1) as shown in Figure 4.2. The angular velocities associated to maximum and minimum engine speed are indicated by horizontal dashed lines. The circles drawn at the intersection points of gear lines with the vehicle velocity represent the shifting speed to the subsequent smaller gear.

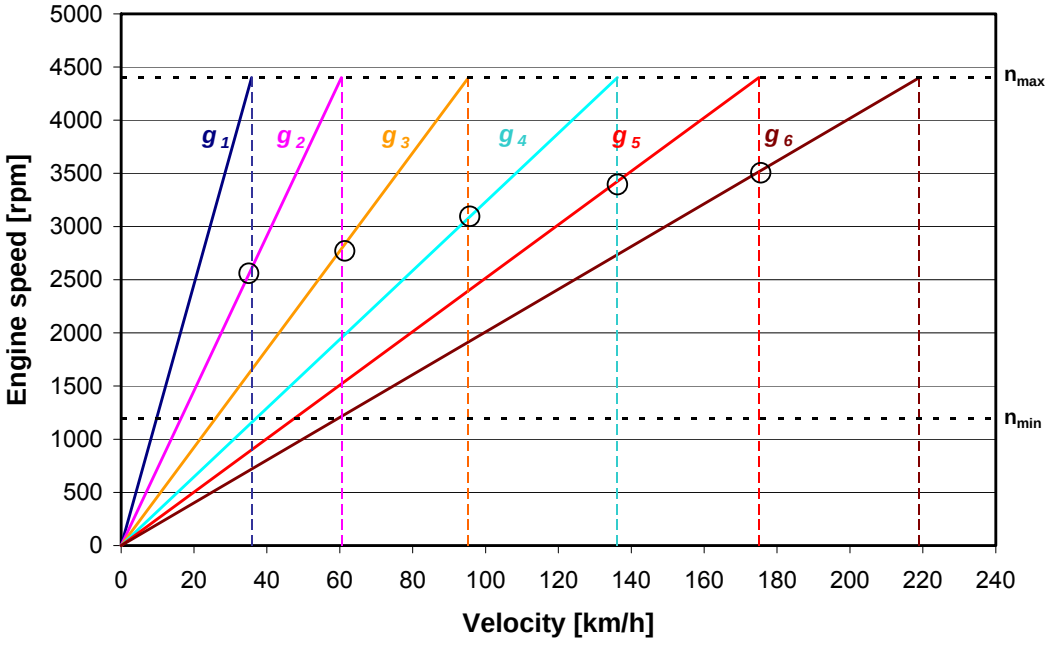

Figure 4.2: Speed-velocity plot for the stepped mechanical driveline

The figure indicates also that the speed margin between maximum speed and shifting speed increases with shifting-up to the next gear.

The larger transmission gap at lower velocity range is tolerated in passenger cars due to the high surplus power being required to accelerate the vehicle [68].

4.3 Mechanical Transmission Analysis

The driveline dynamics model includes the rotational dynamics of dry clutch and gearbox combination, which receives engine torque and delivers tractive torque to the vehicle wheels through the differential and propelshaft. The dynamic equations are used in the different elements of the simulation model that was built in DSH*plus*.

Since the engine is responsible for supplying drive power to the mechanical transmission, the provided ***engine power*** can be expressed as;

$$P_E = M_{ICE}\ \omega_{ICE} \tag{4-2}$$

The engine power is transferred to the transmission through a ***clutch***. The widely used mechanical clutches in mechanical stepped transmissions are in the form of dry single-plate clutches [68]. The torque delivered through the clutch is the input to the transmission and can be determined by application of Newton's second law for rotational motions;

$$M_c = M_E - (J_E + J_c).\ \dot{\omega}_{ICE} \tag{4-3}$$

Depending on which gear is selected, the input torque to the gear box is amplified by the i^{th} gear ratio before being applied to the differential, where ***i*** takes the values from one to six.

Gear ratio; $g_i = \dfrac{Z_{out,i}}{Z_{in,i}} = \dfrac{n_{in,i}}{n_{out,i}} = \dfrac{M_{out,i}}{M_{in,i}}$ (4-4)

The amplified torque at the output of the transmission is decreased by inertial losses in the gears and shafts. If the transmission inertia is characterized by its value on the input side, the output torque of the drive shaft can be approximated by the expression;

$$M_d = (M_C - J_{gi}.\ \dot{\omega}_{ICE})\ g_i \tag{4-5}$$

Similarly, the torque delivered to the ***axles*** to accelerate the rotating wheels and provide tractive force at the ground is amplified by the ***final drive or differential*** ratio

with some reduction from the inertia of the driveline components between the transmission and final drive.

Commonly used models of the differential are reduced to one shaft and not two as in a real vehicle, and can be modeled as a planetary gear set arrangement [69]. Then the expression of axle torque is;

$$M_{axle} = (M_d - J_d \,.\, \dot{\omega}_d)\; g_f \tag{4-6}$$

Now, the torque from the engine (i.e. at the crankshaft) is converted via the gear and differential before being applied to the wheels. The gearing multiplies the torque from the engine by a factor depending on the gear ratios. Hence the wheel torque can be expressed as;

$$M_T = F_w \,.\, r_w = M_{axle} - J_w \,\dot{\omega}_w \tag{4-7}$$

The angular velocity and acceleration of the engine, transmission, and driveline are related to that of the wheels by the gear ratios as follows;

$$\dot{\omega}_E = g_i \;\dot{\omega}_d \text{ , and } \dot{\omega}_d = g_f \;\dot{\omega}_w \text{, then } \dot{\omega}_E = g_i \, g_f \,\dot{\omega}_w \tag{4-8}$$

Recognizing that the vehicle linear acceleration can be expressed in terms of the wheel angular acceleration by the relation;

$$\dot{\omega}_w = \frac{a}{r_w} \tag{4-9}$$

To get the tractive force available at the ground, the equations from (4-3) to (4-9) should be combined while eliminating all intermediate variables to get the traction force on the wheel.

$$F_T = \frac{M_{ICE}\; g_i \, g_f}{r_w} - \left[(J_E + J_c + J_{gi})\; g_i^{\,2}\, g_f^{\,2} + J_d \, g_f^{\,2} + J_w \right] \frac{a}{r_w^{\,2}} \tag{4-10}$$

The effect of mechanical losses can be approximated by adding an efficiency value to the first term on the right-hand side of equation (4-10) to get the final form;

$$F_T = \frac{M_{ICE}\; g_{t,}\, g_f \;\eta_t \;\eta_f}{r_w} - \left[(J_E + J_c + J_{gi})\, g_i^{\,2}\, g_f^{\,2} + J_d \, g_f^{\,2} + J_w \right] \frac{a}{r_w^{\,2}} \tag{4-11}$$

Equation (4-11) shows that the equivalent inertia of each component is "amplified" by the square of the numerical gear ratio between the component and the wheels. For convenience, to obtain a simplified equation the rotational inertias from

Eq. (4-10) are often lumped in with the mass of the vehicle. Here the total rotating parts inertia is reduced to the drive axles for a gear (*i*) and can be expressed as;

$$J_{R,i} = J_w + J_d\, g_f^{\,2} + (J_E + J_{gi})\, g_i^{\,2}\, g_f^{\,2} = m_{r,i}\, r_w^{\,2} \tag{4-12}$$

$$F_T = \frac{M_E\; g_{t,f}\; \eta_t\; \eta_f}{r_w} - m_{r,i}\; a \tag{4-13}$$

Thus Eq. (4-13) provides an expression for the tractive effort which is obtained from the engine to overcome road load forces and accelerate the vehicle. It has two components; the first term on the right side represents the steady-state tractive force available from the engine at the ground to overcome the road load forces of aerodynamics and rolling resistance, to accelerate, or to climb a grade, while the second term represents the "loss" of tractive force due to the rotating inertia of the engine and drivetrain components.

Knowing the available tractive force at the wheels, it is now possible to predict the acceleration performance of a vehicle. The expression for the acceleration must consider all the forces that occur on the drive wheels, as expressed in chapter 3, in equation 3-4, which takes the form;

$$m_g\; a = F_T - F_R - F_{Aer} - F_{Gr} \tag{4-14}$$

Again combining equations (4-13) and (4-14) eliminating common variable leads to;

$$(m_g + m_{r,i})\, a = \frac{M_{ICE}\; g_i\, g_f \eta_t}{r_w} - F_{Aer} - F_R - F_{Gr} \tag{4-15}$$

Referring to the complete form of the vehicle's equation of motion represented by equation (4-15), there are no convenient explicit solutions for acceleration performance. Except for the road gradient term, all other forces vary with speed, and must be evaluated at each speed. An equation as shown above can be used to calculate acceleration performance at specified speeds. The combination of the two masses is an "effective mass" and the ratio of $(m_g + m_{r,i})/m_g$ is the "mass factor". The mass factor will depend on the operating gear. A representative form for the mass factor (λ) is often taken as introduced in [70];

$$\lambda = 1 + 0.04 + 0.0025\; g_i^{\,2} g_f^{\,2} \tag{4-16}$$

The acceleration of a vehicle is determined by the net force and the vehicle's mass. The net force is the difference between the traction force and total resistance force on the vehicle.

$$a = \frac{1}{\lambda . m_g}\left(\frac{M_{ICE}\ g_i\, g_f \eta_t}{r_w} - F_{Aer} - F_R - F_{Gr} \right) \tag{4-17}$$

4.3.1 Driving performance

In mechanical transmission, the required conversion of characteristics between engine and drive wheels takes place through the transmission and final drive gear ratios. The maximum tractive effort available from the engine at steady drive conditions for different gear ratios can be plotted using equation 4.13, as shown in the traction force diagram of Figure 4.3.

The diagram demonstrates that the road resistance curve intersects with the maximum traction curve at the point of maximum vehicle velocity (220 km/h) being obtained by driving the vehicle in the 6th gear. Possible vehicle operating points are indicated by the intersection of the road resistance for different gradient and traction force curves. Moreover, the diagram clearly indicates that, in low gears where the gear ratio is high, a lot of torque on the vehicle's wheels can be delivered but not much speed. While in high gears, more speed can be obtained at the wheel but less torque.

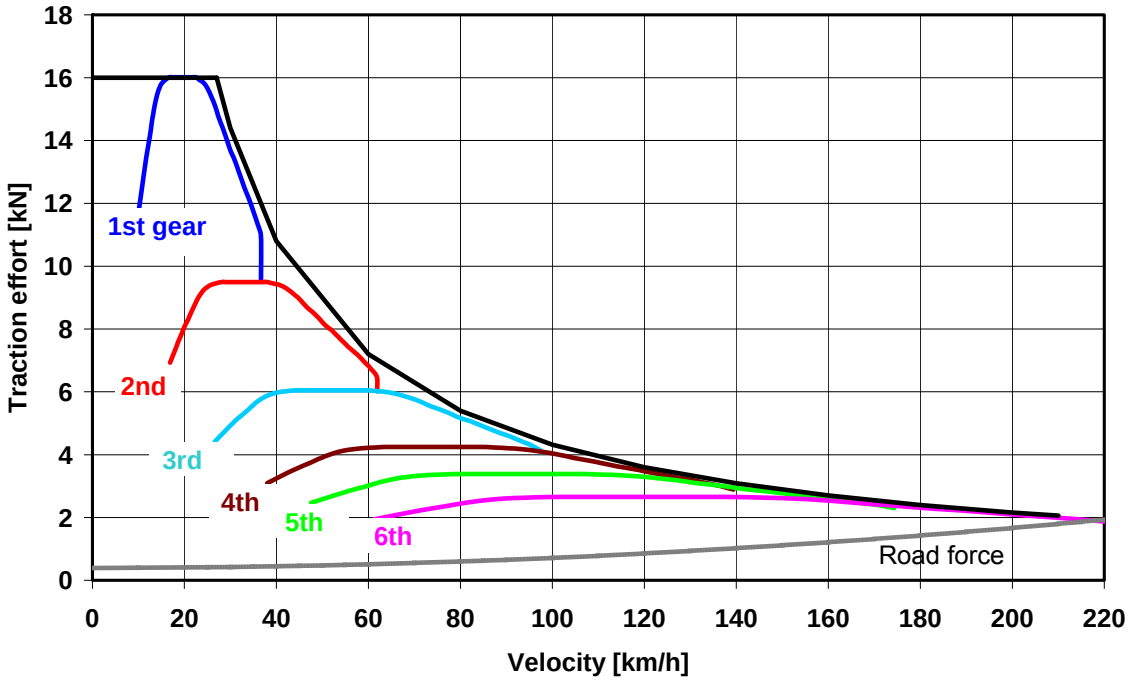

Figure 4.3: Maximum available traction force of geared transmission

The minimum velocity margin for each gear can be obtained by the following equation;

$$v_{\min,i} = \frac{2\pi n_{ICE,\min} . r_w}{g_i g_f} \tag{4-18}$$

Multiplying the respective traction force with the particular driving speed, the full load or maximum power available at the wheel hub at different gears can be represented as shown in Figure 4.4. In addition, demand power necessary for driving at constant velocity over plane road is also indicated.

It is evident from the characteristic of the diagram that the vehicle attains its maximum speed approximately at maximum engine power.

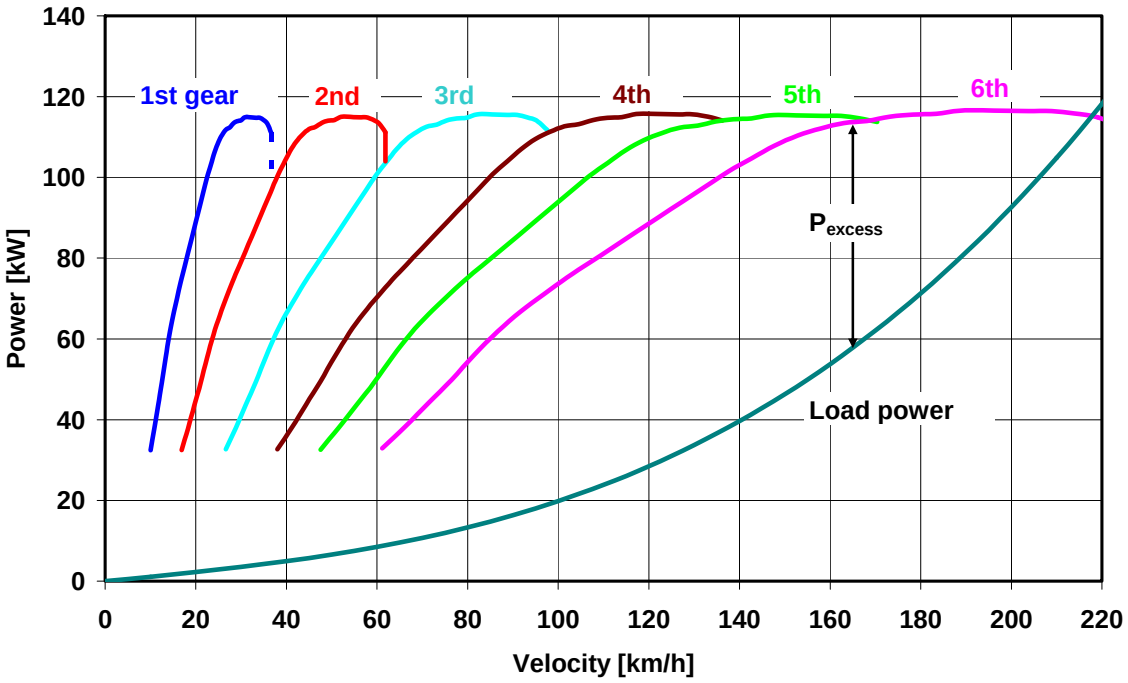

Figure 4.4: Maximum available traction power of the mechanical drivetrain

In both figures (4-3) and (4-4) the difference between the available gear traction force and the demand force is the excess traction force that will be used to climb a road or to accelerate the vehicle. This is also correct for the tractive power and can be represented as follows;

$$p_{ex} = F_{ex} . v_F = \left(F_{T,i} - F_{dem}\right) v_F \tag{4-19}$$

As far as the rotational masses (i.e. $\lambda > 1$) are concerned, the maximum traction force and power will be decreased by a small amount.

4.4 Mechanical Drivetrain Simulation Model

To build a simulation model, the cycle-driver model that controls the clutch pedal gear shifts should be first defined at particular points in time during the NEDC cycle. The expert from the Organization of Motor Vehicle Manufacturers (OICA) has prepared and introduced specific gear shift strategy in line with the requirement of the regulation, where in paragraph 2.3.2 of Annex 4 of vehicles equipped with manual and semi-automatic-shift gearboxes shall be tested by using the gears normally employed for driving as an alternative to the gear shift points as specified in *Table 4-2*. The values used in shift points allow manufacturers to examine produced automobiles during the NEDC driving cycle [71].

Table 4-2: *Manufacturers' specific gear shifting strategy* [71]

Gear	1st gear	2nd gear	3rd gear	4th gear	5th gear	6th gear
Velocity [km/h]	$0 < v < 15$	$15 \leq v < 35$	$35 \leq v < 50$	$50 \leq v < 70$	$70 \leq v < 100$	$100 \leq v \leq 120$
Percentage time sharing during steady speeds	8.2	21.8	22.7	15.6	22.7	9.0

The data represented in *Table 4-2* are plotted on the NEDC indicating the gear shift strategy for city and highway parts of the cycle is indicated in Figure 4.5.

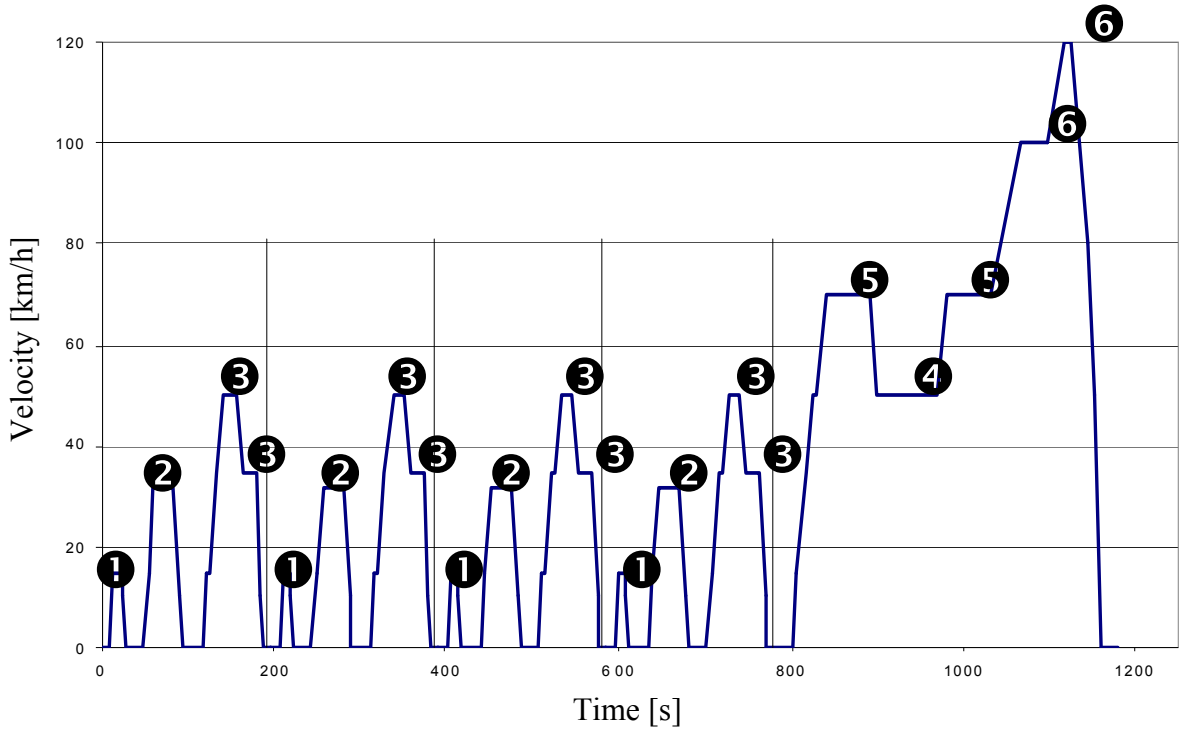

Figure 4.5: The manufacturer specific gear-shift strategy during NEDC [71]

A simulation model using the mechanical and control elements library in DSH*plus* environment was built as shown in Figure 4-6. The simulation model includes a pre-scribed shift points for each level of vehicle speed. It's considered as a semi-automatic transmission combination using dry clutch. Its structure is similar to automatic transmission performance with elimination of a torque converter. The model includes a vehicle driver, controller, ICE, dry clutch, automated-manual shaft transmission, brake system, complete vehicle longitudinal dynamics with tire-road interface characterization. There is no regenerative system in the presented model.

The driver model includes an implicit vehicle velocity controller, with driver velocity error and Proportional-Integral-Derivative (PID) capability, and a drive cycle to provide a vehicle input command. The driver model uses the difference between the simulated vehicle velocity and a commanded vehicle velocity to generate either driving signal to the engine throttle controller or braking signals to the brakes. Command signals are also provided to the clutch and transmission system to drive with the proper gear. In particular, the controller provides engine, clutch and transmission control during shifting or braking.

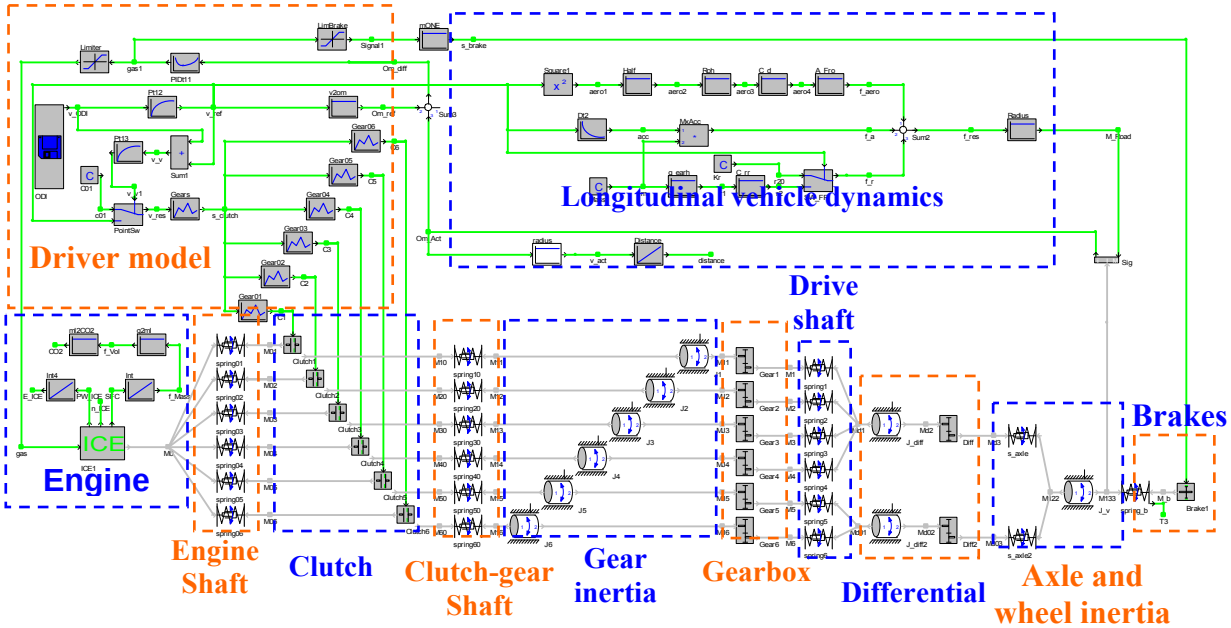

Figure 4.6: DSHplus simulation model for the mechanical drivetrain

Engine controller: It includes throttle with a variable gain PID controller and limiter to provide a specified fuel signal to the engine based on the command from the driver

controller. Also included in the throttle controller are the Wide Open Throttle (WOT) operating logic and the engine idle speed to constrain the engine speed.

Clutch: The clutch uses friction to transmit torque to the gearbox. The clutch will be commanded to engage when engine speed is sufficient and the transmission in gear. The clutch will be commanded to disengage during up / down-shifting, braking or in case engine speed would drop below idle speed.

Transmission controller: It determines when a shift event shall occur and selects the appropriate gear based on transmission's output speed, throttle angle, current gear and clutch state. During deceleration the clutch is disengaged, the engine is ramped to idle speed, and the controller continuous to shift the transmission to be in the proper gear when an engagement is requested. A shift command and gear change are not activated until the controller initiates a disengage signal to the current clutch. The transmission gear shift is emulated by modeling a proper delay based on experimental data.

Brakes: Brake commands are received from the driver model and send directly to the brake element connected to the wheels. While braking the clutch should be open to disconnect the engine shaft from the transmission gearbox avoiding engine stall.

4.5 Results and Discussion

Vehicle velocity, gear changes, engine operating points, as well as engine speed, torque and power consumed along the driving cycle will also be presented and discussed. A summary of fuel consumption and CO_2 resulting from the simulation model is declared and compared to the announced manufacturer data for the baseline mid-sized vehicle.

4.5.1 Engine operating points

The engine's operating points for the prescribed gear-shift mechanical transmission during the NEDC on the engine maps are depicted in Figures 4-7. The figure reveals that the operating points of the mechanical transmission are distributed on the engine map in the region of low engine efficiency. This distributed form of engine operating points is called map-based mode [72]. It shows that the engine is running at low loads, which are typical for average driving conditions in the NEDC,

requiring much less than its maximum torque. The operation of the engine at these low loads leads to high average fuel consumption.

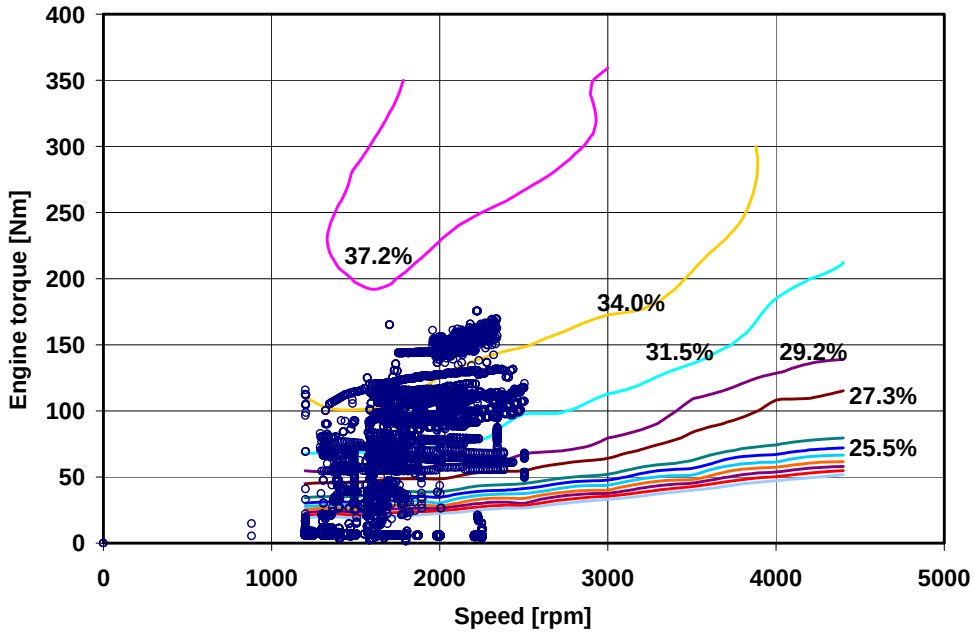

Figure 4-7: Engine operating points of the mechanical drivetrain during the NEDC cycle

4.5.2 Characteristics curves

Figure 4.8 shows some characteristic curves for the main variable of the mechanical drivetrain during the NEDC cycle. Since this thesis investigates different types of hydraulic transmissions compared to the baseline mechanical transmission and in order to be consistent with the standard sign convention, the power provided into the system (i.e. the transmission) is considered negative. Hence, the engine delivered power will carry negative sign since it represents work done on the transmission. On the other hand, restored energy during vehicle's braking is considered positive in order to clearly distinguish it from the external power supplied by the engine as treated in chapters 6 and 7.

The first diagram shows the simulated vehicle velocity tracking the reference commanded value during the mission cycle. The second diagram shows the gearbox shifting status according to driver demand. It agrees with the organization of motor vehicle manufacturers (OCIA) described in this chapter. The 3rd curve shows that the engine speed in some way follows the vehicle speed requirement. The engine speed momentarily drops at each gear change and then increases according to the demand velocity. Maximum engine speed attained is approximately 2500 rpm. Engine torque is

represented in the fourth curve from below. The curve shows that the motor torque is increased at higher vehicle velocities and also drops momentarily at gear changes. It is clear from the figure that the engine is working under low loads, as the maximum attainable torque during the cycle is far below the maximum engine torque of 370 Nm. The top curve in the diagram shows the power consumed by the engine when drive the vehicle during the NEDC cycle.

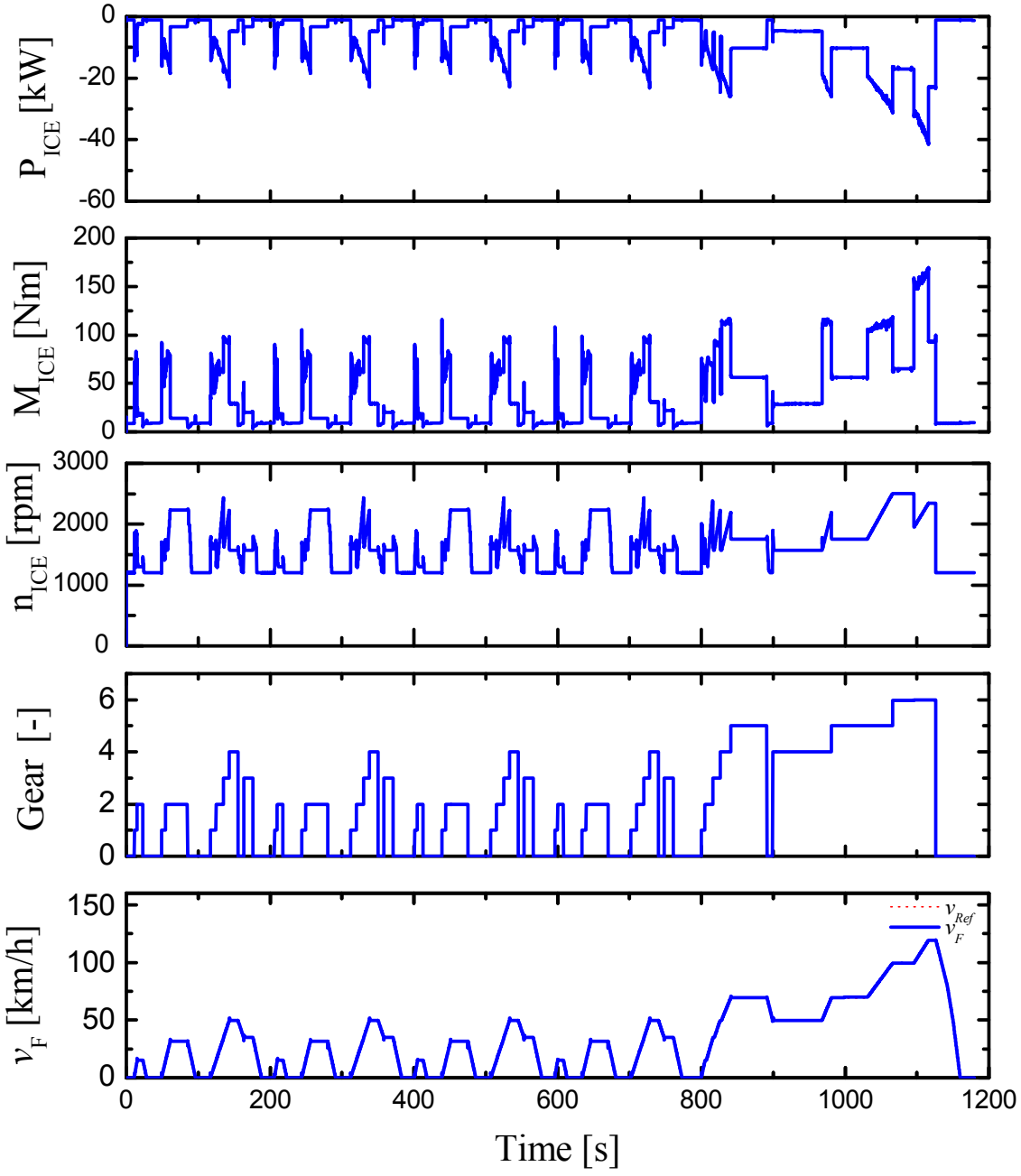

Figure 4-8: Performance curves of the mechanical drivetrain during the NEDC cycle

4.5.3 Fuel consumption and CO_2 emissions

A comparison between the simulation model results and the manufacturer's data of the baseline mid-sized vehicle for fuel consumption in the city and highway scheme is provided in Figure 4.9. Also the CO_2 emission of the simulated and catalogue data of the reference vehicle is provided in Figure 4.10. The resulting values from the simulation look very good when compared to the reference data as there are only small differences between simulation and road test data published by the manufacturer.

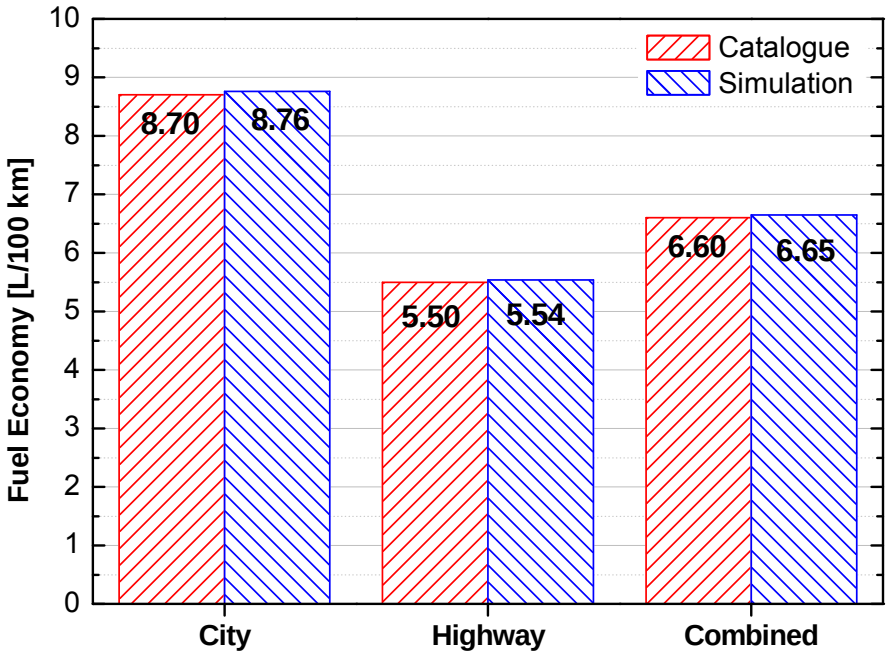

Figure 4-9: Fuel consumption during the NEDC cycle

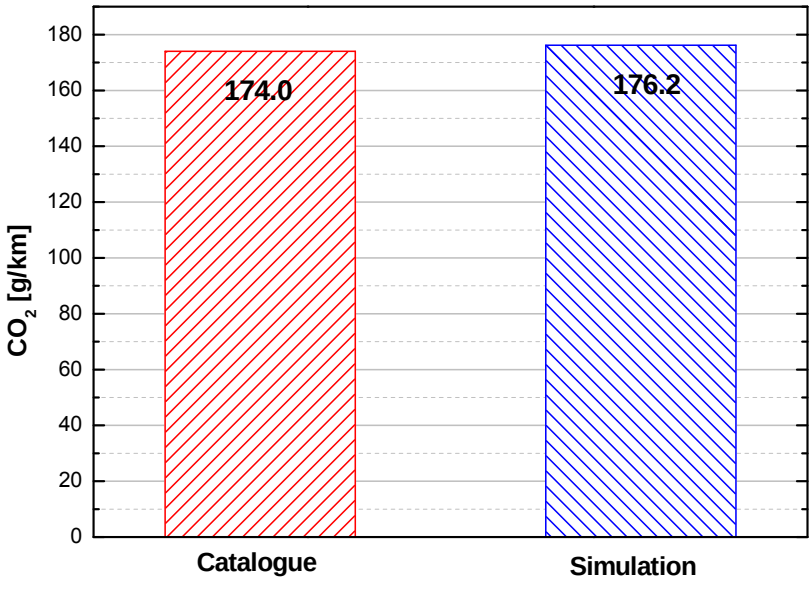

Figure 4-10: Comparison of combined CO_2 emission during the NEDC cycle

During this work, the resulting values of fuel consumption and CO_2 emissions will be used as the comparison criteria to be compared to the similar values obtained for the other proposed hydrostatic and hydraulic hybrid transmissions.

4.6 Conclusion and Outlook

In this chapter a general description for the mechanical transmission that will be used as the baseline vehicle in this work is introduced. Speed behaviour for each gear in the effective range of engine speed was provided showing the velocity range that can be obtained for each gear. Driving performance characteristics including the maximum traction force and power versus the vehicle velocity range was also plotted. The plotted diagrams prove that the road resistance curve intersects the maximum traction curve at the maximum vehicle velocity. In order to build a simulation model, a gear shift strategy obtained from the Organisation of Motor Vehicle manufacturers (OCIA) was used to simulate driver request. The simulation results reveal that the obtained values for the fuel and CO_2 are acceptable compared to the manufacturer's catalogue data. The engine used in the simulation differs slightly from the original one installed in the baseline vehicle, hence the same simulation model including vehicle dynamics, initial conditions as well as the engine model can be used to simulate the proposed alternative transmission methods in this work.

Growing fuel prices year by year and also adequate amount of fossil fuel available on the earth are increasing the demand for producing fuel efficient vehicles. On the other hand, strict environmental issues concerning the hazard emissions resulting from burning fuel in vehicles compound the challenges for vehicle manufactures. Many ideas for developing fuel efficient vehicles arose in the mid of the twentieth century. Some of these ideas concentrate on the use of alternative fuel or energy sources, such as Fuel Cell Vehicles (FCVs) and Electric Vehicles (EVs). Another trend is to replace the conventional mechanical transmission with continuously variable transmissions, allowing the engine to operate in higher efficiency ranges. Other research concentrates on vehicle hybridization. The idea is to use a secondary power source beside the primary power source represented by the engine to reuse the braking energy in order to improve fuel economy and reduce hazard emissions.

Chapter 5

Continuously Variable Hydrostatic Drivetrain

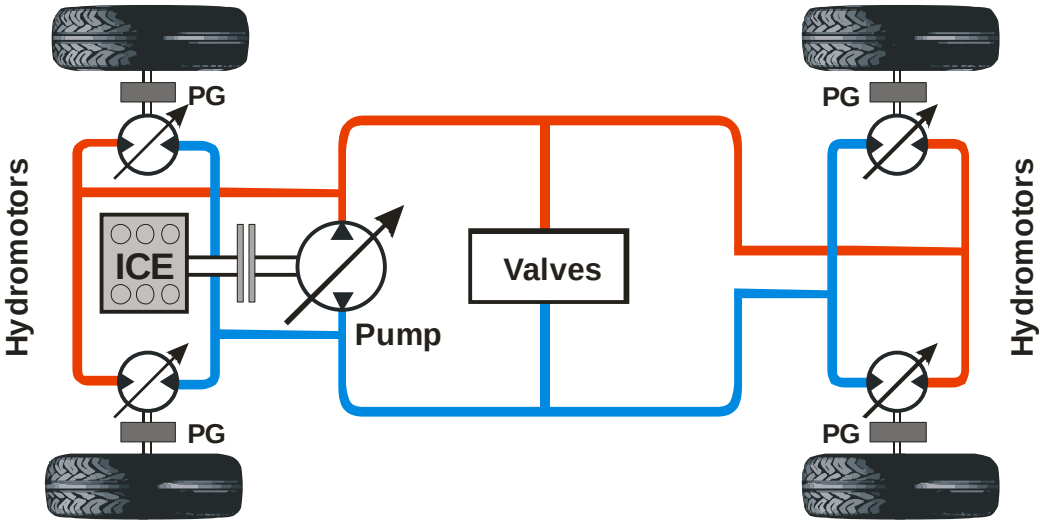

5.1 Introduction

Hydrostatic drives are used in mobile, industrial and aircraft applications when typical advantages such as a high power density, good controllability, flexibility in the system set-up, the excellent dynamic performance as well as the efficient and easy generation of linear movements, especially under high forces are required. This provides a clear advantage for this kind of drive technique over electrical or mechanical solutions [19]. From the vehicle drivetrain point of view, the application of hydrostatic transmissions (HST) has numerous advantages. A continuously variable transmission is possible within full speed range of the drivetrain giving the availability of best matching between the engine and transmission to improve fuel economy and dynamic performance. Moreover, very smooth speed change, ease of control and equal speed in forward and reverse motion are considered additional benefits. Furthermore, convenient layout in the vehicle, as the engine is connected to the wheel motors by hoses or pipes, without regarding their relative positions [73] as well as the robustness of hydraulics should be mentioned as an advantage.

The HST provides continuously variable ratio characteristics with high torque capacity but a slightly low efficiency at a certain operating range, such as at maximum system pressure or minimum motor or pump displacement.

In this chapter, a vehicle with a Continuously Variable Hydrostatic Transmission (CV-HST) integrated with a controlled engine to operate in minimum fuel consumption points will be introduced. The CV-HST represents a flow coupled transmission; where the motor speed depends on the flow delivered from the pump. The torque is hydrostatically determined by system pressure being generated by the pump and also applied at the motor. This configuration is able to form a feasible alternative powertrain due to its potential to choose engine operating points freely, which may lead to a considerable reduction in a vehicle's fuel consumption.

An algorithm based on engine specific fuel consumption is developed to set an Ideal Operating Line (IOL) which represents the locus of the ideal operating points of the engine at various power demands. This allows the engine being connected to the input shaft of the transmission, to operate mostly in efficient operating points. The system includes controllers to continuously vary the displacement of the pump and in-

wheel hydro-motors, so that the adjustable speed range can be covered and the mean efficiency of the vehicle improved.

Contrary to the mechanically stepped transmission, the continuously variable hydrostatic transmission has the possibility to operate the engine in different speeds in a wide range of the vehicle velocity. Figure 5.1 explains this concept; the divergent straight lines in the diagram represent fixed transmission ratios corresponding to each gear for the aforementioned mechanical transmission in chapter 4. For each transmission line a certain velocity range can be covered. For instance, a velocity of 100 km/h can be obtained at three different engine speeds in the stepped transmission as shown by the horizontal dashed line in the diagram. Generally, the CV-HST can theoretically cover all the shaded area shown in the diagram with many transmission ratios satisfying the required speed performance. It can shift the transmission ratio continuously and smoothly by changing the displacements of the pump and/or the motor when power is demanded.

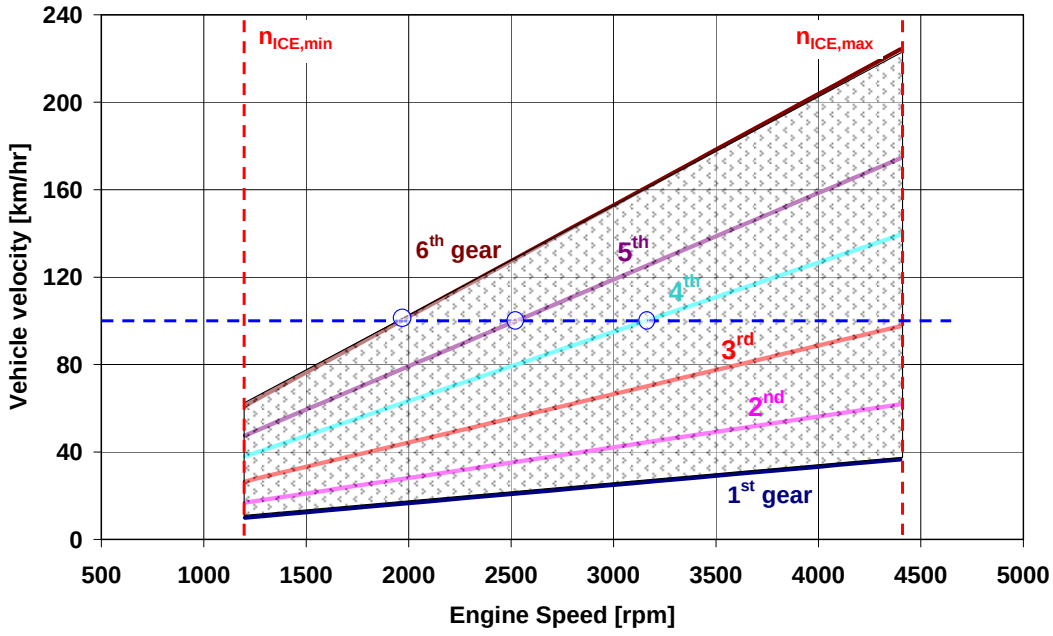

Figure 5.1: Transmission ratio range of the CV-HST versus geared transmission

5.2 Hydrostatic Transmission Structure and Component Selection

The requirements of the hydrostatic transmission drivetrain components are based upon the vehicle requirements. In order to choose the rating of the components (size and ratios design) the demands of the drive must be specified. The performance requirements of a vehicle are maximum torque, acceleration and maximum speed,

which can be represented in a traction curve. Hence, the hydrostatic transmission is limited by torque at low speed and maximum power at high output speeds as shown by full-load curve of Figure 5.2. Beyond this curve, no higher power output or higher torque can be generated [68]. The figure also indicates that the maximum wheel torque is limited by the maximum differential pressure across the hydromotors while the maximum vehicle velocity is limited by the pump size and the maximum available engine power as it intersects the road resistance curve. The maximum vehicle velocity varies inversely with the road gradient, as shown in the diagram by the dashed curves.

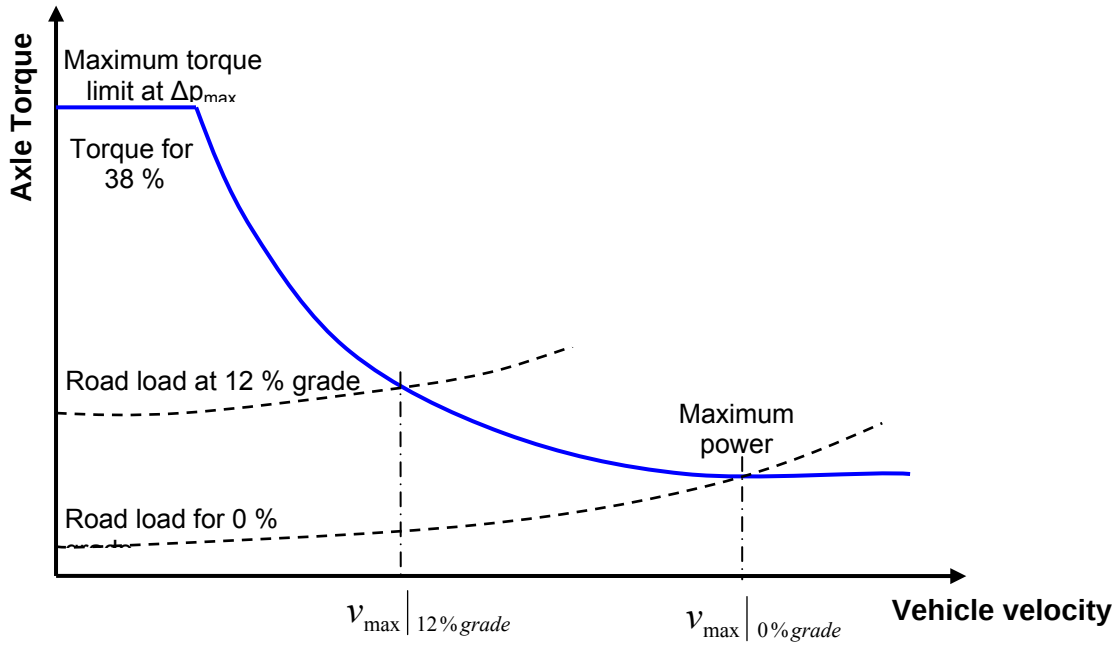

Figure 5.2: Requirements of the CV-HST as based on the vehicle requirements

Most vehicles require high tractive forces during starting and climbing which may be 10-30 times the relatively light load in normal operation [73]. Vehicle speed and load varies over a wide range and requires maximum tractive effort when starting under full load. Hydraulic systems using fixed displacement are inefficient in cases where the desired velocity and load vary over a wide range, since the excess flow is dissipated via relief valves [74].

In some mobile applications, such as wheel loader, an HST system with only variable displacement pump does not satisfy the required torque-speed curve. Hence, the displacement of the pump should basically be variable as well as; the displacement of the wheel motors should also be variable to cover a large speed range of the vehicle. Using variable displacement motor also helps to avoid the reduction of system

pressure during normal operation far from its high efficiency region. This can occur if the displacement of the motor is held constant. At high vehicle velocities the motor displacement can be decreased to increase system pressure which in turn reduces velocity of the oil flow through the circuit in order to reduce flow losses. On the other hand, when the system pressure is increased at low motor displacement the leakage increases and the overall efficiency of the motor is reduced in these operating cases.

5.2.1 Basic principle

The basic layout of a simple hydrostatic transmission system consists mainly of one primary pump and one secondary motor. Figure 5.3 indicates a combination of variable displacement pump and variable displacement motor.

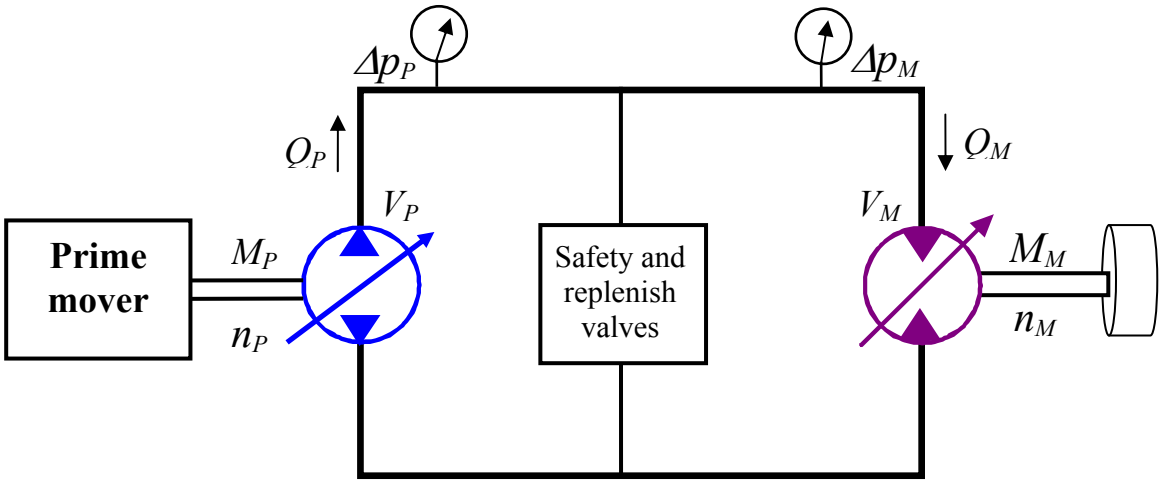

Figure 5.3: A simple hydrostatic transmission system

The relation between pump and motor can be expressed in terms of their basic variables such as, speed, displacement, and pressure. Generally, the pump is coupled to a prime mover (e.g. engine or electric motor) while the hydromotor is connected to the load. The pump is used to transfer the mechanical energy of the prime mover into pressure energy in fluid being delivered to the hydro-motor throughout hydraulic hoses or pipes. The hydromotor in turns converts the fluid pressure energy back into mechanical energy to drive the load connected on its shaft end. The basic equation relating the two hydrostatic units are listed in *Table 5-1* [7, 15]. The flow and torque loss models for hydrostatic pump and motor loaded to the simulation model are taken from the measured data at IFAS on similar units.

The pipeline model used in the simulation model is based on [7]. It accounts for flow loss as well as fluid compressibility and can be expressed as follows;

$$\frac{d\Delta p}{dt} = \frac{1}{C_H}\left[\left(Q_P - Q_{loss,P}\right) - \left(Q_M + Q_{loss.M}\right)\right] \tag{5-1}$$

Table 5-1: *Basic relations of a simple hydrostatic transmission.*

Quantity	Pump	Motor
Displacement setting	$\varepsilon_P = \frac{V_P}{V_{P,\max}}$; $0 \le \varepsilon_P \le 1$	$\varepsilon_M = \frac{V_M}{V_{M,\max}}$; $\varepsilon_{M,\min} \le \varepsilon_M \le 1$
Flowrate	$Q_P = \varepsilon_p . V_{P,\max} . n_P . \eta_{V,P}$	$Q_M = \varepsilon_M . V_{M,\max} . n_M / \eta_{V,M}$
Torque	$M_p = \frac{\varepsilon_p . V_{P,\max} . \Delta p}{2\pi} \times \frac{1}{\eta_{hm,P}}$	$M_M = \frac{\varepsilon_M . V_{M,\max} . \Delta p_M}{2\pi} \times \eta_{hm,M}$
Power	$P_P = 2\pi . n_p . M_p = Q_P . \Delta p_P$ $= \varepsilon_p . V_{P,\max} . n_P . \Delta p_P \frac{1}{\eta_{hm,P}}$	$P_M = 2\pi . n_M . M_M = Q_M . \Delta p_M$ $= \varepsilon_M . V_{M,\max} . n_M . \Delta p_M . \eta_{hm,M}$
Overall efficiency	$\eta_{P,O} = \eta_{v,P} . \eta_{hm,P}$ $\eta_{P,O} = \frac{P_P}{P_{mover}} = \frac{\Delta p_P . Q_p}{M . \omega}$	$\eta_{M,O} = \eta_{v,M} . \eta_{hm,M}$ $\eta_{M,O} = \frac{P_{Load}}{P_M} = \frac{M_L . \omega}{\Delta p_M . Q_M}$

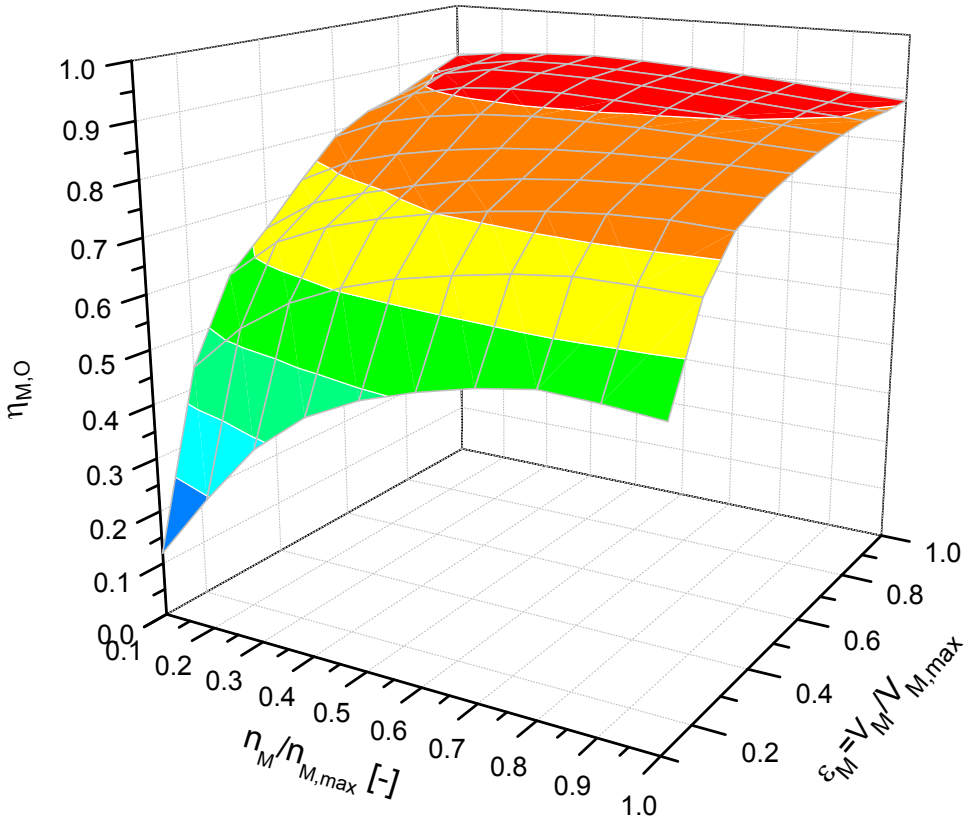

Figure 5.4: Overall efficiency maps of a hydrostatic unit in motoring mode

5.2.2 Hydrostatic transmission design

The design of the hydrostatic transmission is a classic design problem, as its variables are interrelated in a very interesting way [75]. The method described here is one of several designs that also meet the functional requirements of the system.

The proposed hydrostatic transmission configuration is comprised of one main primary variable displacement pump connected to secondary variable displacement wheel motor of the same size. A variable displacement pump and motor enables a variation of the engine speed independent of the vehicle load and will result in a stepless transmission with a wide speed ratio and high efficiency.

The displacement setting of the hydrostatic pump and motors will be controlled in combined/parallel way as described in [7]. Figure 5.5, describes the main performance of the combined/parallel displacement control concept, as the displacement of the pump is increased, the displacement of the hydromotor decreases in controlled manner. The engine is supposed to deliver its maximum power in the defined speed range of the vehicle.

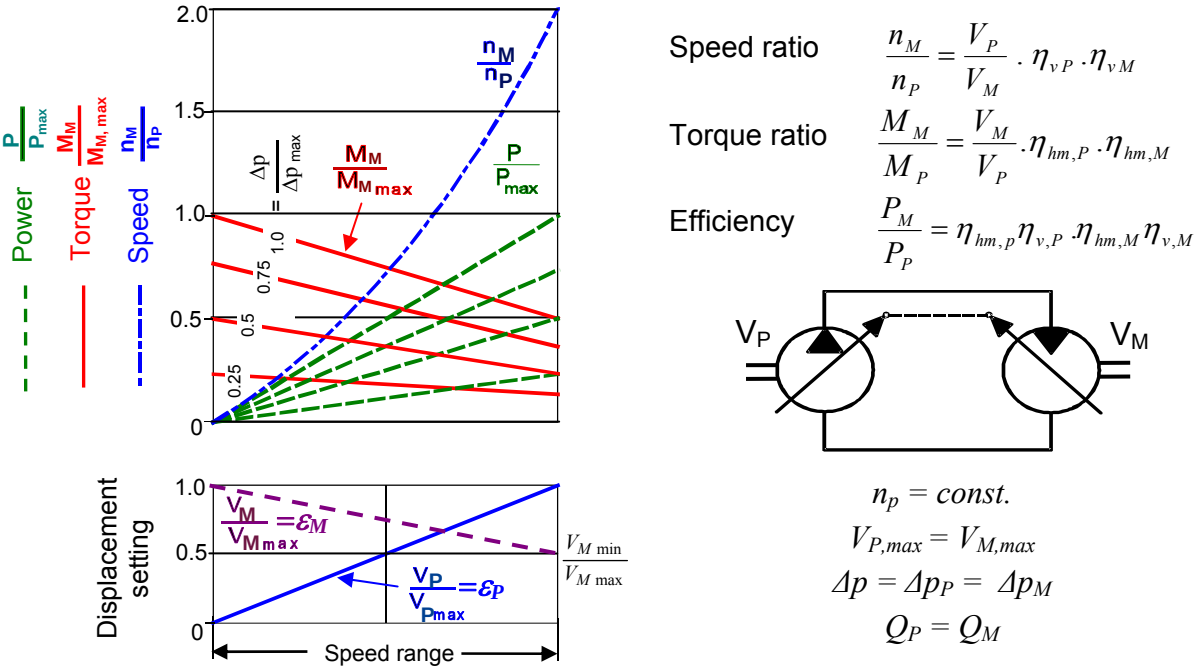

Figure 5.5: Characteristics of the combined displacement setting [7]

To design the transmission it is required to select an appropriate motor and pump size from the available data sheet. The primary choice is to select the hydromotors from a high-speed type mounted in planetary final drive gearbox (PG),

where the efficiency map of this type is available. The alternative is to use high-torque, low speed motors to drive the wheels directly. The efficiency maps of this type are not available for this thesis.

The pump and hydromotors selection depends on the state of the art pump catalogue data sheet of Bosch Rexroth for types A4VG and A6VM [76]. Referring to the data sheet of Bosch-Rexroth A6VM hydromotors, it reveals that the maximum motor speed ranges from 2010 to 8750 rpm for sizes of 1000 ~ 28. But the vehicle should operate normally in the speed range from zero to 1850 rpm or above. Then, a planetary final drive between the hydromotors and wheel hub is a precondition. The final drive converts a high-speed, low-torque input of the motor into a low-speed, high-torque output at the wheel. Also, the engine speed ranges between 1200 ~ 4400 rpm, while the maximum pump speed of Bosch Rexroth A4VG pumps ranges between 2600 ~ 4500 for sizes from 260 to 28 cm^3/rev. A pump mount gearbox between the engine and the motor is also required to operate the pump at proper operational range.

The configuration chosen consists of four hydromotors as shown in Figure 5.6; two hydromotors connected to the front wheels via planetary gear and two others which are used to drive the rear wheels simultaneously. To determine the torque that must be developed at each wheel, the total maximum wheel torque is divided by the number of driving wheels.

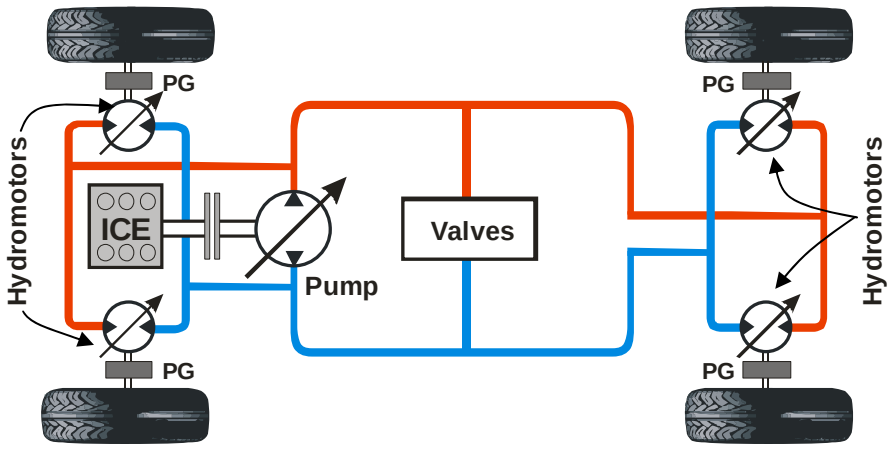

Figure 5.6: The Configuration of the hydrostatic transmission used in CV-HST drivetrain

The design of the transmission components are subject to some constraints such as; maximum engine power is delivered at maximum pump displacement; maximum system pressure which occurs at maximum traction limit, is held just beneath the

opening pressure of the relief valve of 420 bar; maximum engine speed occurs at maximum power is 4100 rpm; minimum permissible displacement for the in-wheel hydro-motors is 25 % from its maximum displacement; and pump mount gearbox and planetary final drive gearbox are assumed to have 98 % constant mechanical efficiency independent from varied load conditions.

The algorithm used to select the motor size is depending on torque ratio at maximum load in an iteration process as shown in the flow chart of Figure 5.7.

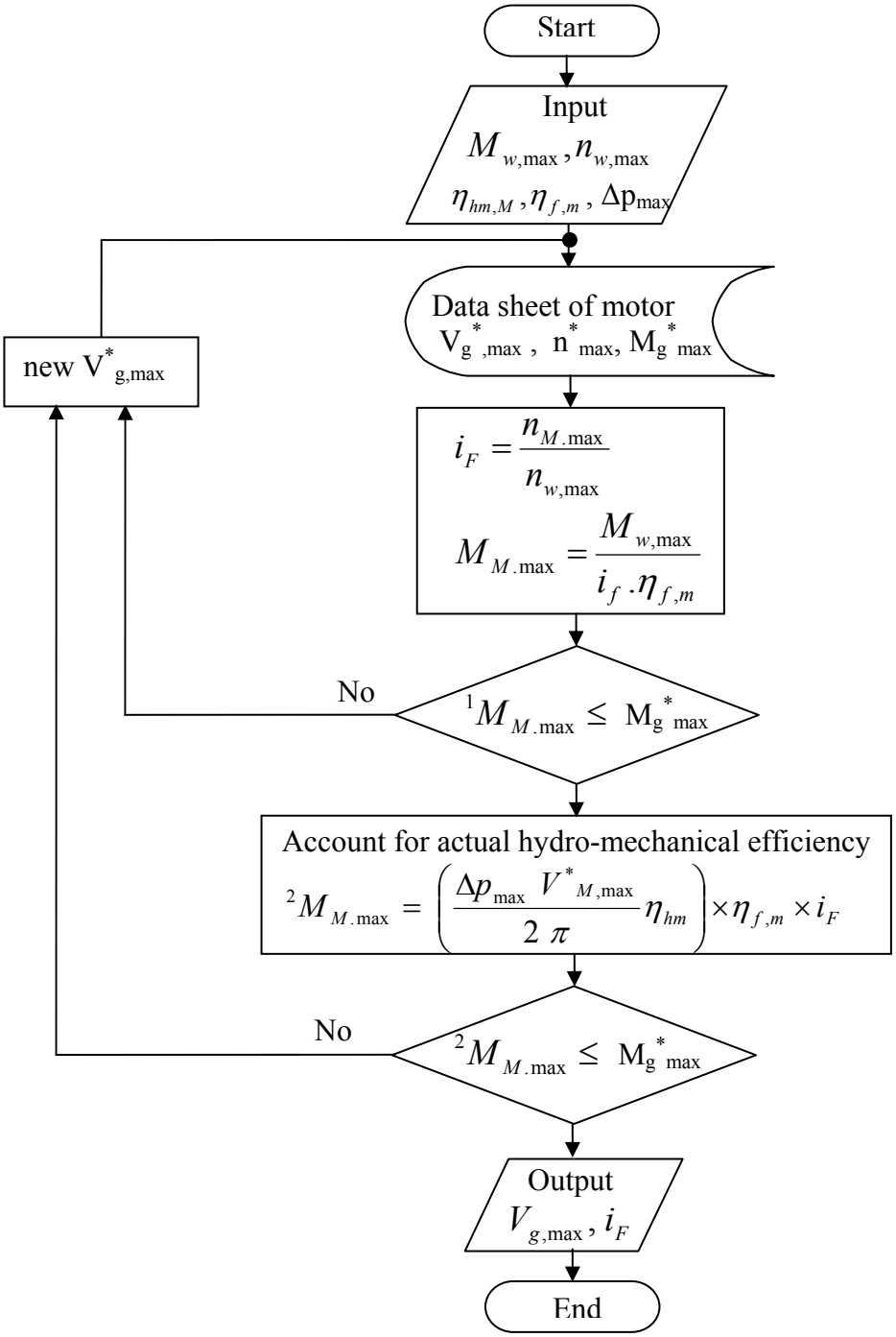

Figure 5.7: Flow rate of the iteration process of hydromotor selection process

The final drive (wheel hub) gear ratio is determined from the maximum permissible motor speed and the maximum speed of the vehicle's wheel which can be expressed as

$$i_F = \frac{n_{M,\max}}{n_{w,\max}} \tag{5-2}$$

Similarly, the pump gear reduction ratio is determined by the engine speed corresponding to maximum power and the maximum pump speed, as follows;

$$i_P = \frac{n_{ICE}\big|_{P_{\max}}}{n_{P.\max}} \tag{5-3}$$

The selection of the pump size is calculated on flow balance basis at maximum vehicle velocity. For initial iteration, the pump volumetric efficiency $\eta_{v.P}$ =86 % at high pressure and 90 % for road travel

$$Q_p = Q_M \tag{5-4}$$

At maximum vehicle speed the motor displacement becomes as small as possible, i.e. $V_{M,min} = 0.25\ V_{M,max}$

$$V_{p,\max} = \left(\frac{i_p}{n_{ICE}\big|_{p_{\max}}\ \eta_{v,P}} \right) \left(\frac{0.25 V_{M,\max}\ n_{w,\max}\ i_f}{\eta_{v,M}} \right) \tag{5-5}$$

As check criteria in the successive iteration process, the pump is sized such that the torque required to drive it, at displacement, is not less than engine torque corresponding to maximum power, where;

$$i_p = \frac{M_P}{M_{ICE}\big|_{P_{\max}}\ \eta_{mech}} \tag{5-6}$$

The design process starts with some initial average values and is looped back several times to restart the design at different points to get the suitable sizes from the point of view of maximum speed and maximum torque limits of the hydraulic pump and motor. The nominal component sizes which can perform the task are listed in *Table 5-2*.

Table 5-2: *Components characteristics of the CV-HST transmission*

Item	Type	Displacement [cm^3]	Max. speed [rpm]	Max. Torque [Nm]	Transmission ratio
		$V_{g,max}$	n_{max}	$M_{g,max}$	$i=n_{in}/n_{out}$
Pump	A4VG	125	2850	795	-
Motor	A6VM	107	5600	681	-
Pump mount	Spur gear				1.45
Motor final drive	Planetary				3

5.3 Description of the CV-HST Drivetrain

The basic principle layout of the proposed continuously variable hydrostatic transmission (CV-HST), including all details is shown in Figure 5.8. The hydrostatic transmission is built in a closed loop as shown. It consists mainly of a bi-directional reversible variable displacement piston pump (3) driven by a diesel engine (1) through a pump mount gearbox (2) which reduces the engine speed to the proper operational range of the pump. High pressure oil from the pump being delivered to the variable displacement motors (4) through the closed hydraulic circuit generates the required tractive torque necessary to propel the vehicle. The hydromotors drive the sun gear of the planetary gearbox (5) which in turn drives planetary gear carrier connected to the wheels.

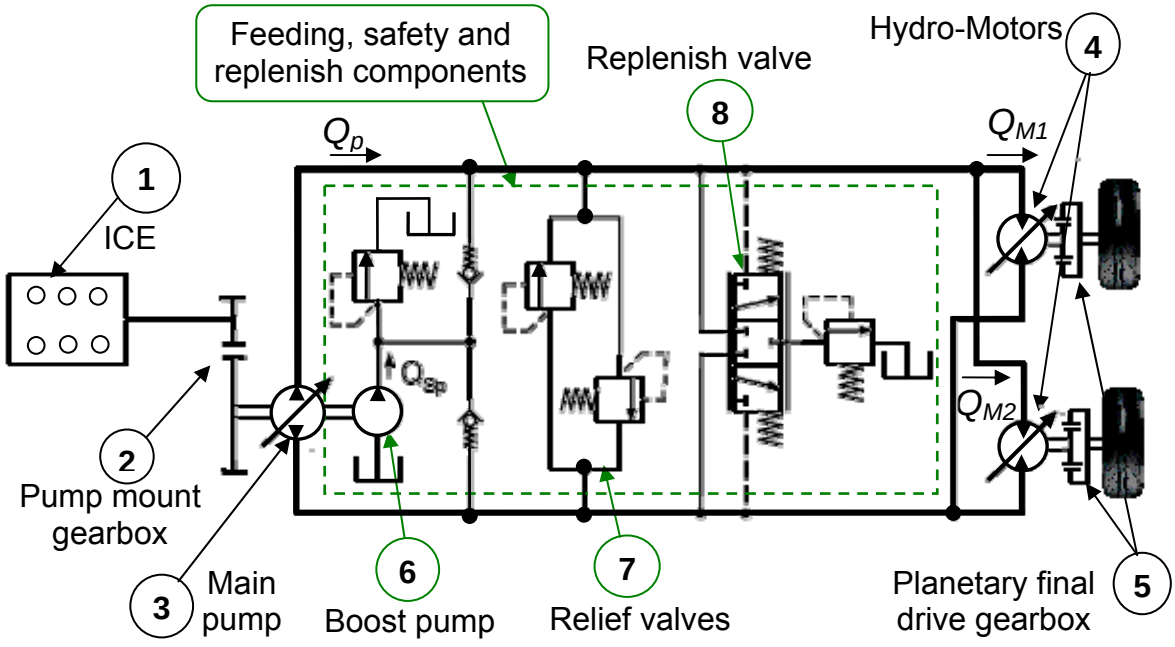

Figure 5.8: Basic layout of the CV-HST drivetrain

For safety purposes, the circuit uses two high pressure relief valves (7) to dump out the high pressure line to the low pressure line in case of overload. A boost pump (6) usually built-in to the main pump provides a separate fluid supply to make-up the leakage in the transmission. It also charges the low pressure line to a level of 15-20 bars to increase the load stiffness and prevent cavitations [75]. Furthermore, When the hydromotors are driven, a replenish or flushing valve (8) is used to pass all returning oil from the main hydraulic circuit to tank throughout the relief valve connected to its output. This keeps the oil temperature at safe levels otherwise more heat could be generated especially during an uphill drive.

5.4 System Control Techniques

The main objective of the control system for the CV-HST drivetrain is to satisfy the required power from the propulsion system while keeping fuel consumption and CO_2 emissions as low as possible. Therefore, the control system regulates simultaneously the amount of fuel supplied to the engine, pump displacement, and motor displacement in such a manner as to achieve optimum performance.

5.4.1 General control system

The CV-HST drivetrain includes some variables to control its operation. These variables are engine speed, pump and motor displacements, system pressure, engine torque and speed. As the drivetrain can operate in the four quadrants of operation, the pump can operate in bi-direction to allow forward, neutral and backward motion, while the hydro-motors' displacement can be varied only in one direction to overcome the vehicle load demand. Figure 5.9 shows the general control system of the vehicle indicating the signal measured from the system and signals supplied from the control unit as used in the DSH*plus* simulation model. For better visibility the front wheel motors are not shown in this picture.

The control unit shown in the figure includes driver requirements as a consequence of the drive cycle characteristics, the engine Ideal Operation Line (IOL) controller, as well as pump and motor displacement controllers. The function of these controllers is to regulate the operation of the whole drivetrain without interrupting the required speed by varying the transmission ratio in a controlled manner, while keeping

the engine running in the range of IOL. It also ensures that driving the engine at the best-efficiency line will not decrease vehicle performance.

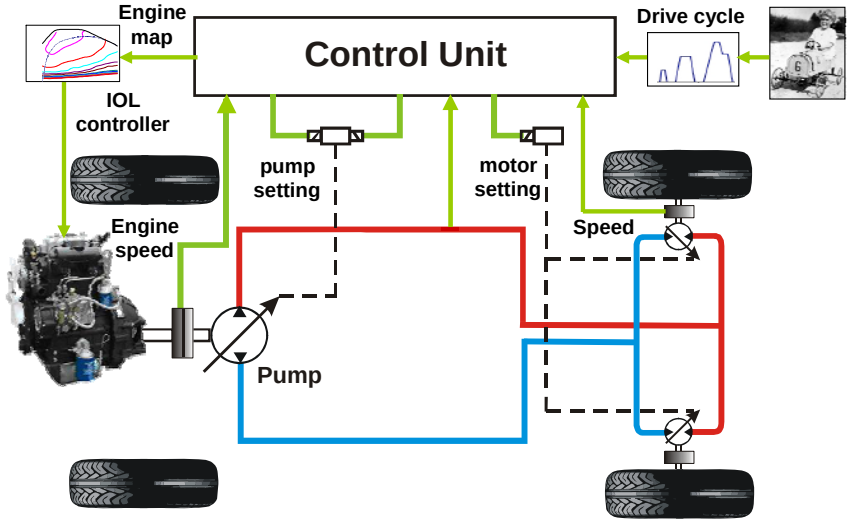

Figure 5.9: General control system of the CV-HST drivetrain

For the given desired velocity and throttle opening, the desired power is calculated from the engine characteristic map by considering component losses. Finally, the desired transmission ratio is obtained from the modified speed ratio map with respect to the vehicle velocity and desired power.

5.4.2 Operating point optimization

A strategy was chosen to operate the engine installed in CV-HST drivetrain at nearly the optimum operating points. The optimization process aims to reduce the fuel consumption of the engine and satisfy the performance requirements without compromise. In fact it will optimize the engine performance characteristics where the engine will neither run at low torque at low demands nor will it run to unnecessary speeds beyond maximum power revolutions. This is done by controlling hydrostatic transmission ratio, which enables the engine to freely operate at optimum speeds independent of the load torque.

The IOL or fuel economy controller is developed based on fuel consumption maps of the engine speed as well as the desired vehicle velocity and acceleration.

The technique applied here is to shift the engine operating points to another region of minimum fuel consumption. Figure 5.10 depicts the engine map with the Brake Specific Fuel Consumption (BSFC) lines. The algorithm of driving the Optimal

Operating Points (OOP) is to calculate the demanded power corresponding to each velocity within the available engine power range. For each demanded power, a point of minimum fuel consumption on the engine map exists. The locus of these points, determining minimum fuel consumption with respect to the iso-power curves over the operating power range of the engine, will form the Ideal Operating Line (IOL). The torque and speed pairs (n_{ICE}, M_{ICE}) can then be obtained for each engine power.

The figure also shows an engine speed corresponding to a certain steady velocity, being about 3000 rpm indicated by point-A. At this point, the developed engine torque is quite low leading to high fuel consumption. The same power required from the engine can be obtained at low specific fuel consumption point by moving the point-A on the same constant iso-power line up to point-B, which is characterized by high torque and low speed. Running the engine at point-B permits it to develop the same required power with a lower fuel consumption compared to point-A.

Hydrostatic continuous variable transmissions offer the possibility to freely choose the engine operating points for a prescribed power demand on the line of constant engine power.

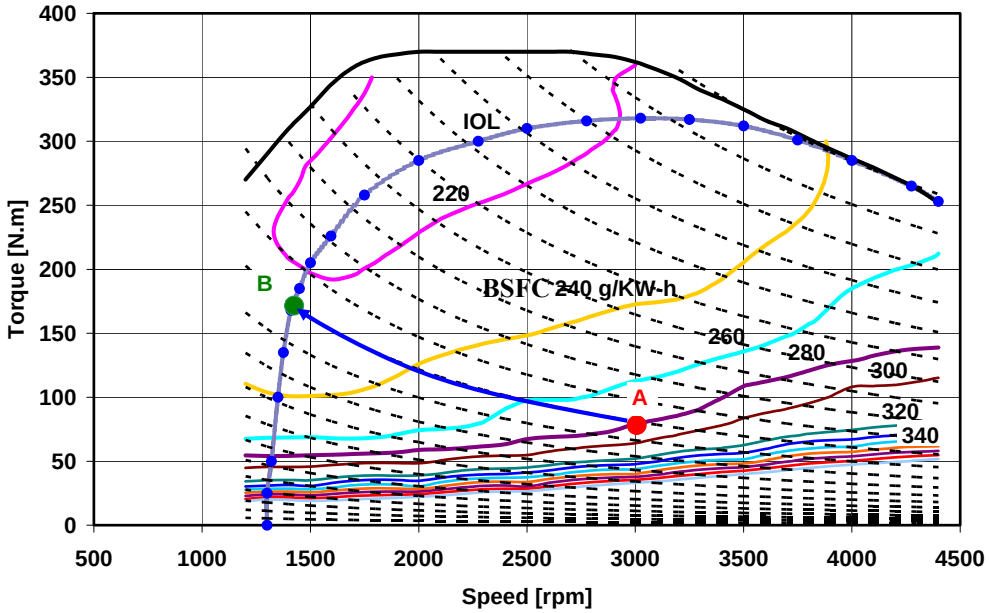

Figure 5.10: Ideal operation line (IOL) across the engine operating range

The controller follows the IOL during the steady periods of operation, allowing the engine to deviate in a controlled manner from the IOL during transients. By doing so, the power is adjusted by varying transmission ratio rather independent on engine torque to provide instantaneous power. Total transmission ratio can be expressed as;

$$i_T = \frac{n_{ICE}}{n_w} = \frac{n_{ICE}}{n_P} \times \frac{n_P}{n_M} \times \frac{n_M}{n_w} \tag{5-7}$$

$$i_T = i_p \times i_{HST} \times i_F \tag{5-8}$$

Where i_P and i_F, describe pump mount and final planetary gear connected to the motor, both of them are greater than 1, to meet pump and motor operation speed range.

During system operation, the pump feeds the motor directly, so that the HST transmission can also be expressed as a function of the pump and motor displacements as follows;

$$i_{HST} = \frac{n_P}{n_M} = \frac{\varepsilon_M \, V_{M,\max}}{\varepsilon_P \, V_{P,\max}} \times \frac{1}{\eta_{v,P} \, \eta_{v.M}} \tag{5-9}$$

$$Where, \quad n_M = \frac{\left(n_P . \varepsilon_p . V_{p,\max} - Q_{Loss,P} - Q_{Loss,,M}\right)}{\varepsilon_M . V_{M,\max}} \tag{5-10}$$

Equation (5-8) indicates that, the transmission ratio of the hydrostatic transmission varies according to the volumetric displacements of its hydraulic components (i.e. pump and hydromotors).

The chosen transmission ratio must comply with the vehicle speed as well as the road load requirements. For instance, the minimum transmission ratio occurs at the maximum attainable vehicle velocity and can be expressed as follows;

$$i_{T,\min} = \frac{n_E\big|_{P_{\max}}}{n_{w.\max}} \tag{5-11}$$

Also, the largest transmission ratio required is calculated at maximum climbing ability which is usually occurs at the smallest possible driving velocity.

$$i_{T,\max} = \frac{M_{w,\max}}{M_{ICE.\max}} \tag{5-12}$$

5.4.3 Transmission ratio controller

The operation of the HST ratio's controller is based on vehicle speed requirements, whereas the vehicle speed is related to the engine speed and the transmission ratio which can be expressed as follows;

$$v_F = \frac{2.\pi.n_{ICE}.r_w}{i_T.60} \tag{5-13}$$

The HST ratio controller is used in the simulation model as a constraint to determine the primary value of the transmission ratio that should be sent to the pump and motor displacement controller in order to satisfy the vehicle speed requirements. The developed primary value from the controller will be subjected to a second constraint considering the road load requirements during operation, to satisfy both vehicle speed and road load requirements.

The transmission ratio of the CV-HST varies between its minimum and maximum values ($i_{T,min}$, $i_{T,max}$) over the appropriate engine speed range ($n_{ICE,1}$, $n_{ICE,2}$), refer to Figure 5.11. In the simulation model, the effective engine speed range varies from 1300 up to 4200 rpm. As illustrated in the diagram, if the engine operates at the lower speed limit $n_{ICE,1}$ then vehicle speeds of $V_{n1,min}$ can be obtained at the maximum transmission ratios while $V_{n1,max}$ can be obtained at the minimum transmission ratio. On the other hand, if the engine operates at $n_{ICE,2}$, vehicle speeds of $V_{n2,min}$ and $V_{n2,max}$ can be obtained at the maximum and minimum transmission ratios respectively.

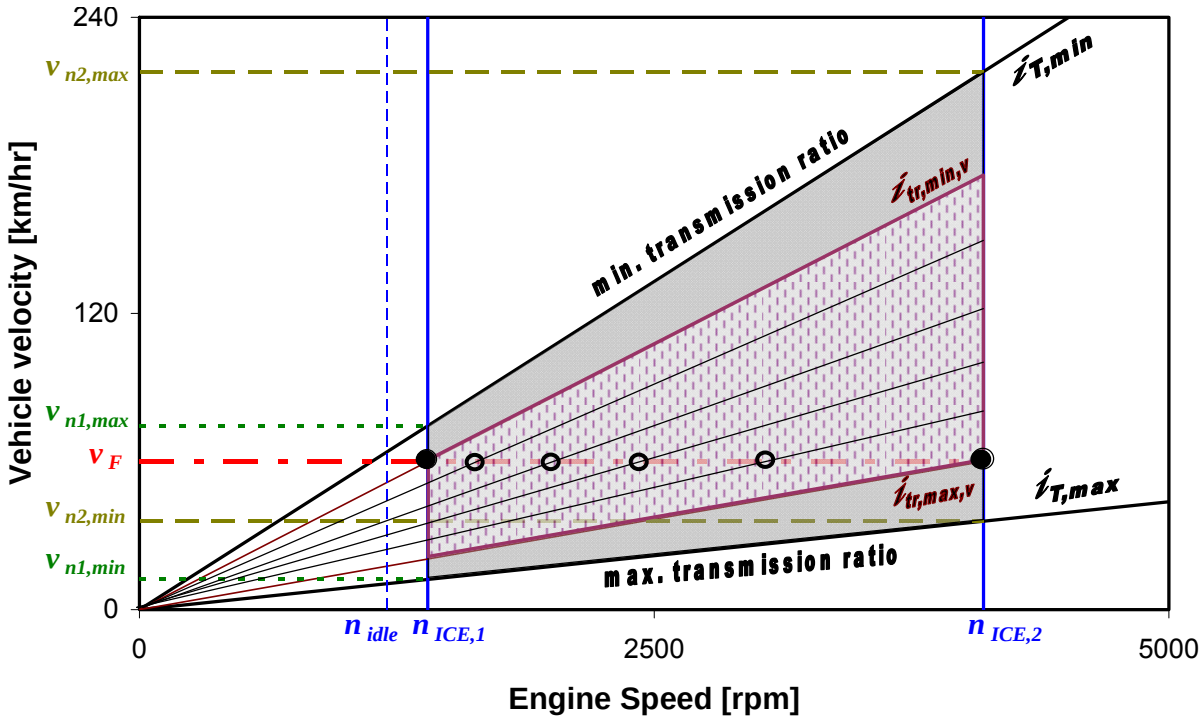

Figure 5.11: Transmission ratio selection based on speed requirements

The vehicle velocity limits are stored in the look-up table of the controller to determine the appropriate transmission ratio. Generally, for each required vehicle velocity there are certain ranges for the transmission ratio to satisfy this speed, but

there is only one transmission ratio where the engine can run in optimum condition of minimum fuel consumption.

For an arbitrary vehicle speed v_F lies in the range between $V_{n2,min}$ and $V_{n1,max.}$ The suitable transmission ratio for this arbitrary velocity is limited in the range of $i_{T,min,v}$ up to $i_{T,max,v}$ indicated by the shaded area. The resulting range can be obtained at the intersection of the horizontal line representing the desired velocity with the engine speed range limit ($n_{ICE,1}$, $n_{ICE,2}$) indicated in the diagram by the two solid circles at the extremes. There are many transmission ratios satisfying the vehicle speed requirements in the obtained range ($i_{T,min,v}$, $i_{T,max,v}$), some of them are indicated by the hollow circles. Within this range there is only one optimum engine speed consuming minimum fuel consumption to drive the vehicle at the desired velocity.

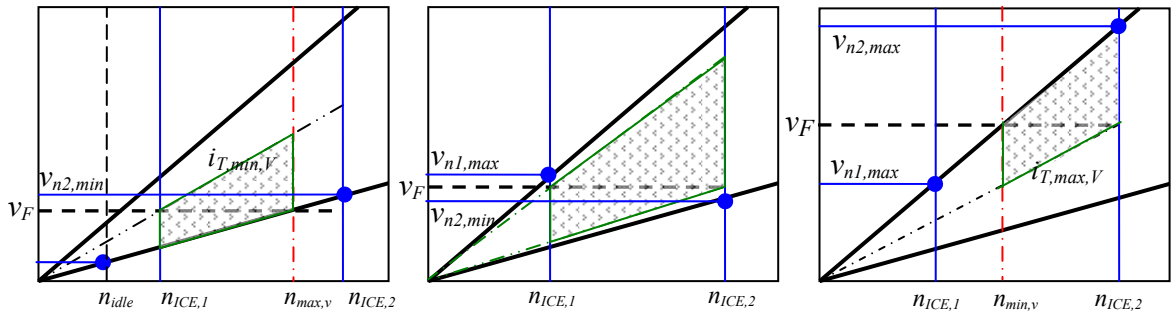

Case: 1
$v_{idle} < v_F < v_{n2,\min}$
$i_{T,\min,v} \le i_T \le i_{T,\max}$

Case: 2
$v_{n2,\min} \le v_F \le v_{n1,\max}$
$i_{T,\min,v} \le i_T \le i_{T,\max,v}$

Case: 3
$v_{n1,\max} < v_F \le v_{n2,\max}$
$i_{T,\max,v} \le i_T \le i_{T,\min}$

Figure 5.12: Transmission ratio limitation based on vehicle speed demand

Figure 5.12 summarizes the possible transmission ratio limits of the controller based on the vehicle speed requirements. The first diagram on the left shows the possible range of the transmission ratio corresponding to a vehicle velocity where demand lies in the range (v_{idle} , $v_{n2,min}$) represented by the shaded area. In this case, the minimum transmission ratio is shifted-down to the new value $i_{T,min,v}$. The upper limit of the engine speed is decreased from $n_{ICE,2}$ to the new upper limit $n_{max,v}$, where the value of $n_{max,v}$ varies depending on the desired vehicle velocity v_F.

The middle diagram, case 2, is already explained in detail in the the general case previously described in Figure 5.11. Contrary to the first case, the third diagram

on the right shows the permissible transmission ratio range corresponding to a vehicle velocity located in the range ($v_{n1,max}$, $v_{n2,max}$). As shown the maximum transmission ratio is shifted up to the new value $i_{T,max,v}$, and the lower limit of the engine speed $n_{ICE,1}$ may increase to the new lower limit $n_{min,v}$ depending on the value of required velocity.

5.4.4 Functional architecture of the vehicle controller

The vehicle controller is developed based on the efficiency maps of the engine, pump and hydromotors, as well as drive cycle required speed and road load. The controller considers the vehicle speed requirements, as well as the road load requirements. Generally any chosen transmission ratio must satisfy vehicle speed and road load requirements, in order to ensure that the engine torque can meet the required load torque of the vehicle and also to avoid operation of the engine above the maximum speed.

The proposed control strategy of the CV-HST drivetrain computes the Optimal Operating Point (OOP) of the engine. It provides the controller with the optimal torque and consequently forces the engine to operate in its optimal speed by choosing the appropriate transmission ratio. Figure 5.13 shows the functional diagram of the vehicle controller, where $n_{ICE,d}$ is the desired engine speed determined by the HST controller. The n_w and M_w are the torque and speed request on the driven wheel, with, n_{ICE} and M_{ICE} being the actual speed and torque requests from the engine respectively.

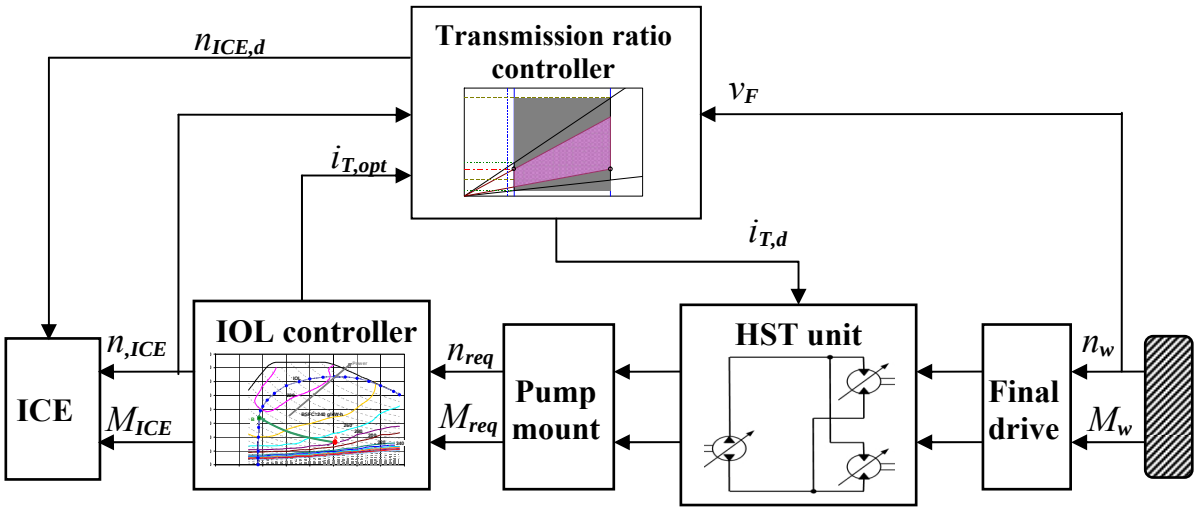

Figure 5.13: Functional diagram of the CV-HST controller

The controller calculates at first a desired transmission ratio based on vehicle speed requirements and compares this primary value with the actual required torque-based transmission ratio depending on the road load. Then the proper transmission ratio is chosen to operate the engine in its optimal operating point. The demand torque on the engine side of the transmission is obtained by dividing the demand torque on the wheels by the primary selected transmission ratio. If the result value is lower than the maximum total capability of the engine implemented in the engine map, then the chosen transmission ratio can satisfy load requirement, otherwise it is discarded and another value is determined in the permissible transmission ratio range. The pump and motor displacement controllers react with the selected transmission ratio by adjusting the displacement of both units simultaneously. This forces the engine to operate at optimal speed of minimum fuel consumption under the demanded load.

Shifting the transmission ratio from one operating point to another operating point is used during normal driving, while the output power is controlled by varying the engine speed. In this case, the specific trajectory by which the new transmission ratio is reached becomes relevant for the driveability of the vehicle.

5.5 Simulation Model

A simulation model for the whole CV-HST drivetrain was built in DSH*plus* environment to study the performance of the system under the aforementioned control strategy. Figure 5.14 depicts the hydrostatic transmission system with input control signals as fed from the pump and motors displacement controllers. The pump and motors controllers are adapted to operate the hydrostatic pump and hydromotors at high displacement whenever possible depending on the vehicle demands, in order to attain high efficiencies in the most frequent velocity range of the vehicle.

Accurate volumetric and hydro-mechanical losses 3D look-up tables based on the measured data described in [34], which are a function of speed, pressure, and swashplate angle, are loaded to the hydrostatic units. The internal combustion engine with its throttle and speed controller components are also shown on the left side of the model. Engine fuel consumption and maximum torque maps are loaded to the engine. The value of the throttle signal supplied to the engine is proportional to the vehicle speed.

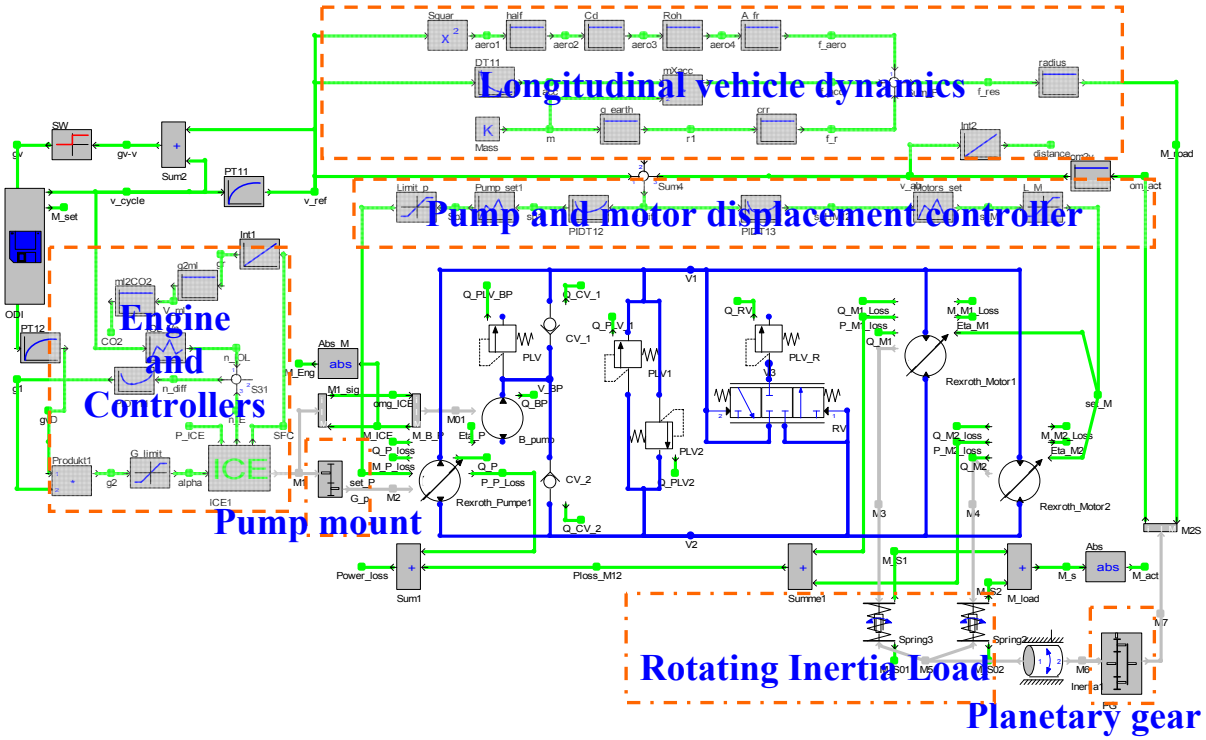

Figure 5.14: DSHplus simulation model for the CV-HST drivetrain

A driver model is represented by the Online Data Input (ODI) and PID type controller is used to manipulate the vehicle operation and also to couple or decouple the pump from the engine according to the travel mode. It feeds the transmission controller with the required motion i.e. acceleration, deceleration, forward or backward travel and manipulates the value of the throttle angle to follow the driving schedule. The controllers integrated in the system force the engine to operate in its Optimal Operating Line (IOL) depending on the vehicle speed requirements and road load torque.

5.6 Results and Discussion

The simulation model was run during the NEDC driving cycle computing fuel consumption and CO_2 emission in comparison to the baseline vehicle on this European standard test cycle which is considered the basic cycle criteria of evaluation in this thesis. Engine operating point according to the introduced control strategy is explained. The characteristic curves of system variable showing its variation during the driving cycle is also indicated.

5.6.1 Engine operating points

The operating point of the engine on the torque-speed diagram is shown in Figure 5.15, which demonstrates that the engine is forced to operate near IOL under the control strategy applied in CV-HST drivetrain. This enables the transition of the operating point from map-based mode as obtained in mechanical drivetrain to best-line mode.

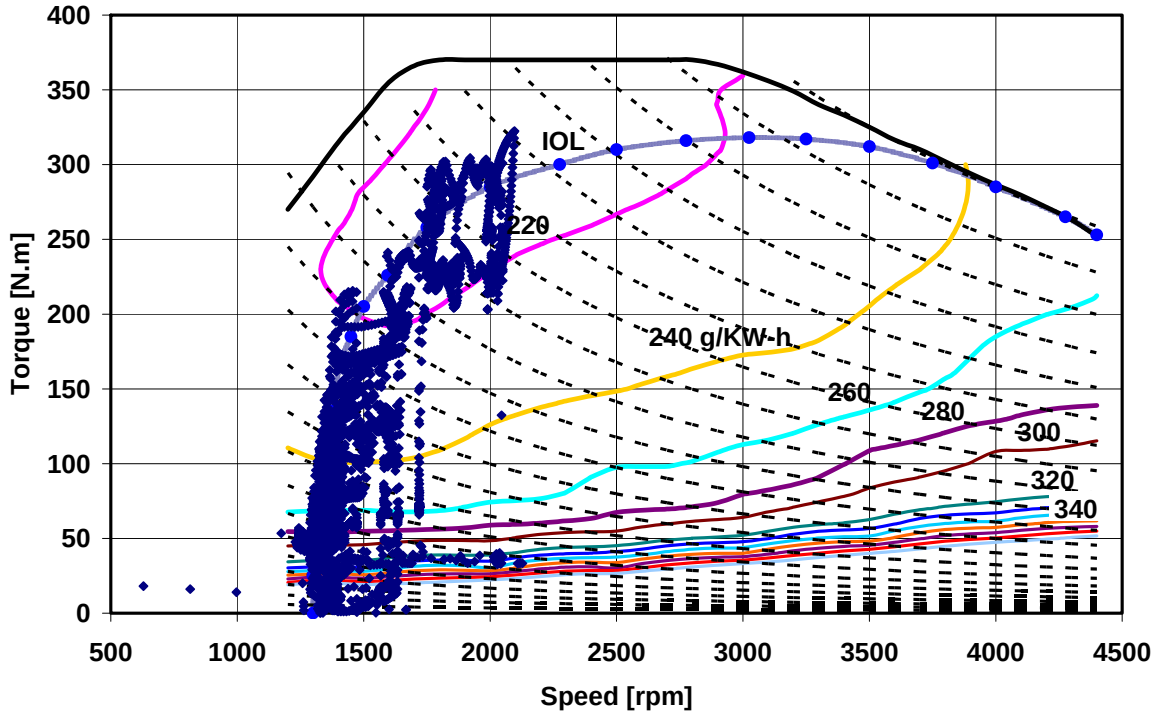

Figure 5.15: Engine operating points of the CV-HST during the NEDC

The engine installed in a mechanical transmission suffers from operation at low loads. The operation of the engine at these low loads leads to high average fuel consumption.

In IOL control strategy, the low loads operation region is shifted to another point of minimum fuel consumption on the same iso-power curve.

5.6.2 Characteristics curves

Figure 5.16 shows the performance analysis curves of the CV-HST variables during the NEDC cycle. The vehicle velocity which is represented by the first curve shows a good match with the desired velocity over the whole drive range. The second curve represents the internal combustion engine speeds. The engine is continuously running for the entire driving time.

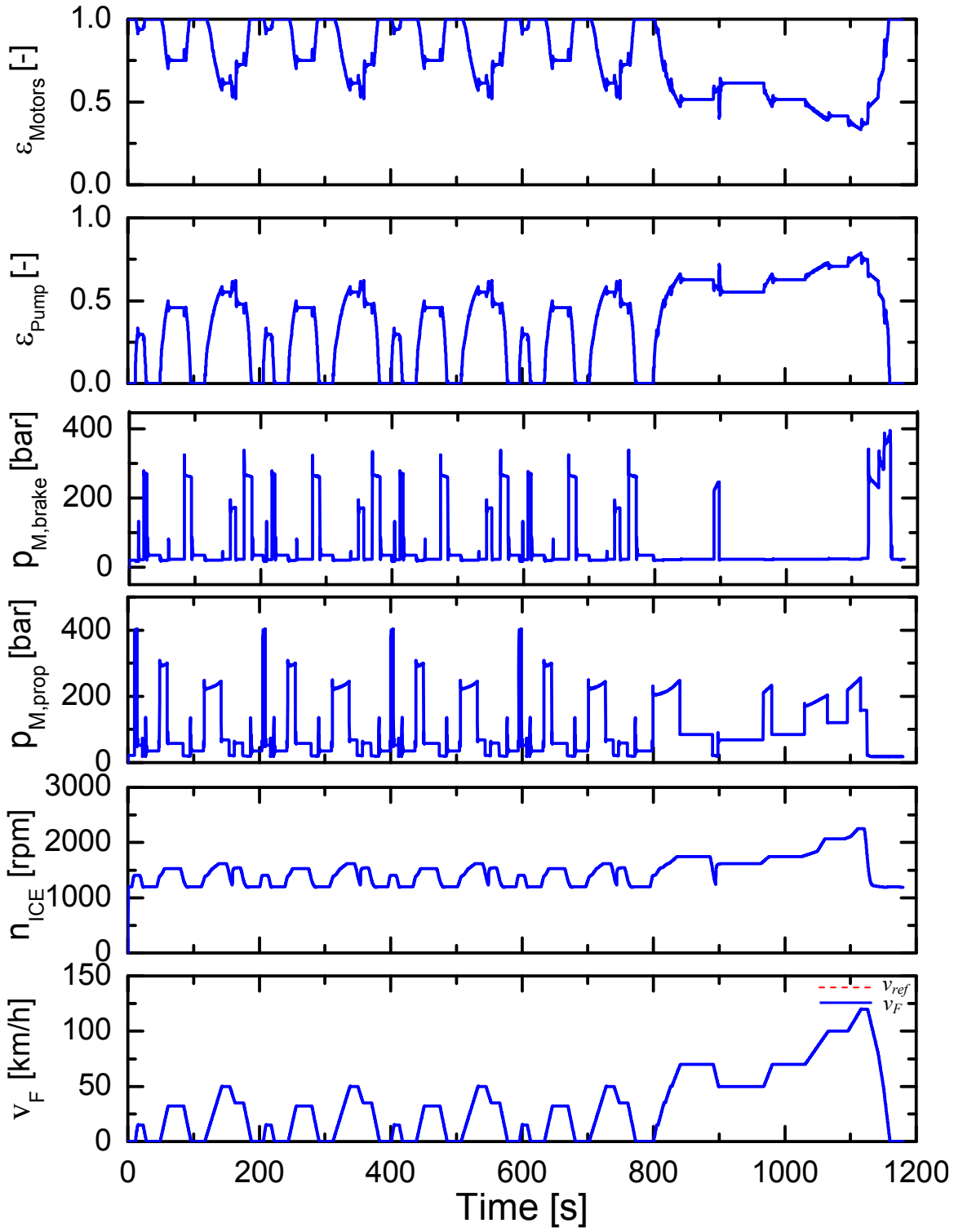

Figure 5.16: characteristic curves of the CV-HST drivetrain during the NEDC cycle

During vehicle stop the engine is running in its idle speed of 1200 rpm otherwise it reacts to the vehicle speed according to the command signal from the controller. Hydromotor pressure in propulsion and braking modes are illustrated respectively in the third and forth diagrams.

Pump displacement setting, ε_P, is indicated in the fifth diagram. The pump displacement increases when the demanded vehicle speed increases. The available control range of the pump displacement lies between 0 to 100 %. At maximum cycle velocity the pump displacement reaches about 76 % of its maximum value, while the hydromotor attains approximately 34 % of the maximum displacement, as indicated in the top curve in the figure. Contrary to the pump displacement, the motor displacement decreases with increasing vehicle speed. The behavior of the performances curves of system variables matches the vehicle requirements as illustrated during the driving cycle.

5.6.3 Hydromotor operating points

Figure 5.17 indicates the operation point of the hydromotor during the drive cycle. The diagram can be divided into two parts with respect to the y-axis which refers to the pressure difference across the hydromotor. The upper part, i.e. the positive pressure difference range, represents the operation point of the hydromotors under road load in forward travelling during the cycle. The lower part, which lies in the negative pressure range of the motor, represents deceleration or braking cases. The average motor efficiency in driving mode is approximately 51 %, with an average of 79 % during braking mode.

During deceleration mode, the hydromotors are swiveled back to their maximum displacements in order to gain maximum braking torque while reducing vehicle speed. In this case, the hydromotors reverse their pressure direction and operate as pumps delivering flow, leading to system pressure rise. The pump controller reacts to this situation by reducing the pump displacement to zero in order to reduce the driving torque on the ICE.

In the current system, there is no energy recuperation for the braking energy of the vehicle. Configurations which recuperate the braking energy will be discussed later in the next two chapters, where a large amount of this unexploited braking energy can be stored in the form of potential energy within a hydro-pneumatic accumulator.

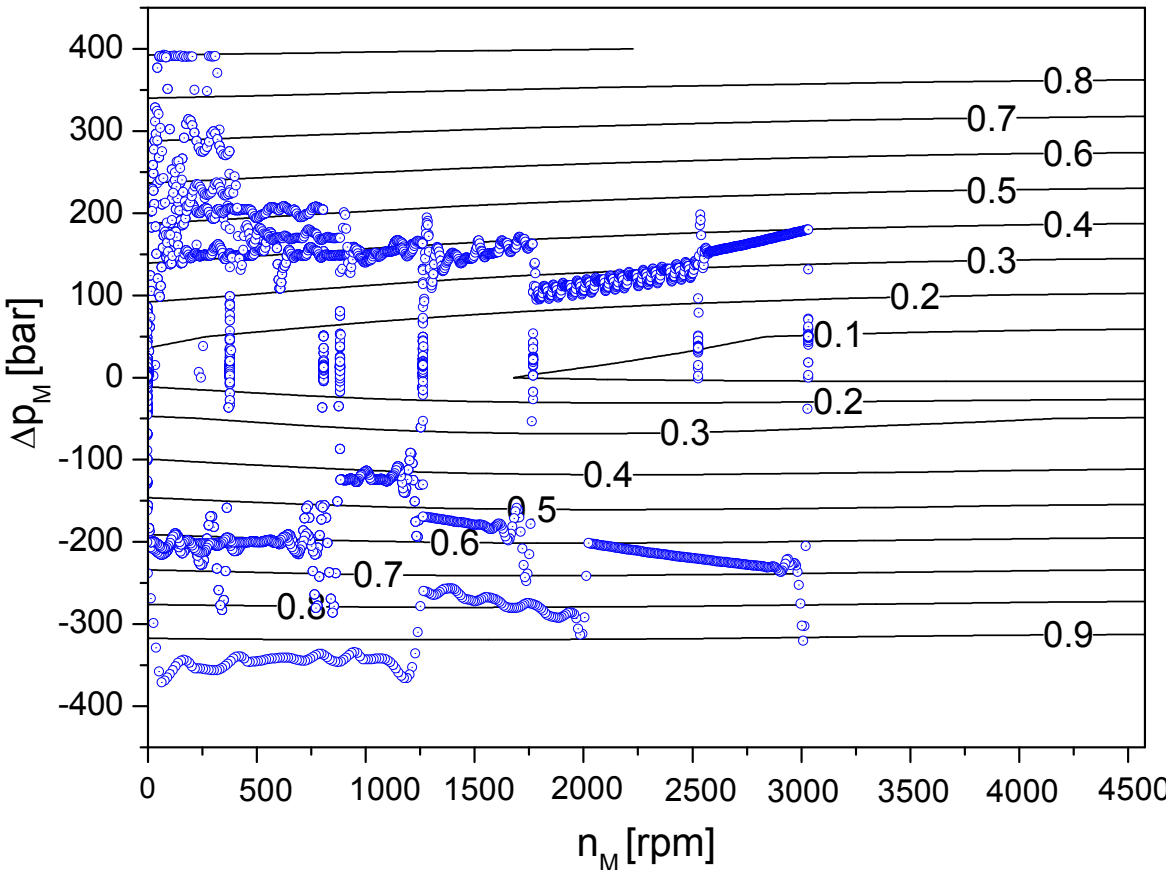

Figure 5.17: Hydromotor operating points during the NEDC cycle

5.7.4 Fuel consumption and CO_2 emissions

Simulation results for fuel consumption and CO_2 emissions for the CV-HST drivetrain compared to the baseline mechanical transmission are illustrated here.

The bar chart shown in Figure 5.18 reveals a reduction of fuel consumption about 37 % in the city drive cycle as a result of running the engine in the best operation line strategy in low loads drive.

Contrary to the city drive, the fuel consumption of the CV-HST drivetrain is increased in highway cycle. The increase in fuel consumption is a direct result of the reduction in hydrostatic transmission system efficiency at these higher speeds. The speed of the engine increases to meet the vehicle requirements, the pump displacement also increases causing a reduction in system efficiency. At these higher speeds the hydromotor operates at small displacements being characterized by low efficiency causing deterioration of total system efficiency. The total reduction of the CO_2 emissions during the cycle is negligible as shown in the bar chart of Figure 5.19.

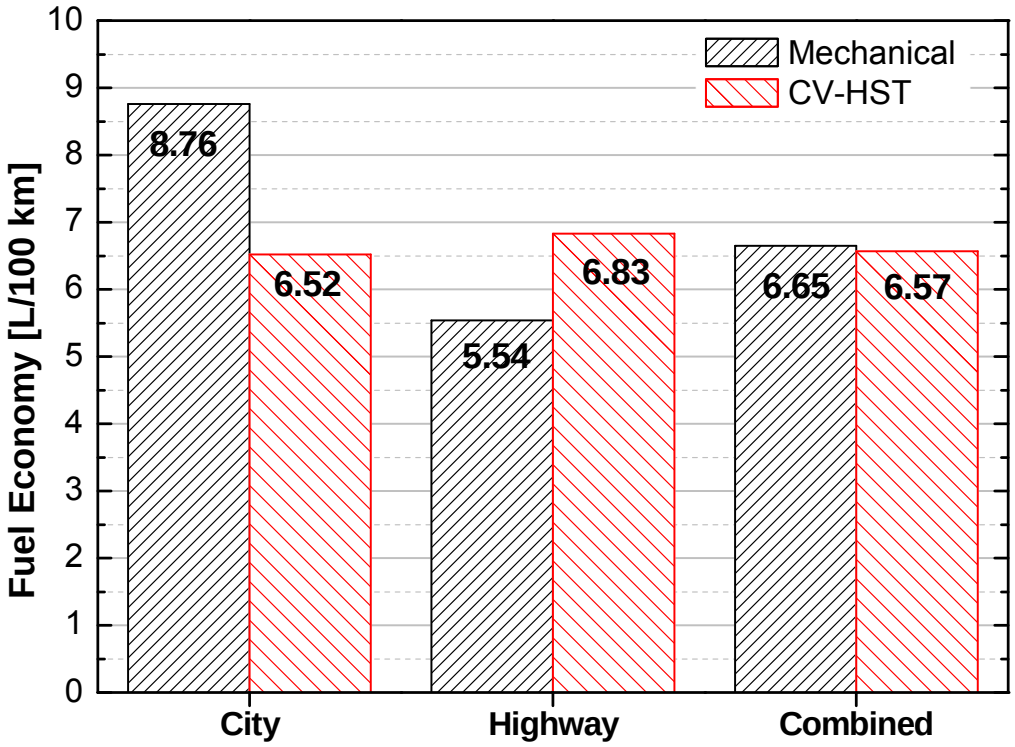

Figure 5.18: Fuel consumption of the CV-HST versus mechanical drivetrain

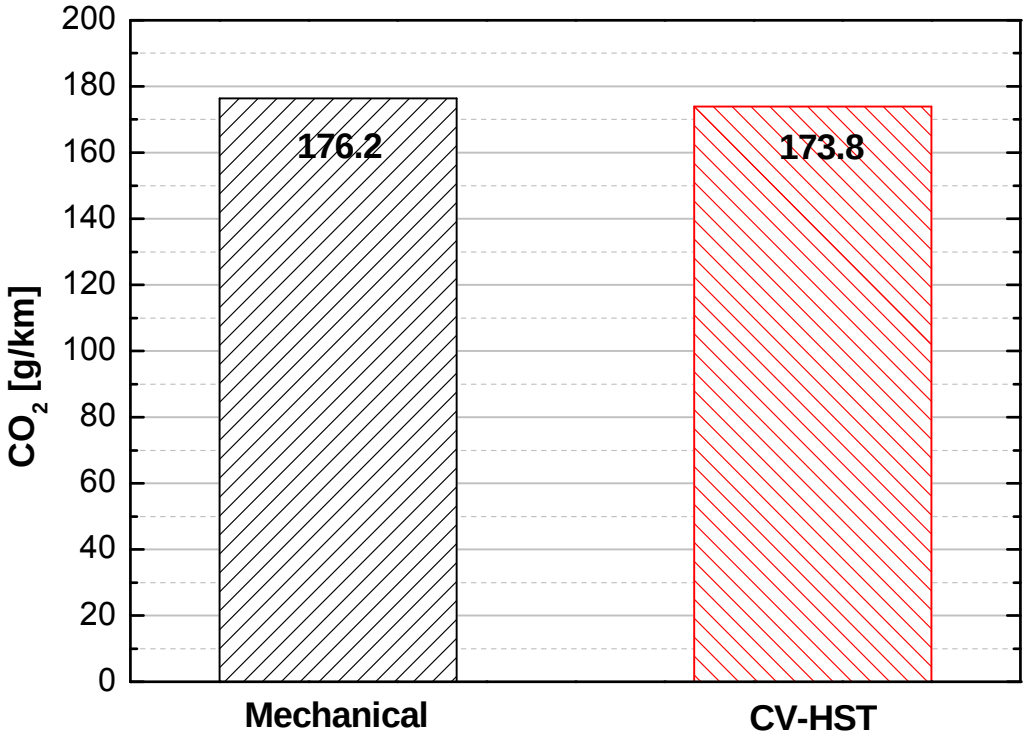

Figure 5.19: CO_2 emissions of the CV-HST versus mechanical drivetrain

5.7 Conclusion

This chapter introduced a detailed description for a hydrostatic transmission system using variable displacement pump and variable displacement motor, integrated with a control strategy to operate the engine in best-line of minimum fuel consumption. The results indicate that it is generally accepted that CV-HST has the potential to provide some desirable attributes specifically in city drive such as; a wider range ratio, good fuel economy, shifting ratio continuously and smoothly. However it is not suited to apply in passenger vehicles due to its huge components size, high weight and cost.

The simulation results show that the continuously variable hydrostatic transmission integrated with the complicated control system has almost no fuel saving compared to the gear-shift transmission, because the gain in running the engine on minimum fuel consumption line will be lost by the low component efficiency especially at high vehicle speed.

Generally, the HST is considered as double energy conversion, its efficiency is not high enough compared with mechanical transmission. To reduce the gap in efficiency, a suitable method and simple control strategy are required to store the lost energy during vehicle braking.

The aim of recuperating the unused braking energy is to raise the net energy efficiency of the system or the round-trip efficiency. In regenerative transmission, part of the energy developed by the engine which is lost in multiple braking can be restored in order to reduce the operation time of the engine and consequently reduce its fuel consumption.

Chapter 6

Secondary Controlled Hydrostatic Drivetrain

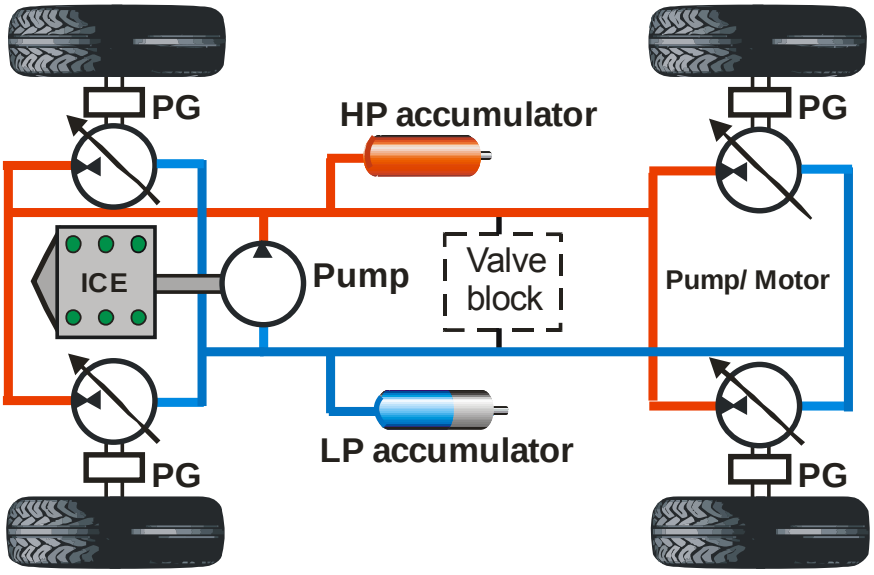

6.1 Introduction

The conventional form of a hydrostatic transmission presented in chapter 5 is known as flow coupling hydrostatic transmission, because the relation between the motor and the pump is basically dependent on the flow delivered from the pump. As the efficiency of the flow coupling hydrostatic transmission configuration is not high enough, the conventional hydrostatic transmission was integrated with a complex control system in order to force the engine to operate along an optimum operation line of minimum fuel consumption according to the required power. The applied strategy causes a further reduction in fuel consumption in the low loads during city drive which is not the case in the highway drive where the losses increase at high vehicle speed as indicated in the results of chapter 5.

By locating an accumulator on the high pressure side of the HST circuit, the relation between pump and motors changes from flow coupling to pressure coupling. Installing an accumulator in the high pressure (HP) line permits the hydraulic system to recuperate most of the lost vehicle kinetic energy in deceleration and braking states [77]. A pump is used to charge the accumulator, while the vehicle speed is controlled by adjusting the displacement of the secondary unit (i.e. the hydromotor). The secondary unit works as a motor in normal driving mode while it can also work as a pump, regenerating the kinetic energy during deceleration and braking cases. The hydraulic accumulator is used for storing the recovered energy through flow coming from the secondary unit. It takes its energy either via the primary flow delivered by the pump or the secondary unit. The system operating pressure is independent of the vehicle load which is not the case in conventional flow coupling hydrostatic transmission. This independence creates several benefits including energy recuperation and the ability to change the rotational direction of the hydraulic motor by displacing it over-center. Therefore the accumulator plays an important role in the Secondary-Controlled Hydrostatic Transmission (SC-HST) where it dominates the overall performance of the drivetrain.

The proposed Secondary-Controlled Hydrostatic Transmission (SC-HST) is considered to be an energy-saving system. A study of the potential of a secondary controlled in vehicle drivetrain is therefore interesting. In this chapter complete system

description and analysis, alongside discussion of system control and operation modes will be introduced. The energy utilization as well as the recuperation potential of the system is investigated by means of DSH*plus* simulation model. The proposed drivetrain can regenerate most of the vehicle's kinetic energy during acceleration which is dissipated in the form of heat via friction brakes.

6.2 Configuration of a Secondary-Controlled Hydrostatic Transmission

The basic idea of a secondary controlled hydrostatic transmission was first patented in 1962 and was applied and developed in the early 1980s [9, 78]. Secondary control is a known technology in the field of hydraulics offering precise positioning and speed as well as the possibility of energy recuperation [79]. Secondary control is currently applied in machinery such as excavators, forklifts and wheel loaders, where it moves high loads in cyclic motions which are ideal conditions for energy recuperating systems [80, 81].

The outstanding features of the secondary control over the conventional hydrostatic transmission are the ability of recovering the braking energy, higher efficiency, higher dynamic response, energy recuperation and better accuracy in speed, torque and positioning [45, 82, 83]. The secondary controlled hydrostatic transmission is considered as a multisource or hybrid driving system. The primary power source, such as electric motor or Internal Combustion Engine (ICE), works in a stable zone independent from the current load of the vehicle. A hydro-pneumatic accumulator is considered the secondary power source. It accumulates the power of the primary power source and the energy recovered from the hydromotor during deceleration.

6.2.1 Basic principle

Theoretical principle of a secondary-controlled hydrostatic transmission is represented in Figure 6.1. A constant or variable displacement hydraulic pump representing the primary unit keeps the high pressure line of the circuit and consequently the accumulator pressure at a predetermined level.

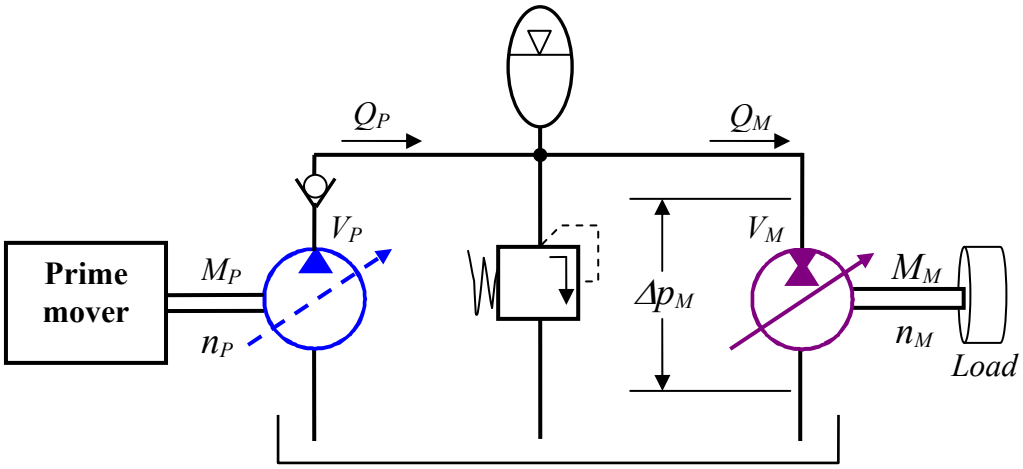

Figure 6.1: A basic secondary controlled system

The dashed line plotted on the pump means that the pump can be used as constant or variable displacement, on the other hand the solid line plotted on the motor means that it must be variable displacement to satisfy a secondary-controlled concept.

A hydromotor representing the secondary unit is a variable displacement unit and can work as both pump and motor. It must be able to be controlled over-center allowing positive and negative torque in any direction of vehicle travel speed which is commonly referred as four quadrant of operation (i.e. forward, backward acceleration and/or deceleration).

When the system pressure is kept constant, the hydromotor output torque is directly proportional to its displacement of the secondary which can be expressed as follows;

$$M_M = \frac{\varepsilon_M . V_{M,\max} . \Delta p_M}{2\pi} \times \eta_{hm,M} \tag{6-1}$$

When increasing the swivel angle the flow requirement raises according to;

$$Q_M = \frac{\varepsilon_M . V_{M,\max} . n_M}{\eta_{V,M}} \tag{6-2}$$

Solving equation (6.1) and (6.2) together yields;

$$Q_M = \frac{2\pi . M_M . n_M}{\Delta p_M . \eta_{hm,M} . \eta_{V,M}} \tag{6-3}$$

If the pressure difference is held constant at predetermined level then the motor flowrate is directly proportional to vehicle speed and load torque. At a certain constant

speed, a change in vehicle load would result in a certain change in flow and the secondary unit reacts with a change in displaced volume. Such a relationship makes the secondary controlled hydrostatic transmission (SC-HST) particularly energy efficient since the high loads can occur at high speeds without necessarily increasing the system pressure avoiding high flow losses.

In a secondary controlled system, if the pump is controlled to keep the same pressure level in the system then the accumulator pressure will also remain constant and consequently the hydromotor pressure. This means that no energy storage can be made in the accumulator during braking. The oil flow will instead be directed back to the pump. A torque can be created which acts to unload the diesel engine. This type of energy recuperation is however not ideal in the vehicle drivetrain application. It may be suitable for other systems driving different loads which demand power from the engine.

Hence, the accumulator pressure level should vary between a minimum and maximum values to achieve as much energy recuperation as possible. The selected pressure range should allow the accumulator to store most of vehicle's kinetic energy during braking while its pressure is being raised from minimum to maximum value.

During braking the load torque becomes negative. The secondary unit starts working as a pump and effectively delivers flow from the low pressure side back to the accumulator on the high pressure side. The motor swivel angle is controlled over-center and the flow is directed back into the high pressure line, converting the kinetic energy of braking into pressure energy. The recovered energy is stored in the accumulator for later use.

6.2.2 SC-HST concept design

Components and units selection of the proposed secondary-controlled hydrostatic drivetrain is done in a similar way as for the conventional hydrostatic transmission. The introduced secondary-controlled hydrostatic transmission is designed using high pressure (HP) and low pressure (LP) accumulators to keep the balance of oil volume in the circuit as shown in Figure 6.2.

To reach the maximum torque a certain motor size is needed which depents on the gear ratio and the chosen pressure level in the circuit. Since the high pressure (HP)

side never changes in a hydraulic circuit and the four quadrants of operation are demanded from the variable displacement hydromotor, then the Rexroth reversible-variable displacement A6VM motor is a suitable to use also as secondary unit in order to meet the above requirements.

The required motor and pump sizes can be calculated when the maximum swivel angle is used as the operation point.

$$V_{M,\max} \geq \frac{2.\pi.M_{w,\max}/i_F}{\varepsilon_M.\Delta p_{M,\max}.\eta_{hm,M}} \tag{6-4}$$

On the primary side, a small constant displacement pump is suitable to charge the accumulator when needed, as it is connected to the engine shaft directly. The same Rexroth A4VG pump type applied in the conventional contentiously hydrostatic transmission represented in chapter 5 is also used in the hydraulic circuit of the secondary-controlled hydrostatic transmission to enable a fair comparison and also to use the same flow and torque losses look-up tables which are integrated in the pump and motor units.

In the SC-HST simulation model described in this chapter, the pump displacement is held constant at maximum swivel angle by supplying a constant value on the displacement controller of the pump in order to work at maximum capacity on constant flow basis as fixed displacement ones.

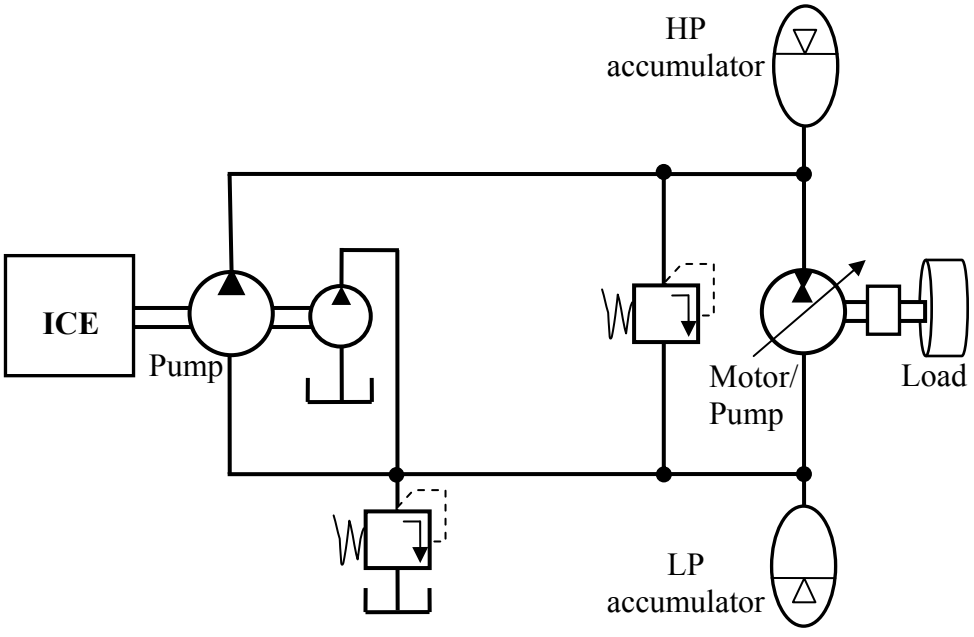

Figure 6.2: Conception design of the Introduced SC-HST circuit

A bypass valve and control switch are required on the pump side in order to run the diesel engine at a predetermined torque level, adjusted by the pressure controller installed on the accumulator as will be explained later in detail. In braking mode, the reversed flow from the hydromotor is delivered to the accumulator, making the kinetic energy available for reuse.

6.3 Hydro-pneumatic Accumulators

Accumulators are fluid power components that store potential energy and return it to the circuit on demand. Accumulators have several functions in the hydraulic circuit of the SC-HST transmission system. However, the primary functions of the accumulators in the hydraulic circuit are to stabilize the working pressure in its secure limits, make the system easier to control and conserve hydraulic energy.

In the introduced SC-HST drivetrain, a high pressure accumulator is mounted between the pump and the hydromotor on the high pressure side to change the flow coupling relationship of the pump and the motor to pressure coupling. In order to maintain the pressure coupling between the fixed displacement pump and the motor, the accumulator is controlled to operate in a certain pressure range, for instance on the high pressure side between 200 and 400 bar.

6.3.1 Sizing the accumulator

Sizing the accumulator accurately is a challenge. The selection of the proper size accumulator is important for an efficient operation. The proper pre-charge gas pressure of two accumulators being installed in each side of the common pressure rail (i.e. high pressure side and low pressure side) are critical to the operation of the system. The pre-charge of the low pressure accumulator is taken as a ratio of the minimum suction pressure of the pump but the pre-charge of the high pressure accumulator is a percentage of the minimum working pressure of the system.

Referring to Figure 6.3, the pre-charge gas pressure of the accumulator, p_o is normally just below the minimum working pressure p_{min} of the hydraulic system. This is to prevent the accumulator bladder constantly closing the anti-extrusion check valve. From the viewpoint of energy conservation; the pre-charge gas pressure can be theoretically equal to 90 % of the minimum pressure denoted by p_1, i.e. $p_o=0.9\ p_{min}$.

The maximum working pressure denoted by $p_{2,}$ is the fluid pressure when the accumulator is fully charged; this pressure should not be greater than three times the minimum working pressure, otherwise the elastomer material of the bladder may be damaged.

The volume and pre-charge gas pressure are discussed in this article from the point of view of energy recovery and reduction of pressure fluctuation; this is because both of them have a close relationship to the performance of the system. To be more conservative in sizing the accumulators, it is best to estimate a change in gas volume.

Systems using fixed-displacement pumps typically respond faster, so that smaller accumulators can be used. The accumulators will be designed according to the amount of inlet and outlet fluid through it to fulfill the actuators demands. This requires knowledge of the motion profile of the hydro-motors to calculate the amount of oil required in the accumulator; also the pump flow as a function of the pressure needs to be taken into account.

As the vehicle speed reduces from the high speed v_{F1} to the low speed v_{F2}, the decrease in kinetic energy can be expressed as,

$$\Delta E_a = \frac{1}{2} J_w \left(\omega_{w1}{}^2 - \omega_{w2}{}^2\right) = \frac{1}{2} \frac{J_w}{r_w{}^2} \left(v_{F1}{}^2 - v_{F2}{}^2\right) = \frac{1}{2} m_F \left(v_{F1}{}^2 - v_{F2}{}^2\right) \tag{6-5}$$

Where, $J_w = m_F \; r_w{}^2$ (6-6)

The energy is stored in the accumulator in the form of potential energy during braking and it is released during the acceleration process. The optimal size of the accumulator is determined by the amount of energy which has to be stored. As the rate of charging and discharging occur rapidly, then energy exchange between nitrogen and atmosphere can be considered adiabatic.

Maximum discharge quantity, optimum pressure ratio and stored energy are calculated according to the following equations neglecting power losses [7];

$$\Delta V_a = V_1 \left[1 - \left(\frac{p_1}{p_2} \right)^{\frac{1}{n}} \right] \tag{6-7}$$

$$W_{12,a} = 0.308 \cdot p_2 \cdot V_1 \tag{6-8}$$

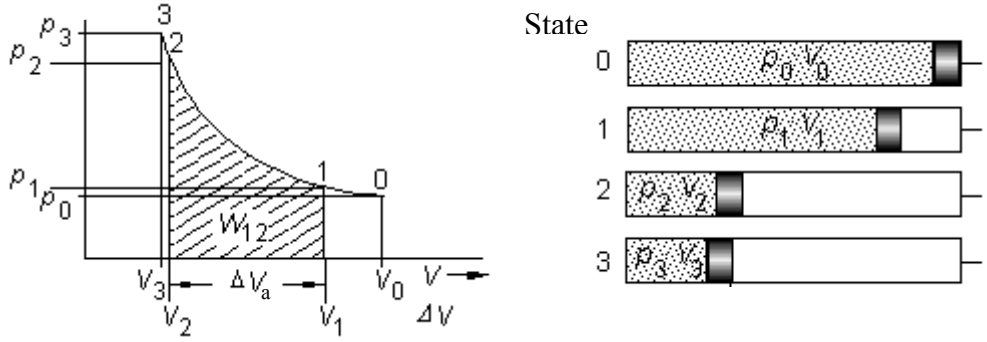

Figure 6.3: Relation between accumulator pressure and volume [7]

The calculation reveals an accumulator volume of 20 liter, which is capable of storing most of the brake energy 258.720 J or 72 Wh and cover most of the power and traction transients of the vehicle. This amount is equivalent to brake the vehicle from 60 km/hr to zero. A larger accumulator will however be both expensive and requiring more space.

For the purpose of a hydraulic circuit, a 22 liter low pressure accumulator will be selected in order to use as a make-up fluid whenever fluid is introduced into the high pressure accumulator, which assures pre-flow during engine start.

6.4 Drivetrain Architecture

A hydraulic fixed displacement axial piston pump type A4VG, size 71 cm^3/rev (Bosch Rexroth), is coupled to the engine output shaft as shown in Figure 6.4. A 20 liter bidirectional hydro-pneumatic accumulator pre-charged with N_2 at 180 bar being used as a secondary power source is located in the high pressure side of the hydraulic circuit to recuperate the braking energy and restore it to the system when needed. Another 22 liter low pressure accumulator is connected to the low pressure side that functions as a fluid reservoir.

A pressure relief valve is installed in the circuit to protect the circuit from overloads when system pressure increases higher than the secure pressure value of 420 bar. The pressure range of the high pressure accumulator which varies between 200 and 400 bar affects the necessary size of the hydromotor. A lower pressure demands a bigger displacement to create the same torque according to motor torque and

displacement relation, refer to equation 6.1. A choice must thus be made of how the primary unit should control the pressure level in the circuit.

Variable displacement bidirectional hydro-motors type A6VM (Bosch Rexroth), each attached directly to the four wheels of the vehicle, each of size 107 cm^3/rev to reduce mechanical losses is suitable to satisfy the vehicle performance.

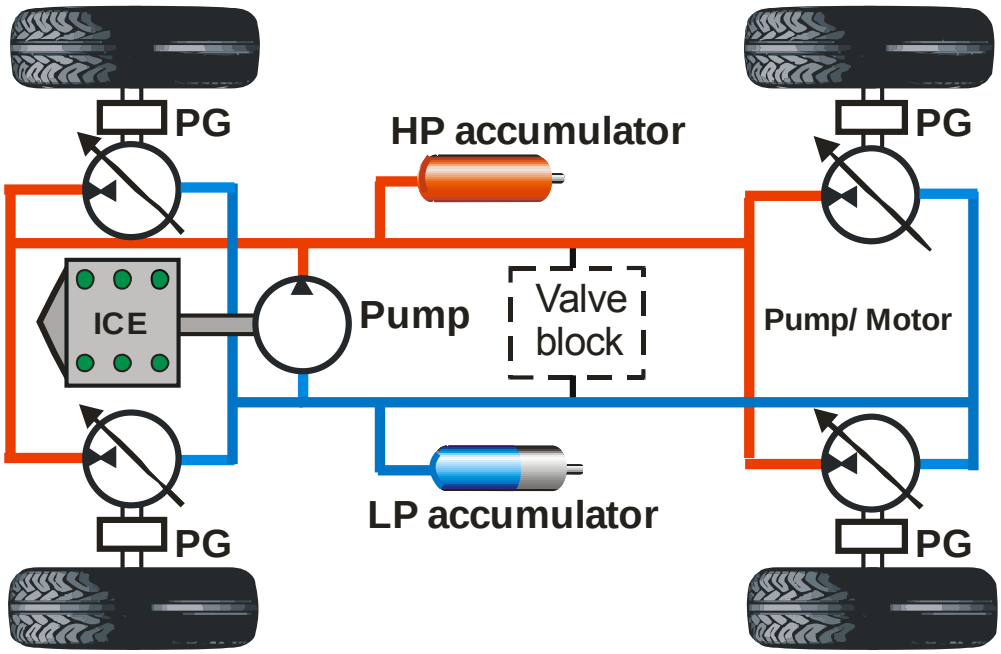

Figure 6.4: Architecture of the SC-HST drivetrain

6.5 Control Strategy

The secondary-controlled drivetrain has a speed control circuit with free variable of swivel angle or torque. When the speed is preselected, the secondary unit searches the required torque automatically in order to keep the given speed at any operating pressure.This means that a reference speed affects the motor displacement so that the speed is always followed-up. An increased load will hence make the secondary unit respond in a higher swivel angle to create an equal torque and keep the reference speed. At higher speeds, a lower pressure difference meaning that the hydromotors work with higher swivel angles to cover the road load torque. This increases the overall efficiency of the motor.

The SC-HST not only regenerates the kinetic energy of the vehicle, but it also performs the tasks of engine manager, having some energy-saving benefits [82].

When a low load is required by the vehicle, the engine can either be shut off while the accumulator alone drives the vehicle or the accumulator increases the engine load to supply extra energy to the accumulator to be stored for later use.

The accumulator pressure level is controlled via a pressure-controller which actuates the engine when the accumulator pressure goes below a specified threshold minimum value i.e. 200 bar. The engine is turned-off when the accumulator pressure goes higher than 400 bar.

Therefore the accumulator plays an important role in the system operation dominating the overall performance of the system. Since a series-hybrid omits a mechanical link between the combustion engine and the wheels, the engine is running at an efficient rate even as the vehicle changes speed. The pressure controller set value of the primary unit is correlated to the vehicle speed $p_{ref} = f(v)$. When vehicle speed increases the set pressure should be decreased, giving the system more possibilities to store energy. The optimal pressure thresholds for the accumulator would therefore be a pressure of 200 *bar* at maximum speed and 400 *bar* at zero speed.

A simplified block diagram of the SC-HST illustrating the overall control strategy is indicated in Figure 6.5.

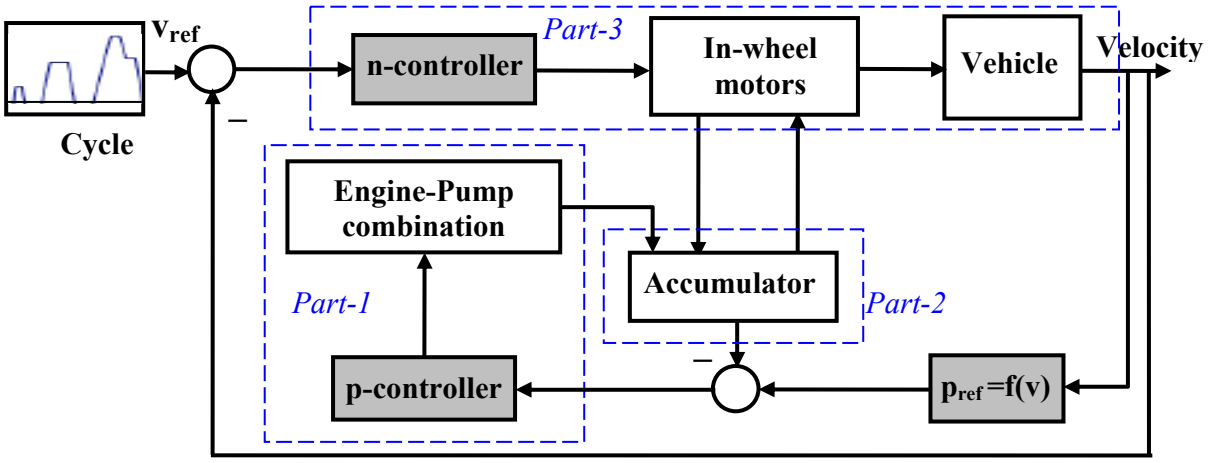

Figure 6.5: Block diagram indicating the overall control strategy of SC-HST

As shown in the block diagram, the system consists of three sub-systems. The first subsystem represents the engine-pump combination and its p-controller which controls the engine on/off according to accumulator pressure level. It is responsible for converting the thermal energy into hydraulic energy to charge the accumulator. Part 2

corresponds to the storage subsystem which is a hydro-pneumatic accumulator. Part 3 represents the traction subsystem which is composed of in-wheel variable displacement hydro-motors and its n-control to control the vehicle velocity. The interaction between these subsystems is managed by the control unit.

6.6 Simulation Model

The simulation model depicted in Figure 6.6 has been built to evaluate the performance of the proposed control strategy developed for the SC-HST drivetrain. The model investigates the effects of driving patterns on the engine and estimates the vehicle's energy use, emissions and fuel consumption for a range as in the NEDC cycle.

There are two independent PID-fixed gain controllers used in the model. The first is a speed-controller located at the hydro-motors side to actuate their displacement according to load demand on the wheels. The resulting error in speed between the commanded and actual velocity is controlled by the speed controller and then saturated to limit the controlled signal. The final saturated signal is used to adjust the hydromotor swivel angle to obtain the required vehicle velocity. The error of saturation is only active in accelerating movements since the flow generated from the secondary unit, at braking motion, is not limited.

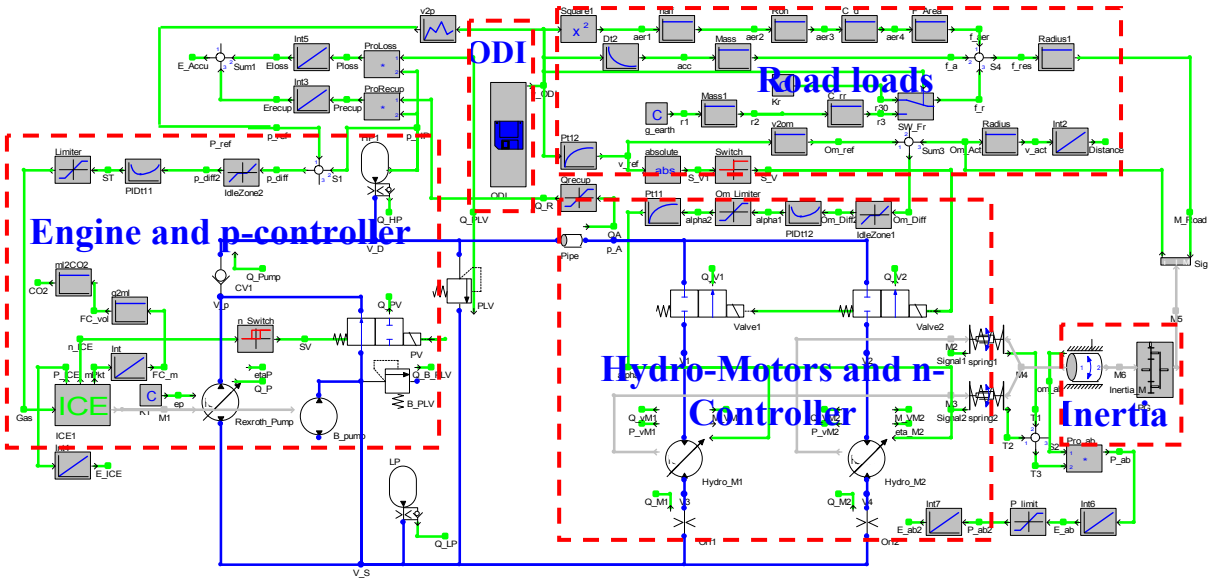

Figure 6.6: Simulation model of SC-HST drivetrain in DSHplus

The basic task of the primary side of SC-HST is to control the energy charge level of the accumulator that is made by means of controlling fuel quantity to the engine. The accumulator pressure level is monitored and regulated so that it stays in a secure operating range by the pressure controller. The pressure controller stands for controlling the high pressure line and consequently the engine operation. The difference between the current set pressure and the accumulator actual pressure in the circuit are compared and controlled with a traditional PID-controller. The output signals from the PID-controller are then saturated to keep the control signal within limits.

The complete engine and pressure controller comprises of an input pressure signal from the accumulator, limiter, noise filter, gas throttle valve signal, an angular velocity switch and a solenoid venting valve (shuttle valve). The solenoid valve will also be connected to the ICE starter, so that the pump can start the engine under no-load from stand-still through stored energy in the HP accumulator. The hydraulic circuit is equipped with a check valve at the pump output to prevent the stored energy from escaping through the pump, and an electrically controlled shut-off valve to block-out the flow to the motors during standstill. An additional pressure relief valve sets the maximum pressure in the circuit. The Online Data Import (ODI) is used for implementing the NEDC cycle in the simulation while the controller tracks the required vehicle speeds.

6.7 Results and Discussion

Similar to the conventional hydrostatic transmission the SC-HST simulation model was also run for the NEDC driving cycle to get fuel consumption and CO_2 emissions as well as the drivetrain is variable performance during the cycle. This cycle is selected for purpose of analysis as it includes hard acceleration, cruising at constant velocities and braking phases. The simulation results are performed on the on-off control strategy. All of the initial conditions and input data such as vehicle parameters and command velocity from the cycle are the same as the previous CV-HST simulation model described in chapter 5.

6.7.1 Engine operating points

The engine's operating points for the SC-HST transmissions during the NEDC is depicted in *Figure 6.7*. It is clear for the figure that, by using SC-HST in the vehicle drivetrain, the operating points were moved to the highest efficiency region. This is a direct result of using the pressure controller which permits the engine to run under high load only in the defined range of operation of the accumulator of 200 to 400 bar.

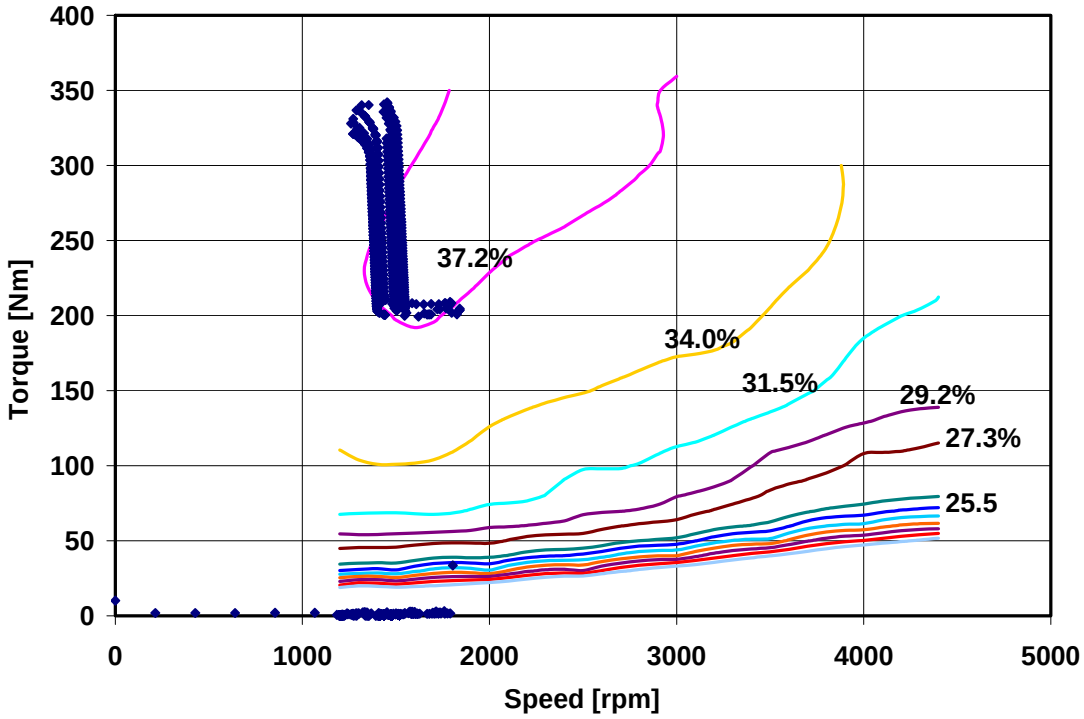

Figure 6.7: Engine operating points of the SC-HST drivetrain

6.7.2 Characteristics curves

A complete profile of the simulation result for the driving mission in NEDC cycle is shown in Figure 6.8. The first curve shows that the actual vehicle velocity is completely tracking the commanded velocity along the mission NEDC cycle. The system pressure in the drivetrains is maintained in the secure range of the accumulator ranging from 200 to 400 bar as indicated by the 2nd curve.

The vehicle begins and ends operation with a fully charged accumulator. The accumulator pressure decreases with increasing vehicle speed until it reaches 200 bar. At this minimum threshold value, the pressure controller actuates the engine on. Referring to the third curve, it shows the engine speed profile during the driving cycle. The curve shows that the engine is turned on corresponding to each lowest pressure

valley, at which the pressure controller actuates the engine on to recharge the accumulator again, up to the upper secure limit. The engine first run is at 75.5 sec from cycle start, as the energy of the accumulator reaches the minimum limit.

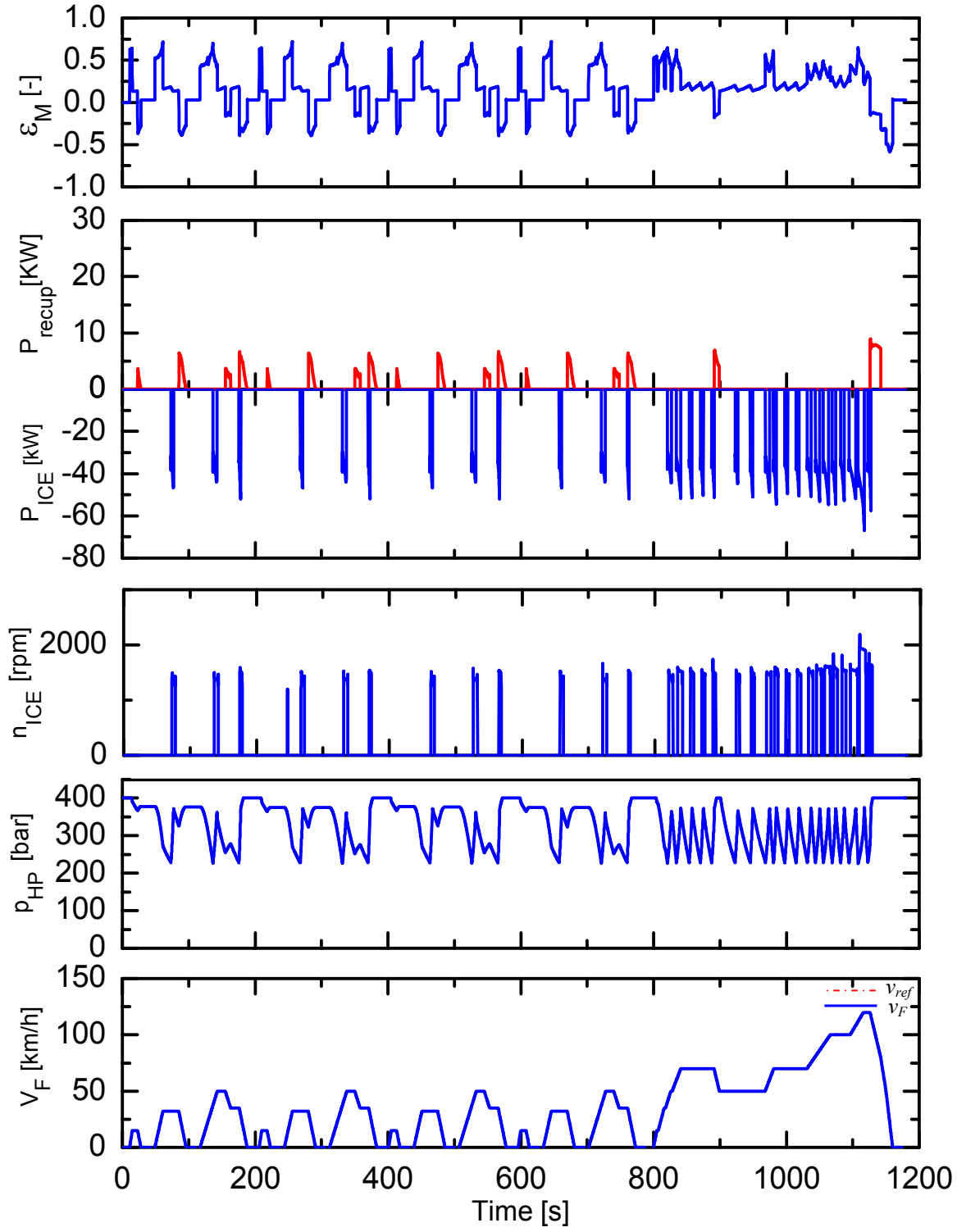

Figure 6.8: Characteristics operation curves of SC-HST during the NEDC cycle

The system analysis reveals that the engine run approximately 21 % of the mission cycle time. The engine in the SC-HST drivetrain runs nervously on short times as shown by the engine speed curve. This is due to the pressure difference on the accumulator being the same as that on the wheel motor, i.e. the pressure on load side is the same on the accumulator side, causing high variations in the working pressure during the cycle. The fourth curve shows the power consumed for each period of engine run. The fifth curve shows the recuperated power during the driving cycle which corresponds to each braking phase in the vehicle.

The swivel angle setting ratio of the variable displacement hydromotor is shown in the top curve of the diagram. As shown, the swivel angles have positive angles in propulsion mode and negative angles during braking mode.

6.7.3 Hydromotor operating points

The operating points of the hydro-motors are depicted during the drive cycle in Figure 6.9.

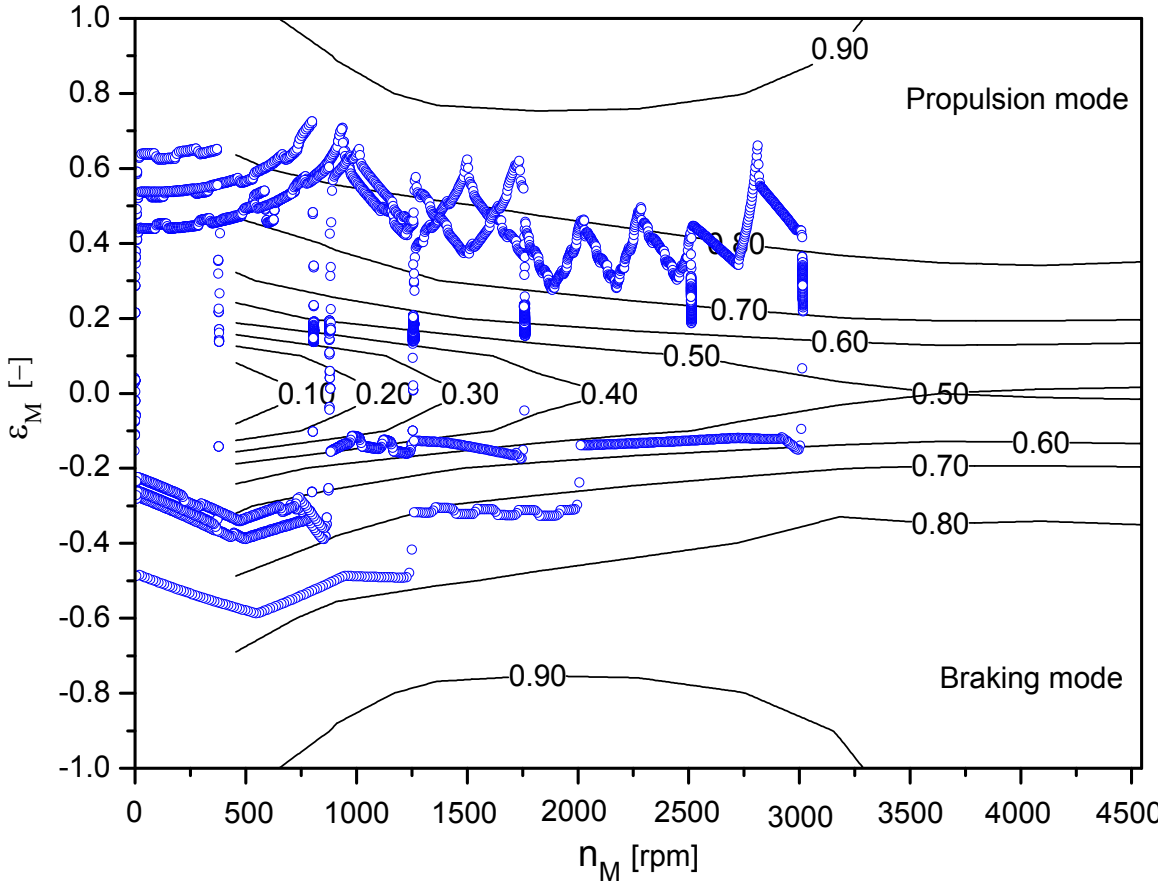

Figure 6.9: Hydro-motor's operating points during the NEDC cycle

The shown diagram can be divided into two parts with respect to the y-axis which refer to the displacement setting of the hydromotor. The upper part, i.e. the positive displacement range, represents the operation point of the hydromotors under road load in the travelled distance during the cycle. The lower part which lies in the negative displacement range of the motor represents deceleration case.

The average motor efficiency in driving mode is approximately 79 % and average of 67 % during braking mode. During deceleration operation the hydromotors are swiveled over-center to the negative swivel angle in order to gain maximum braking torque while reducing vehicle speed. In this case, the hydromotors reverse their flow direction and operate as pumps delivering flow streams against the main flow stream which cause a momentarily rise in system pressure.

6.7.4 Fuel consumption and CO_2 emissions

Fuel consumption and CO_2 emission resulting from the simulation models of the SC-HST are compared to the baseline vehicle as shown in figures 6.10 and 6.11.

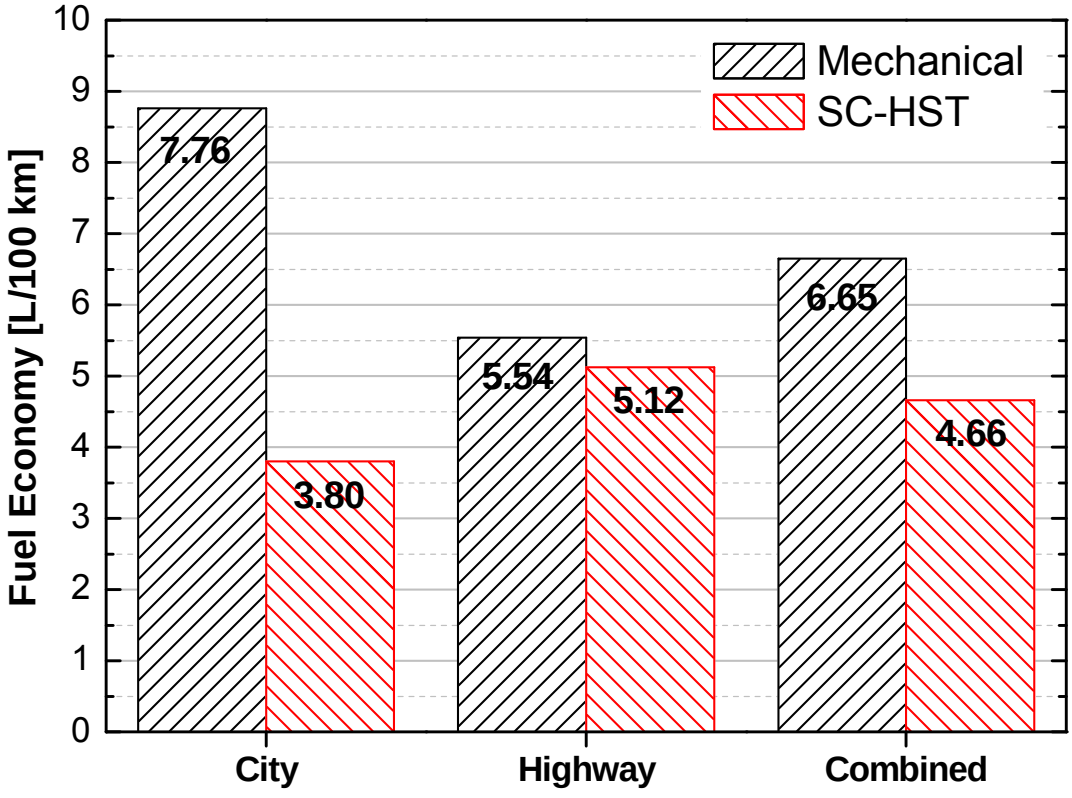

Figure 6.10: Fuel consumption of the SC-HST versus mechanical during the NEDC cycle

The results show that the fuel consumption and consequently CO_2 emissions are reduced by amount of 30 % in the SC-HST compared to the conventional baseline vehicle.

The CO_2 emission is reduced to about 123.37 g/km. The additional total reduction of fuel and CO_2 during the NEDC cycle was gained by SC-HST drivetrain due to its abilities to recuperate a part of the braking energy in the high pressure accumulator and reusing it during propulsion and also due to shutting the engine off when the accumulator pressure is above the minimum value or during braking. The reuse of the system energy substitutes some of the losses in the transmission system.

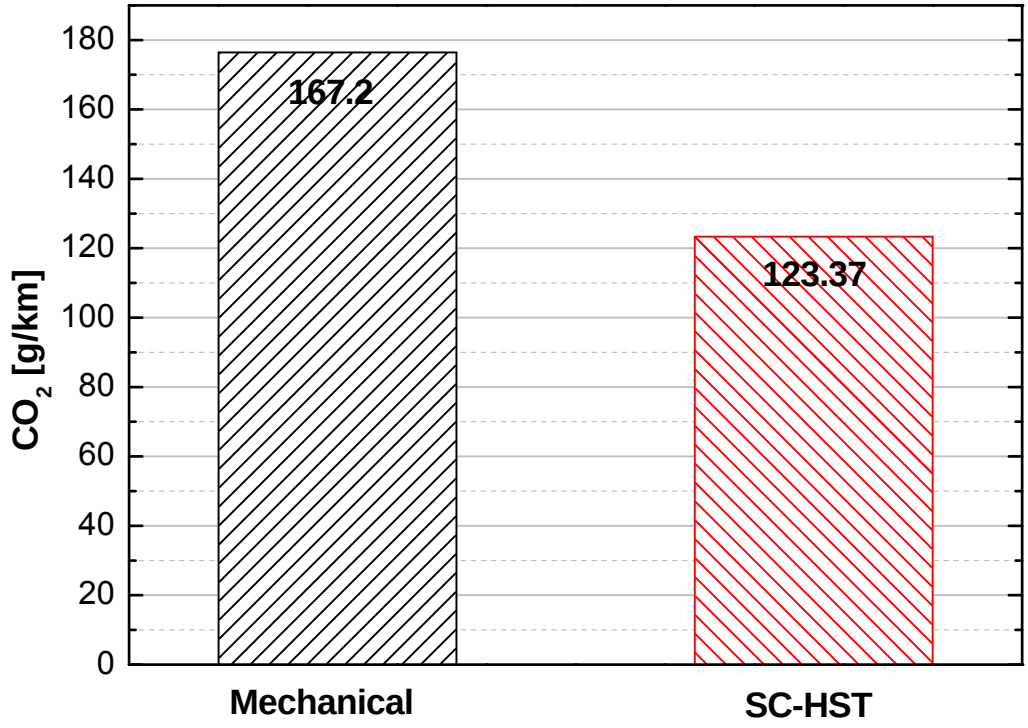

Figure 6.11: CO_2 emissions of the CV-HST versus mechanical during the NEDC cycle

6.8 Conclusion

Generally, the secondary-controlled hydrostatic transmission is considered as the basic form of the series hydraulic hybrid, which uses one of the current market hydraulic components. Fuel consumption and consequently CO_2 emissions can be reduced considerably by adding a hydraulic accumulator as a secondary power source to the primary combustion engine which will tend to improve the round-trip efficiency.

The aim of using this type of standard series hydraulic hybrid or the secondary-controlled hydrostatic transmission is to increase the whole system efficiency with

efficient use of the primary power source, efficient management of energy for motion and efficient recovering and reuse of braking energy.

This chapter assesses the potential fuel savings and emissions reductions associated with hydraulic hybridization for the baseline vehicle. Two traditional PID-controllers were used to regulate the operation of the drivetrain. A speed controller is responsible to track the desired velocity input, and a pressure controller is responsible for keeping the high pressure accumulator, and consequently the high pressure line, in effective secure limits between 200 to 400 bar.

The strategy implemented on the introduced SC-HST drivetrain forced the engine to run only under medium to high loads avoiding low and partial operation which consumes large amounts of fuel. Furthermore, it is highly efficient even under partial road loads conditions. By doing so, the engine off time reaches approximately 79 % the cycle time.

The results indicate that secondary-controlled hydrostatic transmission as a conventional hydraulic hybrid system has the potential to reduce fuel consumption and consequently CO_2 emissions. SC-HST offers good fuel saving of approximately 30 % compared to the mechanical transmission during the standard NEDC driving cycle, but the SC-HST drivetrain still suffers from high pressure variations. These variations in pressure arise from that the road load changes which have a direct effect on the accumulator pressure, i.e. all the load needs should be covered by the accumulator.

Furthermore, the secondary controlled hydromotor suffer from low level of efficiency at low motor displacement during low loads. The efficiency of the variable displacement motors is very low at low speed and torque, i.e. at low power demands, which are typical for average driving condition in the NEDC. Therefore there are still some deficiencies in applying SC-HST such as variable displacement motors being large units, heavy and less efficient than constant ones. The high mass of the motors increase the suspended weight of the wheels. Also the current motors may suffer from slip-stiction friction, which might reduce the torque at brake-away conditions.

It is better if possible to choose a fixed displacement motors at the vehicle wheel which can operate at a high pressure range over the current units, in order to reduce drivetrain weight and increase efficiency. A hydraulic transformer can separate

the accumulator from the pressure variation on the load side to increase the stability of the system. It can manage system pressure according to load demands and cover the pressure gap between pressure source and load side avoiding repeated on-off run for the engine. It can also amplify the high pressure line even if the accumulator pressure reaches the minimum threshold of 200 bar or amplify the pressure in the motor side to the accumulator during braking to increase the stored energy.

In this case the speed controller should be moved from the motor to the transformer. If a state of the art transformer is used, it will suffer from the same problems as conventional motors, such as low efficiency, big size and high weight. A new design of hydraulic transformer and high pressure range fixed displacement units is required to accomplish the required performance.

Chapter 7

Novel Series Hydraulic Hybrid Vehicle

“The Hy*d*rid”

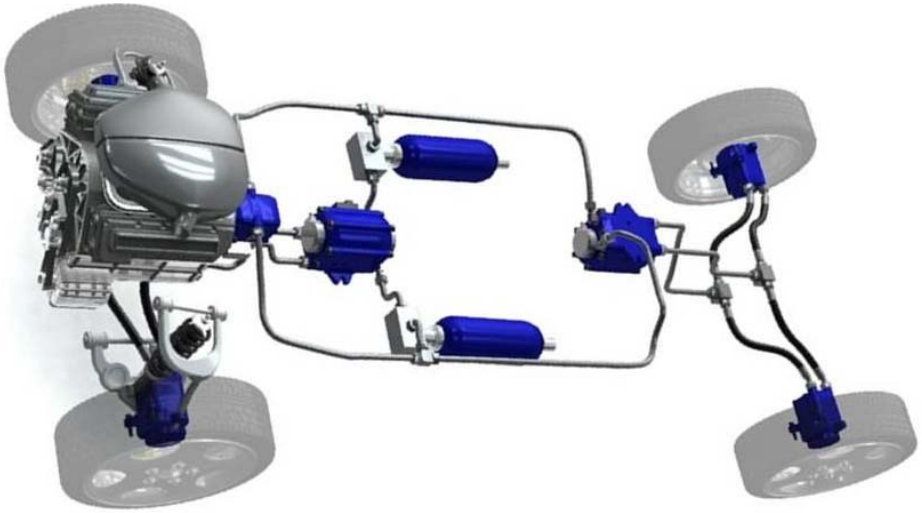

7.1 Introduction

Automobile and vehicle manufacturers are directing their effort towards designing and producing less polluting and more fuel efficient vehicles in order to meet the new tough emissions regulations issued by many committees such as the American EPA and the European Environmental Agency (EEA) to help reduce air pollutions. The development of new vehicles to reduce fuel consumption and emissions is a prerequisite to protect humans and the environment.

One way to improve fuel economy and reduce the emissions of a vehicle is to hybridize it. The word "Hybrid" has its origin in the Latin language and means: "a Mixture or combination of two things" [84].

A hybrid drivetrain consists of at least two energy conversion devices. The first one is an irreversible primary power source such as an internal combustion engine (ICE) which converts the long-term chemical energy stored in a fuel into mechanical rotation. The second is a reversible secondary power source such as an electro-chemical battery or a hydro-pneumatic accumulator which converts the short-term chemical energy stored in a battery or the potential energy in the accumulator to propel the vehicle's wheels. The ICE uses the long-term chemical energy stored in a fuel, while a battery/accumulator use the short-term chemical/potential energy to drive the wheels.

By vehicle hybridization, the whole drivetrain efficiency can be increased by optimal use of the primary power source, efficient transformation of energy for motion and efficient recovering and reuse of braking energy [2].

7.1.1 Hybrid drivetrain configurations

Hybrid vehicles can have three different system configurations; series, parallel and series-parallel as depicted in Figure 7.1. These configurations can be divided into two main common technologies, electric hybrid and hydraulic hybrid. Hydraulic hybrids operate basically the same way as electric hybrids, using a motor-pump instead of an electric motor-generator and a hydraulic accumulator rather than the battery pack to store recuperated energy. A control strategy is necessary to control the power flow from both the primary and secondary power sources to the vehicle's

wheels. Nowadays, the electric hybrids are promoted and successfully applied in the automobile industry, but hydraulic hybrids are still under development.

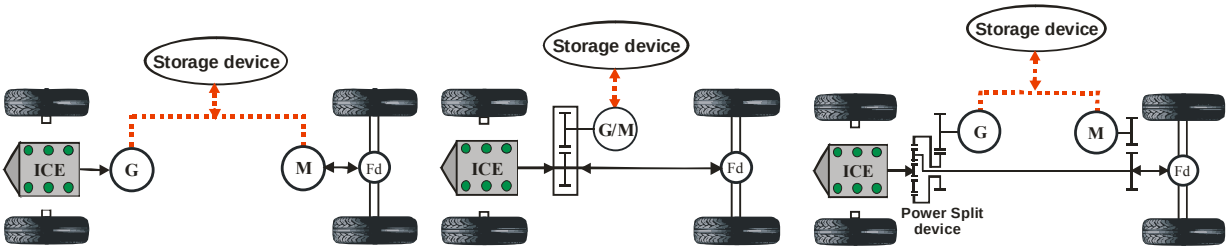

(a) Series (b) Parallel (c) Series-Parallel

ICE= Internal Combustion Engine, G=Generator/pump, M=Motor, Fd= Final drive

Mechanical connection, - - - - Hydraulic/ Electric connections

Figure 7.1: General configuration of hybrid drivetrains

***Series configuration**:* Figure 7.1-a; shows the simple layout of series hybrid vehicles. Power is supplied by an engine-driven generator/pump and/ or a storage device such as a battery or hydraulic accumulator to the motors. In this case the engine is decoupled from the vehicle load and can run in an efficient range, but all system components need to have maximum efficiency to overcome the loss of efficiency during transforming the power from one source to another. During cruises or accelerations, both the ICE and storage device supply energy to the motors. At deceleration or braking, motors works as generators/pumps to store the vehicle's kinetic energy in the storage medium for later use.

Parallel configuration: Figure 7.1-b; indicates the main components of the parallel hybrid vehicle. Both the primary and secondary power sources are connected mechanically to the main drive shaft. Power is supplied to the wheel either by the ICE or the storage device individually or simultaneously. Regenerative braking is also possible.

Series- parallel configuration: it is also known as a power split unit. It incorporates both characteristics of series and parallel configurations by using a split device connecting the engine, a generator/pump and the motor as shown Figure 7.1-c. Power is partially transferred hydraulically/electrically from the pump/generator to the motor or to the storage device and the rest is transmitted mechanically through the planetary gear set. This configuration enables the continuous variation of the speed of the

combustion engine, letting the control algorithm choose the adequate ratio between input and output, for fuel economy and performance requirements.

In hybrid systems, both serial and parallel, it is possible to eliminate idle losses (the losses that occur when the vehicle stops while the engine still runs). They also allow a better and more energy efficient integration and operation of auxiliary loads, like power steering and air conditioning system.

A series hybrid vehicle represents a second generation or second-phase of hybrid vehicles. In a series hybrid, the mechanical transmission can be completely deleted, but it requires a well done control system. Since the engine is completely de-coupled from the wheel load then it can be fully optimized for power supply and efficient operation near its peak efficiency, which is not the case in parallel hybrids. Also in series hybrid, the engine can be turned-off at those times where the vehicle is not in motion or where there is sufficient stored energy to propel the vehicle, which in turn saves fuel.

7.1.2 Characteristics of electric and hydraulic hybrid

Nowadays all hope seems to be focused on the (parallel) hybrid electric drivetrain, with the all-electric transmission on the horizon as the ultimate solution. The electric components however cause a strong increase in the manufacturing cost, resulting in limited market acceptance. Recent studies showed a very limited potential for hybrid electric vehicles of less than 10 % of the total sales volume by the year 2035. The hybrid electric transmission is also by far the most expensive option for CO_2 subsidence [85]. The cost increase of hybrid electric transmissions is inevitable. Being a parallel hybrid solution, the electric system is an add-on to the mechanical transmission, and by definition increases complexity, weight and cost of the vehicle. Despite mass production, electric transmission components remain too expensive [86]. Furthermore, the poor average cycle efficiency of the batteries and the electric motors result in a limited reduction of fuel consumption.

There are some similarities and differences between electric and hydraulic energy. It is important in hybrid vehicles to specify some characteristics of storing energy in the secondary power source (i.e. batteries or accumulator) used.

In electric hybrid; excess engine power is continually stored during a longer period of time in a battery (coarse shading) of Figure 7.2-a, and accessed only as needed (soft shading). The battery can accept a large amount of energy, but the charging process takes long time.

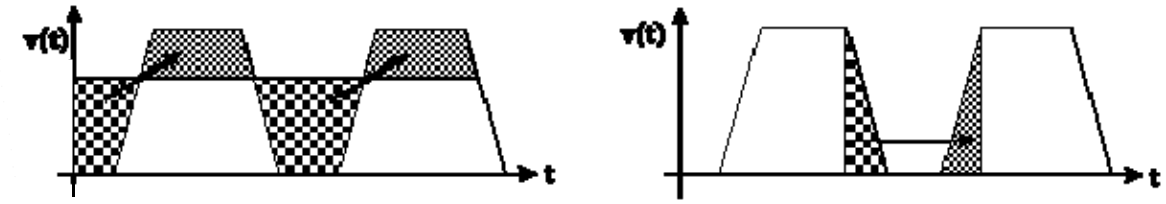

(a) *Electric hybrid* (b) *Hydraulic hybrid*

Figure 7.2: General characteristics of electric hybrid und hydraulic hybrid [84]

In hydraulic hybrid; during braking the kinetic energy is transferred to a hydraulic accumulator (coarse shading) of Figure 7.2-b, and used during accelerating (soft shading). A large amount of energy can be stored in a very short time and immediately accessed. Virtually all of the braking energy can be stored [84].

Generally, it is well known that hybrid drivetrains, electric or hydraulic, can reduce fuel consumption and carbon dioxide (CO_2) emissions, especially if a serial system could be applied. Serial systems require a maximum efficiency of the transmission components to get high transmission efficiency. Electric components have a poor power density, which increases weight and cost of the vehicle, even when considering large scale production. This would result in an increase of the fuel consumption and CO_2 emissions. Due to these shortages, most current hybrid electric vehicles are applied with parallel systems, in which the electric system does not replace the mechanical transmission, but is added to it. Parallel hybrid systems therefore have several shortcomings. They are heavier, thus more expensive and offer only a limited reduction of fuel consumption and CO_2 emission [87]. The alternative is a full hydraulic hybrid transmission.

Hydraulic systems have proven to be extremely reliable and robust. They allow a flexible layout and easy control for the drivetrain, including energy storage in accumulators. Although hydraulic accumulators have an inferior energy density, they have an excellent power density, much higher than electric batteries as shown in the Ragone diagram Figure 7.3. The low power densities of fuel cells as well as batteries

are due to their high internal resistance. They are only marginally suitable for recovering brake energy. Moreover, cyclical charging and discharging at high power rates considerably reduces their service life [88].

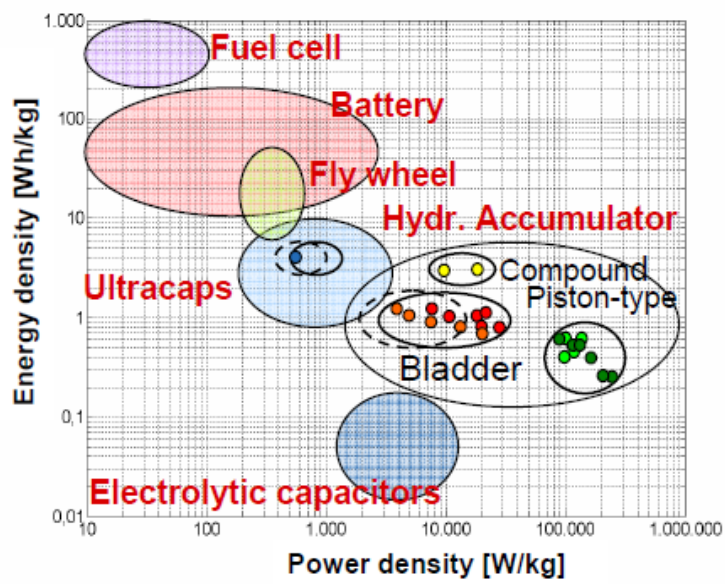

Figure 7.3: Ragone diagram of storage devices [88]

Previously, the efficiency of hydraulic pumps and motors was rather poor (similar to electric motors and generators applied in vehicles), but the recent development of the floating cup units by INNAS and digital displacement units by ARTEMIS has changed this situation [2]. Tests of the floating cup units have already resulted in total efficiency of up to 98 % [89]. They also offer a reduction in size, weight and cost, as well as noise and pulsation levels. They will be discussed in more detail within this chapter.

A hydraulic hybrid is characterized by its ability to capture regenerative braking energy quickly, compared to electric batteries which absorb about 30 % of the braking energy [2]. The high power density of hydraulic pumps/motors and hydro-pneumatic accumulators make hydraulic technology look promising for vehicles. It should be integrated in the automobile industry due to its low price and the recently developed units of high efficiency compared to electric machines [77].

The hydraulic hybrid drivetrain that will be dealt within this chapter has a particular configuration and will be referred to as “the Hy*d*rid”.

7.1.3 Tasks

- Exploring and investigating the "Hy*d*rid" drivetrain configuration and components.
- Choosing and optimizing the size of the Hy*d*rid drivetrain components (Engine, accumulators and hydrostatic units) to match the performance and requirements of the baseline vehicle, in order to minimize fuel consumption.
- Building up a simulation model of the introduced series hydraulic hybrid drivetrain using precise models for the system components (taking into account component efficiencies).
- Improving the controller setup on the basis of system performance.
- Introducing energy management strategy to obtain the highest efficiency.
- Analyzing the simulated results of fuel consumption and CO_2 emissions with the baseline vehicle data.

7.2 The Hy*d*rid Drivetrain

The general architecture of the Hy*d*rid drivetrain was introduced by the Dutch organization for scientific research Innas B.V [62], replacing the mechanical transmission with a novel series hydraulic hybrid transmission. It is tested and analyzed using DSH*plus* 3.6.1 simulation software tool at IFAS of RWTH Aachen University to evaluate its capabilities of application in passenger cars [87, 90].

The Hy*d*rid is a generic term characterized by the full hydraulic hybrid of a distinct series configuration. It includes innovative hydrostatic units such as the recently developed three port-plate Innas Hydraulic Transformer designated by IHT, a fixed displacement pump, and in-wheel hydro-motors designed on the new high efficiency floating cup technology. In addition to this a high pressure accumulator is fitted between the pump and the IHT to store the braking energy and utilizing it back during propulsion mode. The hydrostatic units used in the Hy*d*rid are designed according to the floating cup technology which is characterized by high efficiency, low torque fluctuation and low noise.

The novel series hydraulic hybrid vehicle or shortly the Hy*d*rid, is expected to compete with today's well known electric hybrid vehicle because hydraulic drives are

generally used when power to weight ratio, controllability and dynamic performance are important features. Furthermore they should to be realized at reasonable investment costs combined with long life times and low maintenance.

7.2.1 The Hy*d*rid drivetrain configurations

The drivetrain components of the Hydrid can be combined in a flexible manner resulting in different configurations. They can be used for 2WD in front or rear wheels or for 4WD i.e. all wheel drive, according to the design requirements and vehicle size.

In each configuration, the hydraulic circuit should mainly include a Floating Cup type fixed displacement hydraulic pump coupled to the combustion engine output shaft to charge the primary side. A High Pressure (HP) accumulator pre-charged with N_2 at 180 bar is mounted on the high pressure side of what is called common pressure rail (CPR), and another low pressure (LP) accumulator is connected to the other side of the CPR. The high pressure accumulator discharges (at propulsion) or receives (at braking) its charge through the Innas hydraulic transformer (IHT) of the floating cup type. The IHT is responsible for transforming power from CPR to the fixed displacement hydro-motors mounted in-line with the vehicle wheels according to demand load in the four quadrants of operation. In addition, the entire system has auxiliary components such as pressure relief valves, cooling units, oil filters and an auxiliary pump for feeding the circuit with extra fluid to prevent cavitation in the low pressure side and also to compensate for leakage in the system.

This study will focused in on the all wheel drive to be comparable with the selected baseline vehicle. In all wheel drive there are two concepts, both of them must include two units of the IHT. One feeds the front wheel motors and the other feeds the rear wheel motors.

The first concept depicted in Figure 7.4-a uses two engines of different or equal capacity as that introduced in the 6th IFK in Dresden [87]. The small capacity of engine-pump combination will drive the vehicle at low to medium demands, for instance in city operation, while the second unit is only needed to operate simultaneously for situations in which the power demand exceeds the installed power of a single engine. But this concept is expected to face many difficulties in finding space for two engines with their accessories e.g. exhaust and cooling … etc.

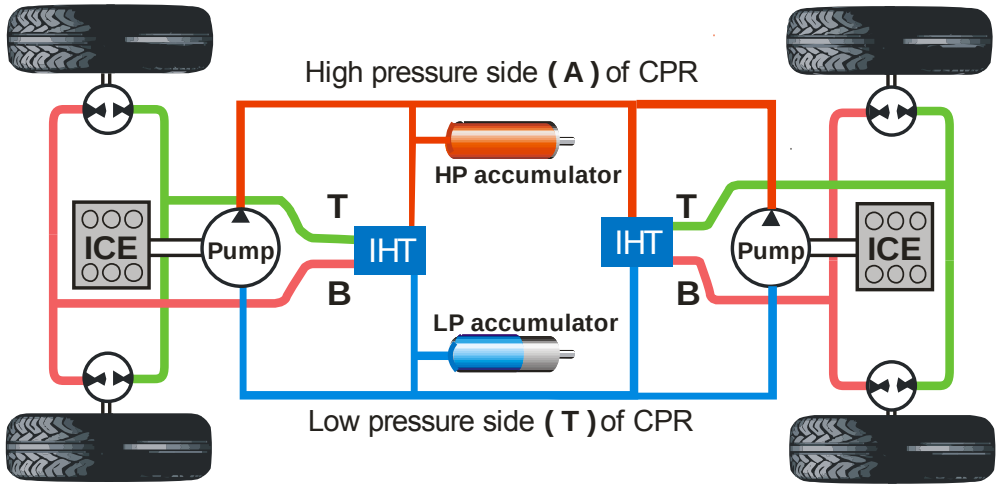

Figure 7.4-a: The Hydrid drivetrain with two engine-pump combinations for 4WD

The second concept employs only one engine-pump combination to drive the vehicle with full engine capacity are shown in Figure 7.4-b. This concept will be considered as the base of the work in this study to apply in mid-sized passenger cars and is considered in detail in this chapter.

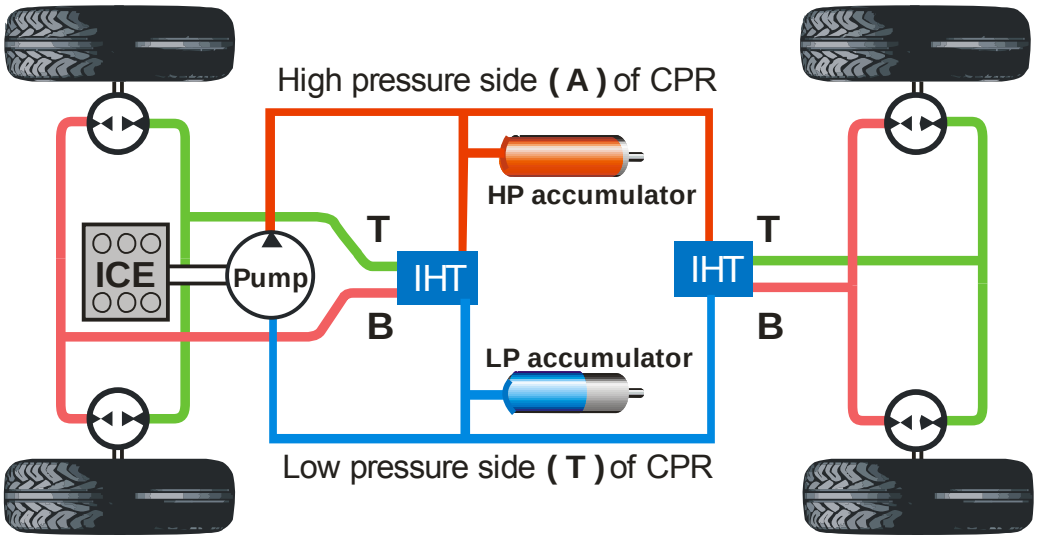

Figure 7.4-b: The Hydrid drivetrain with one engine-pump combination for 4WD

7.3 Drivetrain Components

A hydraulic hybrid will likely have a hydraulic regenerative braking system due to the existence of hydro-pneumatic accumulator. The Hydrid drivetrain, as explained above includes two power sources, i.e. combustion engine and accumulator, interacting in controlled manner with the other system components to obtain the required motion.

The basic components of the drivetrain, including the recently developed hydrostatic unit are presented in the following sub-articles.

7.3.1 The internal combustion engine

The internal combustion engine represents the primary power source in the Hy*d*rid drivetrain which is necessary to charge the hydro-pneumatic accumulator during driving. The installed power of the engine is 120 kW. It is completely disconnected from the road load in the proposed drivetrain. It is solely responsible for charging the hydro-pneumatic accumulator via a coupled fixed displacement pump with the required pressure during driving.

Depending on the effective operating pressure range of the accumulator, the torque range of the engine-pump combination will be constrained between minimum and maximum values corresponding to the maximum and minimum pressure of the accumulator. For instance the engine torque will vary between 50 % (@ 200 bar) and 100 % (@ 400 bar) of the maximum torque. The internal combustion engine is therefore forced to operate at medium to high loads, where optimum performance and high efficiency can be obtained.

7.3.2 The hydrostatic units

The hydrostatic units used in the Hy*d*rid powertrain such as the pump, motors, and Innas hydro-transformer IHT are axial piston units designed following the innovative highly efficient floating cup technology developed by Innas B.V. The three-port plate IHT and the floating cup design are considered key components for introducing the Hy*d*rid drivetrain. The IHT is used for power control and the new multi-piston principle of the floating cup units strongly increase the transmission efficiency and reduce the noise, vibration and harshness issues related to conventional hydrostatic units.

7.3.2.1 Hydrostatic pump and motor

The breakthrough technology for the Hy*d*rid is the floating cup principle for the design of its hydrostatic units. It aims to increase the average efficiency of all the hydrostatic components in the Hy*d*rid such as axial piston pump, transformer(s) and hydro-motors and consequently the overall transmission efficiency. Figure 7.5 depicts

a floating cup unit having 24 pistons arranged in a double ring back to-back configuration.

The Floating Cup Principle (FCP) was constructed with double faced pistons to create a mirrored design. An important advantage of this concept is the complete balancing of hydraulic forces in axial direction. This enables the use of small, simple bearings. The torque on the shaft is still very small compared with conventional axial displacement units.

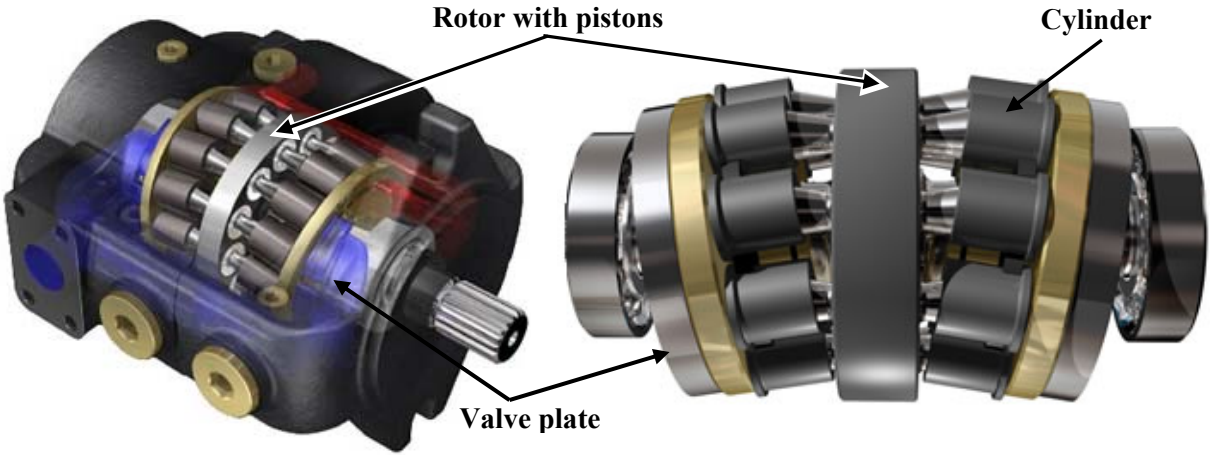

Figure 7.5: A floating cup hydrostatic unit [60]

A floating cup pump was investigated by IFAS of RWTH Aachen University. Two basic types of hydrostatic units were compared to the floating cup unit. The study reveals that key features of the floating cup unit are low flow pulsation and low piston friction losses.

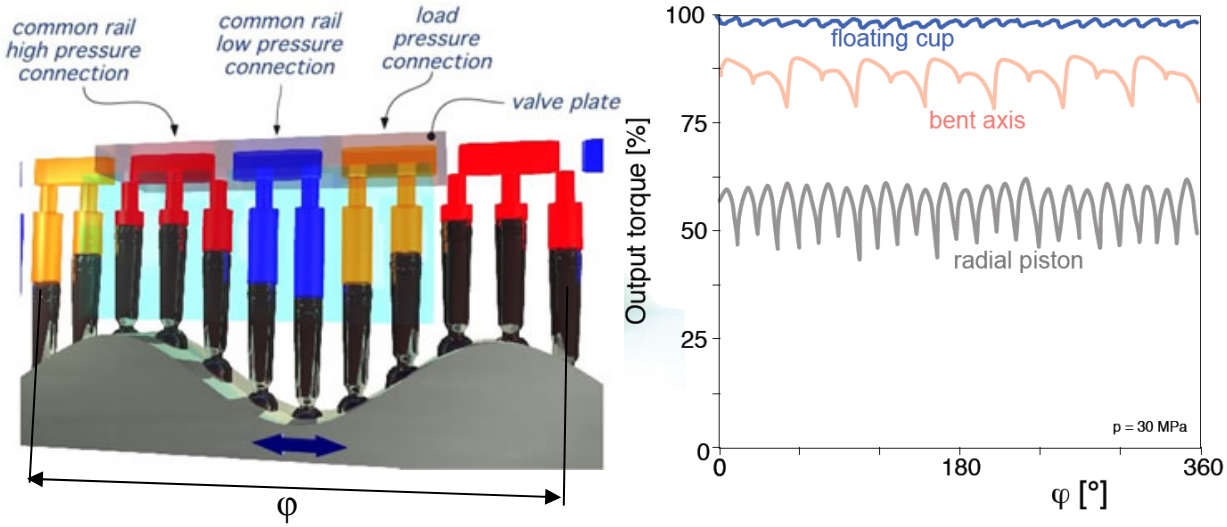

Figure 7.6: Variation of output torque of FC motor versus state of the art axial piston units [89]

The effect of the low friction losses and the high number of pistons can be seen in the diagram of Figure 7.6 which shows the torque output (relative to the maximum theoretical torque) measured at a low rotational speed (< 1 rpm) of a floating cup motor, compared to a bent axis and a radial piston motor. Noise and vibration are low as a result of low pulsations especially due to the high number of pistons (24 pistons) compared to the traditional units having from 7 to 9 pistons.

The floating cup principle exhibits the optimum performance with minimum losses and higher efficiency in a wide range of operating conditions with an efficiency exceeding 95 % as shown in Figure 7.7. In addition, the hydro-mechanical losses are very low at the operating condition of low speeds in combination with high loads. This makes the floating cup principle very attractive for application in hydrostatic motors. The power density of the slipper type, bent axis and floating cup machine are comparable.

Normally, hydraulic motors suffer severely from stick-slip friction, which strongly reduces the torque at brake-away conditions. Furthermore most motors have a smaller number of pistons (or other displacement volumes). This results in a large variation of the drive torque of these motors, which is not the case in the floating cup design. The floating cup machines also exhibit hardly any coulomb friction. Therefore, the torque delivered by the floating cup motors is close to the theoretical torque, as evaluated by IFAS of RWTH Aachen [90].

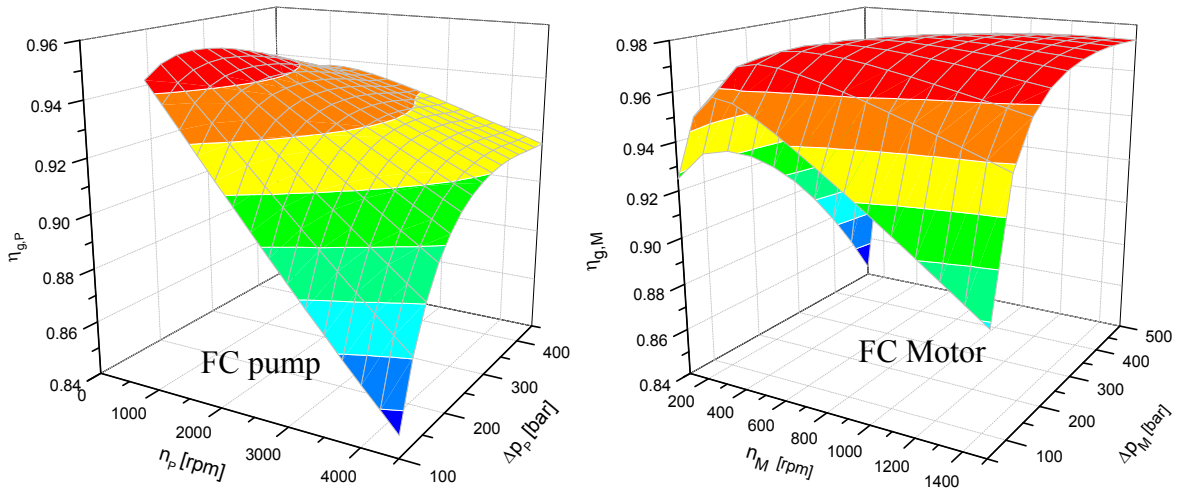

Figure 7.7: Efficiency of the FC pump and FC motor

7.3.2.2 Innas Hydraulic transformer

The Innas Hydraulic Transformer (IHT), depicted in the left part of Figure 7.8, is responsible for transforming power from the high pressure side of the common pressure rail (CPR) to the in-wheel hydro-motors, according to demand load in the four quadrants of operation on constant power basis with high efficiency. IHT converts the difference in pressure between the power source side and that required by the in-wheel motors on the demand side by simultaneously changing the ratio between its inlet and outlet flow. The possibility of transferring a flowrate at a relatively low pressure level to another at a higher pressure level offers the option to recuperate energy from the wheel motors to the CPR and store it in the accumulator. It can transfer energy in both directions, i.e. from higher to lower level on constant power basis and vice versa with high efficiency like an electric transformer [60]. It is used for power control and is characterized by its high flexibility, high efficiency and small weight.

The IHT is used to convert hydraulic energy by keeping the product of pressure and flow at the input side (A) equal to the product of the pressure and flow at its output (B) with the consideration of it's high efficiency as shown by its characteristic curve on the right part of Figure 7.8, the conversion is also reversible. In case of throttling as in valves, pressure drops while the output flow equals the input flow. A pressure decrease through the IHT will result in an increase of flow. A third flow connection is added to the tank to fulfill mass conservation. The transformation can also occur in the other direction, i.e. during deceleration, where a low load pressure can be transformed to the common pressure rail level with a smaller flow enabling energy recuperation.

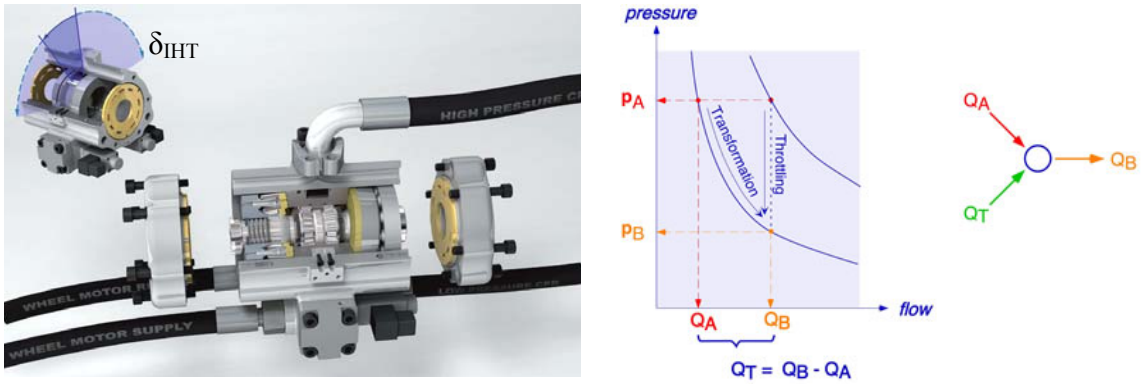

Figure 7.8: IHT unit and its operation principle [60]

The ratio between input pressure and output pressure as well as that between supply flow and delivered flow can be chosen by setting the angular position of the port-plate (δ_{IHT}). The IHT principle could best be compared to an electric transformer where the product of voltage and current in principle remains constant. A small servo-positioning mechanism installed inside the IHT determines the angular position of the port-plate that controls the inlet and outlet pressure of the transformer according to the required vehicle speed [60].

The transformer used in the Hy*d*rid is a four quadrant design and it has basically three ports in its port-plate. Port-A is connected to the high pressure line; it represents the supply port during vehicle propulsion. Port-B is connected to the load side feeding of the hydro-motors. Port-T is connected to the low pressure side or the tank. The transformation ratio can be expressed as,

$$\Pi = \frac{p_B}{p_A} = \frac{Q_A}{Q_B} = \frac{-\sin\frac{\alpha}{2}.\sin\delta_{IHT} - \frac{p_T}{p_A}.\sin\frac{\gamma}{2}.\sin(\delta + \frac{\alpha}{2} + \frac{\gamma}{2})}{\sin\frac{\beta}{2}.\sin(\delta_{IHT} - \frac{\alpha}{2} - \frac{\beta}{2})} \qquad (7\text{-}1)$$

Where δ_{IHT} is the port-plate control angle and α, β and γ are the arc length of the ports A, B and T, respectively.

This equation has been plotted in Figure 7.9 for an ideal IHT, with three kidneys spanning an arc of 120° each and with the make-up pressure put to zero. The figure shows that an IHT can transform the pressure down or up.

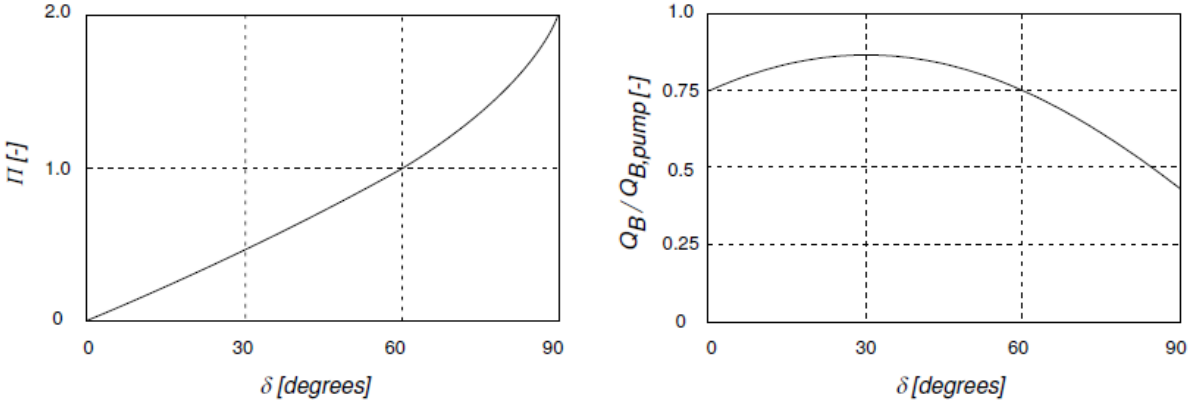

Figure 7.9: Pressure transformation curve and scaled flow [58]

The efficiency of the IHT can be expressed by the following formula during propulsion and braking modes respectively.

$$\eta_{IHT,P} = \frac{p_B Q_B}{p_A Q_A + p_T Q_T} \tag{7-2}$$

$$\eta_{IHT,B} = \frac{p_B Q_B + p_T Q_T}{p_A Q_A} \tag{7-3}$$

The left part of Figure 7.9 shows the theoretical pressure transformation of an IHT, each spanning an arc length of 120°. Π is only a function of the port plate control angle.

The diagram shows that the supply pressure can also be amplified. Here the curve is given up to $\delta_{IHT} = 90°$, which gives a theoretical maximum value of $\Pi = 2$. The port plate can be turned further to reach even higher amplification factors, but at higher values of δ_{IHT} the transformation efficiency will gradually worsen [58]. The efficiency of the IHT is shown in Figure 7.10.

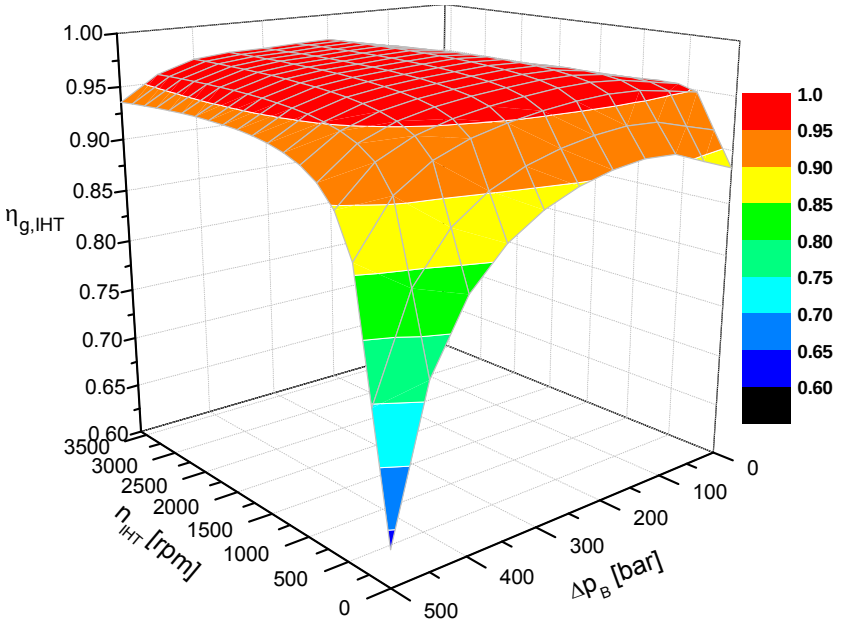

Figure 7.10: Total efficiency of the IHT

7.3.3 Common pressure rail

The common pressure rail (CPR) is considered a new approach in hydraulic systems. It separates the hydraulic power unit (pump) from the loads (motors and cylinders) as shown in Figure 7.11 i.e. loads do not influence each other. A high and a low pressure bladder gas accumulator is mounted on each side of the CPR.

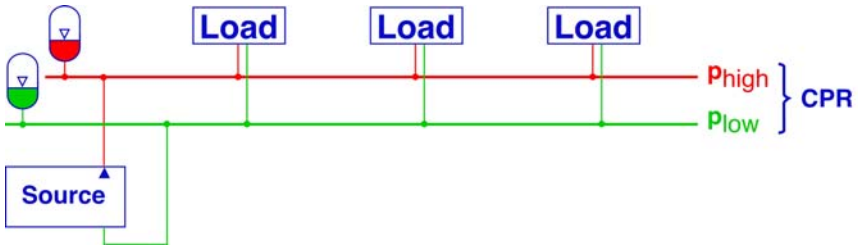

Figure 7.11: Common pressure rail [58]

By means of hydro-pneumatic accumulators the pressure level of the common pressure rail can be varied in a controlled manner. The energy that is stored in accumulators can be used for power management and energy recuperation. The pressure does not necessarily have to be constant, as hydraulic transformers are used as control devices between the pressure side and load side. The CPR technology enables a much simpler and more flexible 'plug-and-play' approach of hydraulic circuits, in analogy to constant voltage electric systems by the electricity grid [58].

7.3.4 Accumulator State Of Charge (SOC)

The hydro-pneumatic accumulator stores energy in a similar way to electric batteries. The accumulator is subjected to frequent charge and discharge phases, which leads to use the same terminology of the battery State Of Charge (SOC).

In the Hy*d*rid drivetrain, the accumulator attains its energy either from the in-wheel motors during vehicle deceleration or directly from the engine depending on its SOC. The effective band of the accumulator SOC is related to its gas pressure. The effective pressure range of the accumulator varies between 200 and 400 bar. So the state of charge of a hydro-pneumatic accumulator will be defined as the ratio of the difference in instantaneous fluid pressure and the pre-charge pressure to the difference in maximum fluid pressure and pre-charge fluid pressure.

Figure 7.12 illustrates the SOC of an accumulator in terms of pressure. For the purpose of conserving energy, the effective fluid volume (ΔV) is corresponding to the effective band of the SOC. The minimum state of charge SOC for the high pressure accumulator occurs when it has very little fluid in it, and the bulk of the fluid is in the low pressure reservoir.

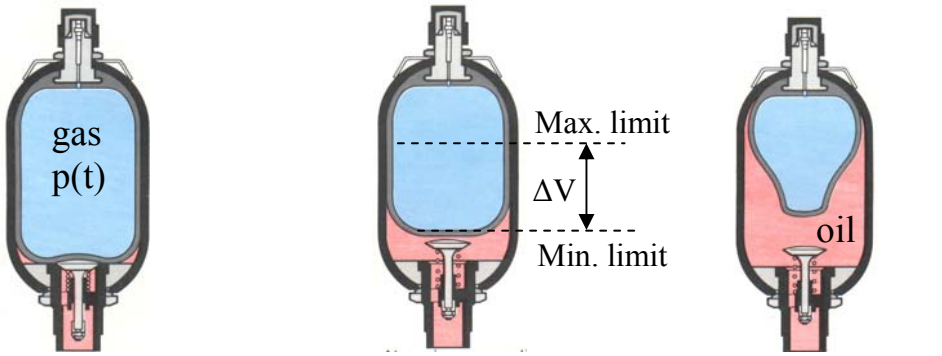

(a) Pre-charge pressure
p (t) = p_o= 180 bar
SOC=0

(b) Working pressure
180 bar< p (t) <420 bar
0<SOC<1

(c) Maximum charged
p_{max} = 420 bar
SOC=1

Figure 7.12: State of charge (SOC) of the accumulator in terms of pressure

7.3.5 Dimension and characteristics of the hydraulic components

The hydraulic transmission must fulfill the same demands as the mechanical transmission and therefore has to deliver the same peak power, speed and torque performance as the conventional drivetrain. Aside from this, the Hy*d*rid drivetrain shown in Figure 7.13 can be optimized to meet the requirements of the more modest normal drive and to match the performance and requirements of the conventional vehicle and to minimize fuel consumption. The system components were sized to achieve a performance similar to that of existing midsize vehicles. Component limitations, such as maximum speed or torque, are taken into account to ensure the proper behavior of each component.

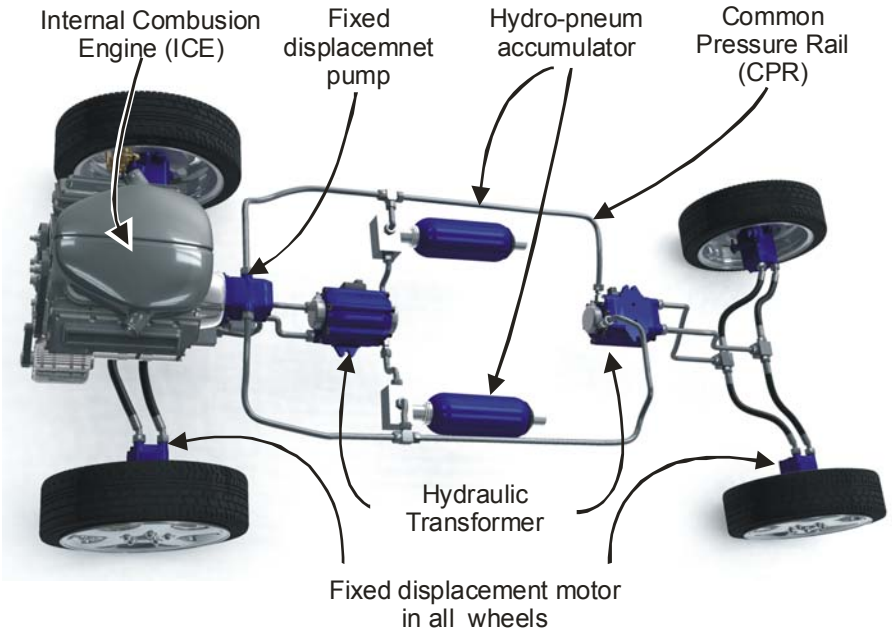

Figure 7.13: Layout of the series Hydrid drivetrain [87]

The cycle simulation is performed with a 60 cm^3/rev pump, 60 cc/rev transformers 65 cm^3/rev in-wheel motors with accumulator size equal to 20 L which can be charged to a maximum pressure of 420 bar. All hydrostatic units are selected to operate on the floating cup principle which have 24 pistons and therefore deliver flow at only 1.4 % torque variation. The analysis will concentrate on one of many possible configurations of the Hy*d*rid.

Table 7-1: *Dimensions and characteristics of hydrostatic components of the Hydrid*

Component	**Pump**	**Hydraulic transformers**	**Motors**
Quantity	1	2	4
Size of each unit	60 cm^3/rev	60 cm^3/rev	65 cm^3/rev
Maximum Δp	420 bar	CPR-side: 420 bar Motor-side: 500 bar	500 bar
Maximum rotational speed	6000 rpm	3000 rpm	1900 rpm

7.4 Simulation Model and System Control

The simulation model of the Hy*d*rid drivetrain was done in DSH*plus* 3.6.1 software, including components loss model and static component models to study the benefits of implementing hydraulic hybrid in the baseline vehicle. One of the main objectives of the simulation was to develop a simulated environment for testing the proposed control strategy developed for the Hy*d*rid drivetrain. Therefore, the system should have the ability to operate the load in four quadrants of operation, i.e. forward and backward motion - acceleration or deceleration, the ability to brake or drive the vehicle and the ability to operate under various load conditions.

However, more than the aforementioned drivetrains, the robustness of the applied power and control strategy of the Hy*d*rid is dependent on the driving cycles which may include aggressive or smooth patterns. Therefore, two additional practical world-wide driving cycles are implemented in the Hy*d*rid simulation model. These cycles are the Japanese 10/15-mode and the American Federal Test Procedure FTP-75.

The Japanese cycle is a modal cycle representing congested driving. This is particularly relevant for an evaluation of hybrid vehicles because the two electrical hybrids that have been commercially introduced so far – Prius and Insight – are both

Japanese and have been tested on this cycle. The American FTP-75 is a transient cycle which gives a better representation of real driving patterns [86].

Operation performance, system variables behavior, fuel consumption and CO_2 emissions will be evaluated for each cycle.

7.4.1 Simulation model building

Throughout the simulation the command input of the vehicle speed is dependant upon the input driving cycle. One of the purposes of the simulation model is to investigate the effects of different driving patterns on the engine and to estimate the vehicle's energy use, emissions and fuel consumption for a range of driving cycles.

As shown in Figure 7.14, the hydraulic circuit is equipped with a check valve at the pump output to prevent the stored energy from escaping through the pump. An additional pressure relief valve sets the maximum pressure at the pump side to 420 bar and at the motor side to 500 bar. The Online Data import (ODI) module is used for implementing the driving cycle in the simulation model while the controller tracks the required vehicle speeds.

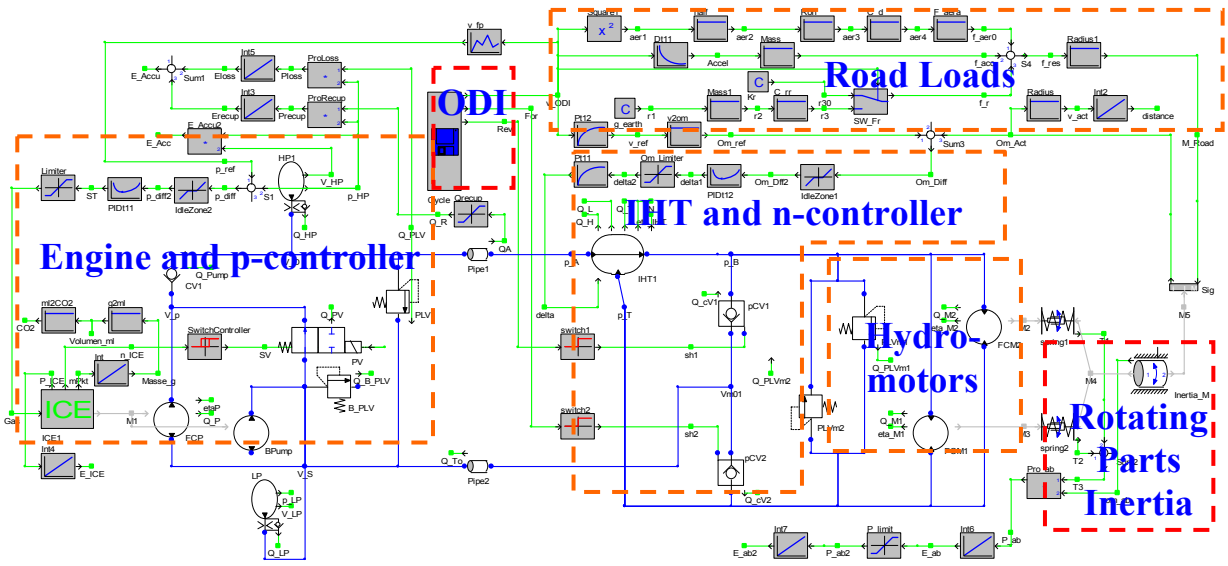

Figure 7.14: Simulation model of the Hydrid drivetrain in DSHplus

A separate fluid supply achieved by a feed pump must be provided to compensate the leakage in the pump, IHT and motor units on the low pressure side.

A part of the simulation model indicating the motor side is depicted in figure

7.15-a. As shown, the hydro-motors are equipped with two cross-line pressure relief valves to limit the hydro-motor pressure to 500 bar.

There are also two pilot-operated check valves (CVs) installed on the motors side which are used to control the flow passes depending on the direction of motion. During stand still, valves are normally closed and work as brake valves to prevent vehicle motion.

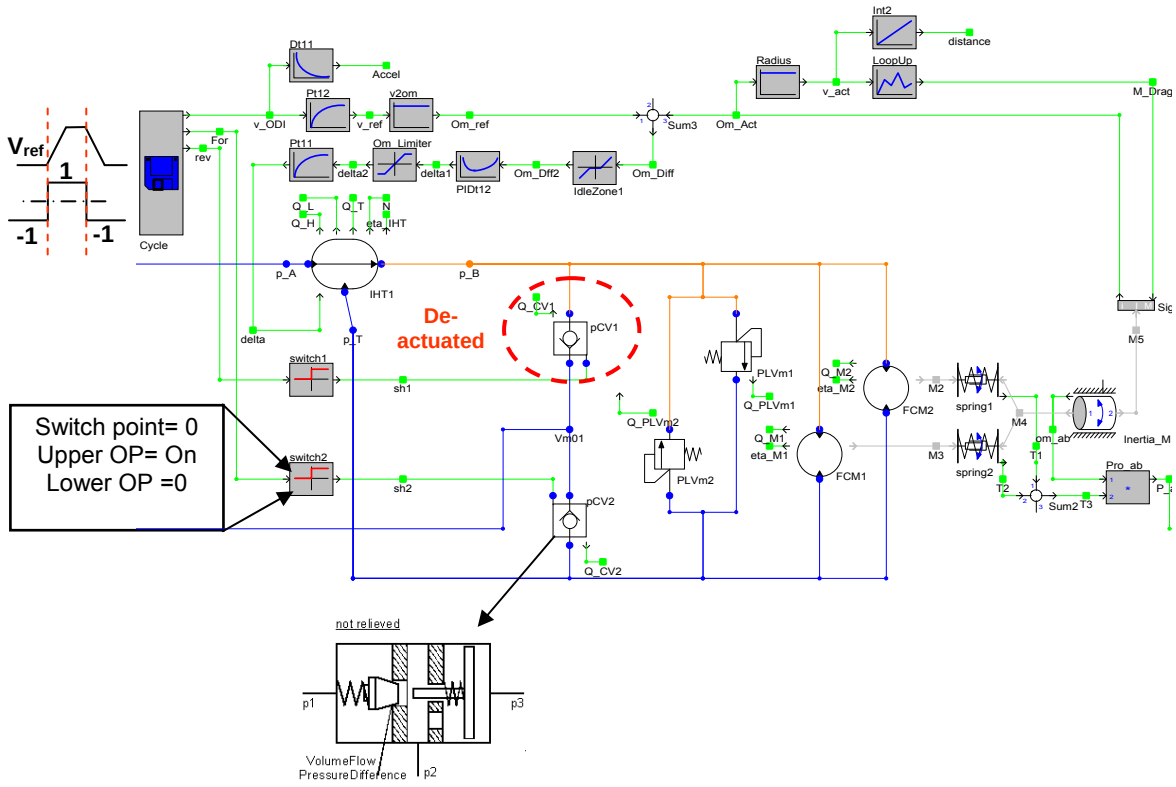

Figure 7.15-a: Pilot-operated check valves description in propulsion mode

According to the direction control signal from the control unit, check valve number one (CV_1) is always closed during forward propulsion and braking as shown in Figure 7.15-b. Check valve number two (CV_2) is actuated-on by the driver during forward propulsion to allow flow balance on the motors satisfying mass conservation.

On the other side during braking, CV_2 is de-energized from the control unit allowing flow from the reservoir to pass to the hydro-motors in order to prevent cavitation and also to prevent further motion after vehicle stopping.

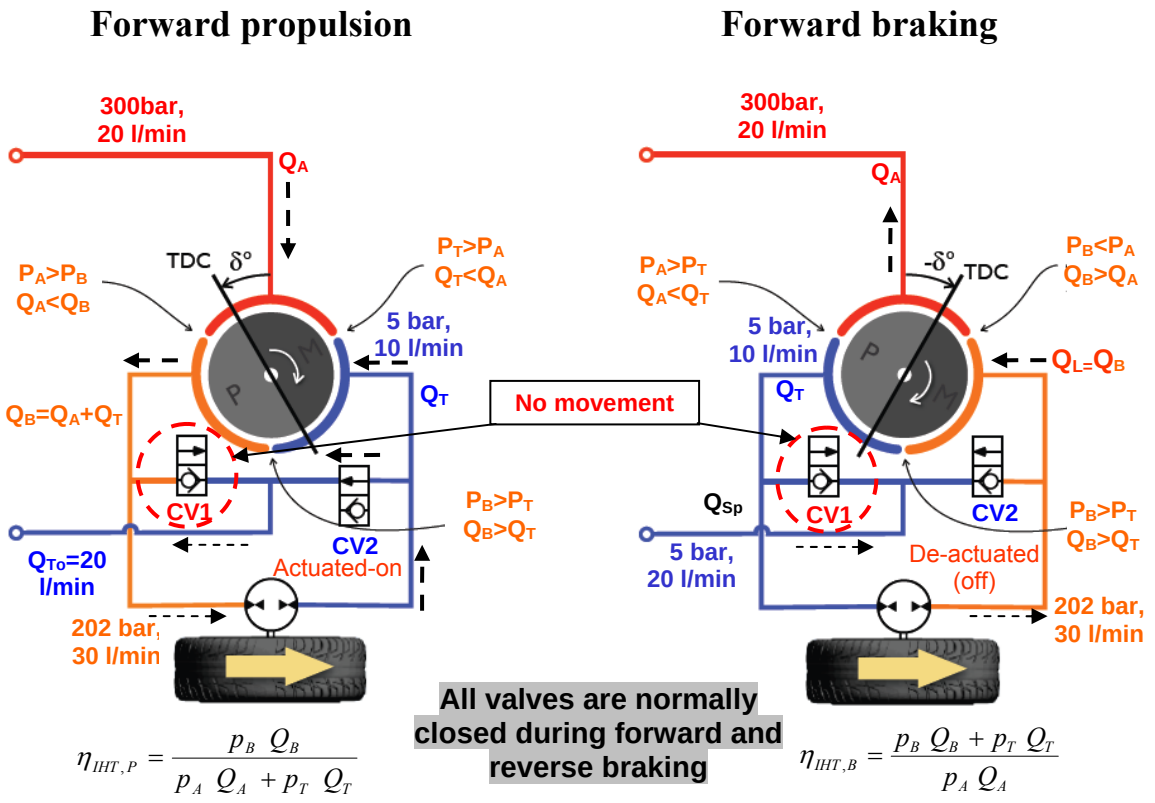

Figure 7.15-b: Pilot-operated check valves operation

7.4.2 System control concept

The drivetrain control concept has to fulfill safe and stable operation of the vehicle. The system control model basically includes two independent PID fixed-gain controllers. One stands for controlling the high pressure line of the CPR and consequently the engine operation. The other stands for controlling the speed of the in-wheel hydro-motors and consequently the vehicle speed under mission cycle by changing the port-plat angle (δ_{IHT}) of the hydraulic transformer. Both of the controllers attempt to correct the error between the measured value and the desired set point by calculating and then outputting a corrective action which can adjust the operation of the system. Unlike the SC-HST, the speed n-controller is shifted from the in-wheel motor to the hydro-transformer. PID controller parameters (the gains of the proportional, integral and derivative terms) of the pressure and speed control loops were tuned and adjusted to the optimum values to obtain the desired response and to stabilize the operation of the system. The tuning process was done at two different operating ranges. These are the low speed and high speed of the drivetrain.

The aims of the controllers are:

- Stopping the engine whenever this is possible, thereby eliminating idle losses;
- Recuperating the kinetic energy of the vehicle during braking;
- Improving the average efficiency of the engine by running it at high loads only.

A simplified block diagram illustrating the overall control strategy of the system components is indicated in Figure 7.16. As shown in the block diagram, the Hydrid drivetrain consists of four subsystems. The first subsystem represents the engine-pump combination and its p-controller which turns the engine on/off according to accumulator SOC. It is responsible for converting the thermal energy of the engine into hydraulic energy to charge the accumulator. Part-2 corresponds to the storage subsystem represented by a hydro-pneumatic accumulator. Part-3 represents the traction subsystem which is composed of in-wheel constant displacement hydro-motors. Part-4 consists of the CPR and hydraulic power transformation in addition to the n-controller which is responsible for controlling the vehicle velocity. In order to control these different behavior components (ICE, accumulators, hydraulic transformer, and in-wheel hydro-motors), the energy flow coming from each element has to be managed by the control unit.

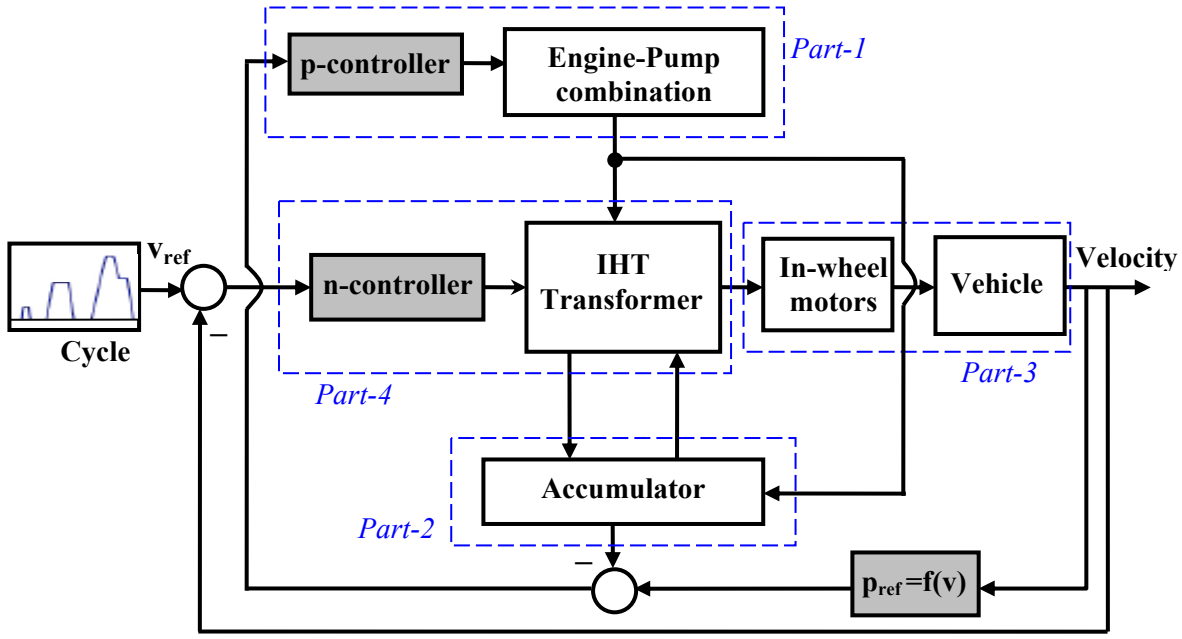

Figure 7.16: Block diagram indicating the overall control strategy of the Hydrid [76]

7.4.2.1 Pressure Controller (p-controller)

The pressure controller is located at the primary side of the Hy*d*rid drivetrain. It can be considered as the master controller of the system. It mainly determines the command value for the engine depending on the working pressure of the high pressure side. For the sake of conserving energy, the pressure controller must possess logic in order to ensure that the speed of the engine is always positive (i.e. the speed of the engine is kept either positive or zero). The control effort, which is sent from the pressure controller to the engine, is zero when the pressure at the high-pressure line is above the maximum threshold pressure, and the engine does not start operation until the working pressure becomes smaller than a certain minimum threshold pressure.

The pressure controller comprises of a pressure signal, limiter, noise filter, gas throttle valve, an angular velocity switch and a solenoid venting valve (shuttle valve). The solenoid valve will also be connected to the ICE starter, so that the pump can start the engine under no-load from stand-still through stored energy in the HP accumulator.

The pressure p-controller is responsible to keep the working pressure in the high pressure line within secure limits, i.e. between 200 and 400 bar. The controller reference pressure is correlated to the vehicle velocity and initially set to 300 bar. The controller output error signal has a dead zone of -100 and +70, bar in order to permit a high pressure line changing range of 200 bar during the system operation and also to prevent unstable engine operation. The angular velocity switch which takes its signal from the engine speed is set to operate between the range 1200-2200 rpm to de-energize the solenoid venting valve in order to permit unloading of the pump. The solenoid valve will also be connected to the ICE starter, so that the pump can be started under no-load from stand-still or idle conditions through the stored energy in the accumulator.

7.4.2.2 Speed controller (n-controller)

The speed controller is responsible to track the commanded velocity signal. The rotational speed of the in-wheel motors is fed back to the controller thus forming the closed loop. With a closed loop controller for the speed, the output vehicle velocity will follow the command cycle velocity independent on the load changes.

In propulsion mode, the n-controller produces a positive signal which adjusts the IHT port-plate angle to run in positive direction depending on the pressure ratio of the accumulator and the load ports. It also causes the displacement of the hydraulic transformer to become negative in order to produce negative output torque on the in-wheel motors as the vehicle decelerates. The motor subsequently pumps oil from the low pressure line to the high pressure line. This in turn also causes the working pressure to become higher than the set pressure. However, the logic in the pressure controller restricts the speed of the engine to zero via controller limiter. The oil pumped by the in-wheel motors therefore cannot be discharged to the pump but rather stored in the accumulator until it is used again.

7.5 Power Management Strategy

The goal of power management is to minimize fuel consumption and to supply the required power by controlling the power flow of the system. In general, a series hybrid protects the engine from transient operation conditions associated with the delivery of power directly to the vehicle. This originates the idea of the simple on/off control strategy. Under this strategy, the engine can operate only from medium to high loads at optimum points and will be turned-on or -off according to the State Of Charge (SOC) status of the accumulator.

7.5.1 Drivetrain power flow

The Hy*d*rid vehicle has distinct characteristics that make it different from other types of hybridization such as electric hybrids. Conceptually, the Hy*d*rid drivetrain can be considered as an engine-assisted hydraulic vehicle. When the accumulator is completely charged and power demand is low, the engine can be turned off.

As shown in the flow diagram indicated in Figure 7.17, the power flow path from the primary power source, i.e. combustion engine, is unidirectional because it represents the irreversible combustion process. But the power flow path from the hydraulic storage accumulator, the IHT and the in-wheel hydro-motors are bidirectional to satisfy propulsion and braking modes. This takes into account the possibility of starting the engine through the power stored in the accumulator.

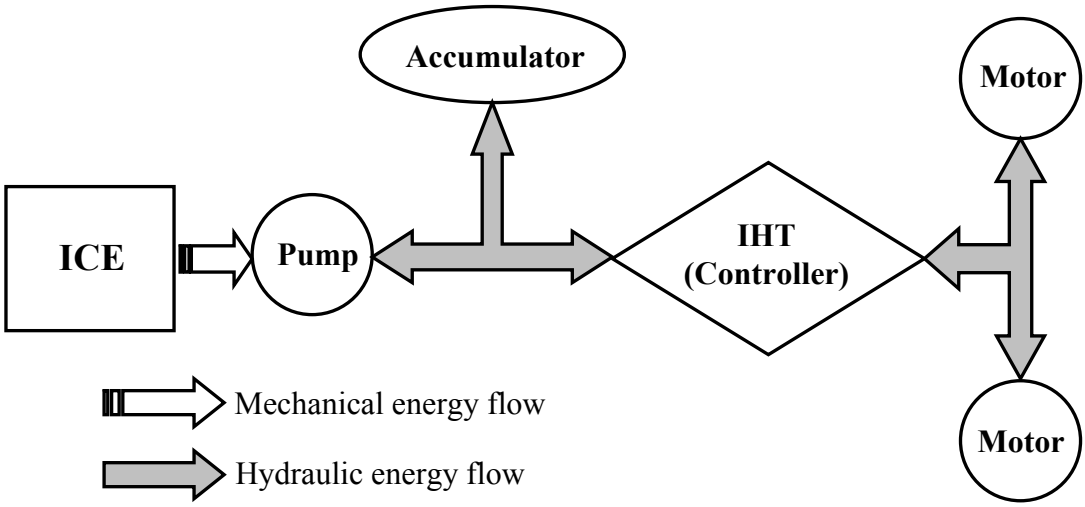

Figure 7.16: Energy flow diagram for typical Hydrid drivetrain

Due to hybridization of a vehicle, the power flow inside the drivetrain can go through various paths in different directions. Each possibility can be represented by a driving mode. The different operation modes for the Hy*d*rid powertrain can be divided into four modes as described below and indicated in Figure 7.18 [91].

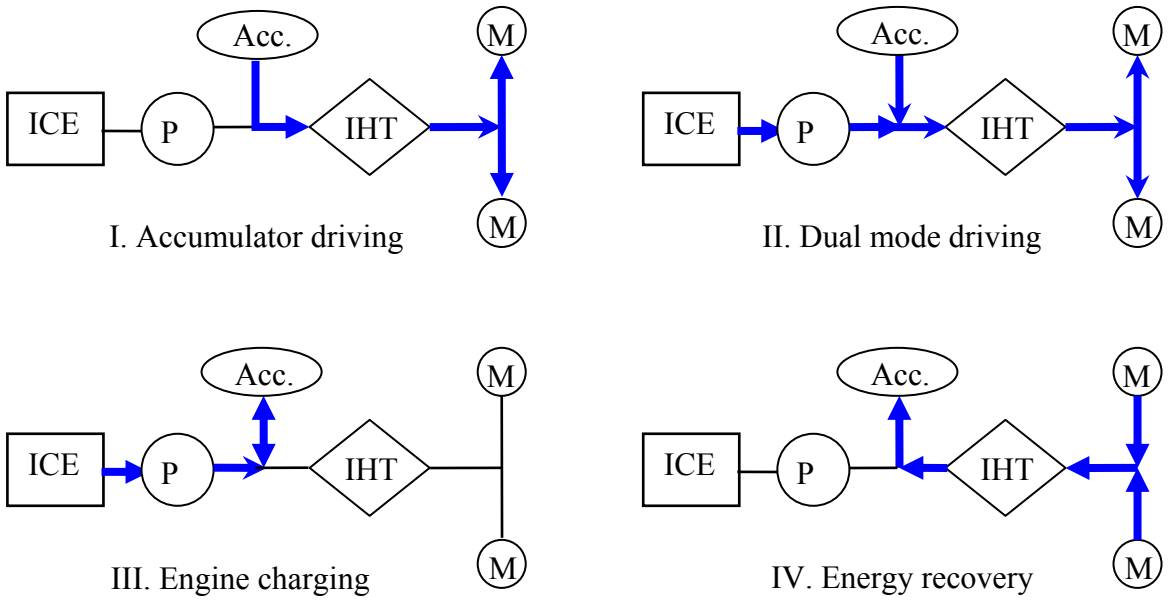

ICE = Internal Combustion Engine, P = Pump; Acc. = Accumulator, IHT = Innas hydraulic transformer, and M = In-wheel hydro-motor

Figure 7.18: The four driving energy flow modes of the Hydrid drivetrain

The power management strategy of the system has been applied through a rule-based approach. Several rules are used to determine how much power to get from each power source during propulsion based on the power demand value which will be considered as positive during propulsion.

On the other hand, during braking mode, regenerative braking will be activated if the power demand is negative. Other rules are used permitting the accumulator to operate within an effective range of SOC and to ensure that some limits are not exceeded, for instance 48 ~ 95 % which is corresponding to the effective pressure range of the accumulator, i.e. 200 to 400 bar. These limits represent the maximum allowable charging and discharging power ratios of the accumulator during braking and driving modes.

7.5.2 Rule-based power algorithm

A rule-based strategy is based on heuristics, i.e. it is based on engineering intuition. It is powerful method in on/off control strategy and can be easily implemented in the system. Moreover, an on/off approach is simple and more robust.

Under this strategy, the engine will run at high efficiency operating points. These operating points are selected based on the efficiency maps. A region of best efficiency is defined on engine maps, whereas the range of delivered engine torques is limited by minimum $M_{ICE,min}$ and maximum $M_{ICE,max}$ values which correspond to the accumulator pressure thresholds (200 ~ 400 bar).

As described by the following rules, system behavior is divided into discrete events. Each event is connected to the other one by certain rules. If the rule is performed, the system moves from one state to another depending on the resolution of the rules.

I- ***Accumulator driving:***

In this mode, the power demand is supplied only by the energy stored in the accumulator without consuming power from the engine. The accumulator SOC value is within its two effective limits, i.e, $SOC_{min} < SOC(t) < SOC_{max}$, and the available accumulator discharging power $P_{A,d}$ is sufficient to drive the in-wheel motors load P_M. The engine is typically off until the accumulator SOC reaches its minimum effective limit.

II. ***Dual driving mode****:*

This occurs only when the demand power P_d is extremely higher than the available accumulator power, and the accumulator SOC is not high enough. Then both sources will supply power to maintain the dynamic performance of the vehicle.

III. ***Engine charging:***

If $SOC(t) \leq SOC_{min}$, during stand-still and before driving, the controller will actuate the engine to charge the HP accumulator up to the maximum limit. This relies on the logic of the pressure controller which keeps the accumulator SOC within preset effective limits (48 ~ 95 %). During charging mode, the accumulator charging power is treated as a net demand power (i.e. $P_{A,c} = P_d$) from the engine.

IV. ***Braking recovery mode:***

When the vehicle begins to decelerate, the demand power becomes negative ($P_d < 0$) and the engine is turned-off. In this mode, the hydro-motors work as pumps to recuperate the kinetic energy of the braking. The IHT in turn transfers this energy to the HP accumulator and is stored there. If the braking energy exceeds the maximum allowable capacity of the accumulator, the conventional braking system will be activated. A summary of the logic sets of rule-based algorithms that have been used are listed in *Table 7-2*.

Table 7-2*: Summery of rule-based control rules*

1- Accumulator mode ($P_d > 0$)	**2- Dual driving mode** ($P_d > 0$)
IF $SOC_{min} < SOC(t) < SOC_{max}$ IF $P_M < P_{A,d}$ THEN $P_{ICE} = 0$ & $P_{A,d} = P_M$ ELSE IF $P_M > P_{A,d}$ Switch to dual mode	IF $SOC_{min} < SOC(t) < SOC_{max}$ IF $P_M >> P_{A,d}$ THEN Engine is on where $P_{E,min} < P_E < P_{E,max}$ and $P_{A,d} + P_{ICE} = P_M$
3- Engine charging mode ($P_d > P_{A,d,max}$)	**4- Braking mode** ($P_d < 0$)
IF $SOC(t) \leq SOC_{min}$ THEN Engine is on where $P_{ICE,min} < P_{ICE} < P_{ICE,max}$ $P_E = P_{A,c}$ or $P_{ICE} = P_d$	IF $SOC_{min} < SOC(t) < SOC_{max}$ THEN $P_{ICE} = 0$ & $P_M = P_{A,c}$ ELSE IF $SOC >= SOC_{max}$ & ($P_d \geq P_{A,c}$) Release Energy

Generally, the rules show that, if the traction power is positive and the pressure of the accumulator is lower or equal to 48 % of its maximum value, the engine is turned-on. When the pressure of the accumulator is between its working limits the engine is off. In any case, when the traction power becomes negative during

deceleration the engine is off. In order to avoid rapid frequent start and stop process of the ICE, it has to stop when the pressure of the accumulator reaches 95 % of its maximum value.

7.6 Results and Discussion

Operation performance, system variables behaviour, fuel economy and CO_2 emissions of the introduced drivetrain during transient and modal cycles are presented in this section. The transient cycles give a better representation of real driving patterns than the modal cycles. The American Federal Test Procedure (FTP-75) is a transient cycle, whereas both the official New European Drive Cycle (NEDC) and the Japanese 10/15-Mode cycles are considered modal cycles.

A summary of the selected driving cycle characteristics is listed in *Table 7-3*. Fuel consumption and CO_2 emissions data are not calculated in the first part of the Japanese cycle represented by an initial 15 mode cycle (231 s) as well as first part of the American cycle which take 505 s, according to the description found in [86].

Table 7-3: *Characteristics of the European, American and Japanese driving cycles* [86]

	Driving cycle		
property	**NEDC**	**10/15- mode**	**FTP-75**
Test time duration [s]	1180	660	1370
Travelled distance [km]	11.02	4.16	17.77
Average speed v_{av} [km/h]	33.6	22.7	34.1
Maximum speed v_{max} [km/h]	120	70	91.25
Maximum deceleration d_{max} [m/s^2]	-1.07	- 0.8	-1.47
Maximum acceleration a_{max} [m/s^2]	2.2	0.8	1.47
% stopping time [-]	23.73	31.36	18.04
% braking time [-]	17.88	21.06	34.9

The energy consumption for starting the engine and the power consumption for auxiliaries are not considered in simulation.

7.6.1 Performance analysis

Complete profiles of the drivetrain variables during the NEDC, 10/15 mode and FTP-75 driving cycles are shown respectively in the multi-curves of Figures 7.19-a, b, c to assess system operation.

The first curves from below in each diagram shows that the actual vehicle velocity coincides with the reference velocity along the mission cycles.

The accumulator pressure plotted in the second curve in each cycle is maintained in the secure operating range of 200 to 400 bar. It is clear from the behavior of the accumulator pressure that it follows the power transients of the vehicle more than a need for storing energy. The accumulator pressure level decreases during propulsion and rises during braking or when charging the accumulator with the engine power.

During the beginning of the cycles the vehicle can run completely depending on stored energy in the high-pressure accumulator. When the pressure level in the accumulator drops below the minimum threshold value, i.e. 200 bar, the engine is started and supplies energy to the system up to the upper threshold of the accumulator pressure, unless the vehicle decelerates or braking mode occurs, permitting the braking energy to be recuperated in the accumulator as shown by the third curve in the diagram from below.

The engine run times are about 16 %, 14.3 %, and 18.6 % for the NEDC, and 10/15-mode FTP-75 cycles respectively and at the rest of the time it is shut-off. A direct reason is the principle of operation of the IHT, as it can cover the gap in pressure differences between load and source sides as long as the accumulator pressure is greater than or equal 200 bar, allowing smooth and steady operation for the engine.

The engine delivered power is indicated in the fourth curve. In the highway part of the cycles, approximately half of the installed engine power is required, which gives a possibility of downsizing the engine if necessary. In the FTP-75 cycle, pressure, engine speed, and consequently engine power behavior are transient, which is not the case for the NEDC and 10/15-mode cycles. This is due to the high transient patterns of the American cycle otherwise the same control methodology was applied.

The recuperated power of the Hy*d*rid during braking is indicated in the 5th curve. The FTP-75 cycle exhibits high recuperated energy which corresponds to high braking time of 34.9 % compared to other two cycles (see *Table 7-3*).

The top curve in each diagram shows that the angular position of the IHT port-plate δ_{IHT} has positive angles in propulsion mode and negative angles during braking

mode. The negative angles are a result of working the in-wheel motors in pumping mode as the vehicle is causing a negative pressure difference across the hydro-motors. Thereby they are supplying power back to the high-pressure accumulator while braking the vehicle.

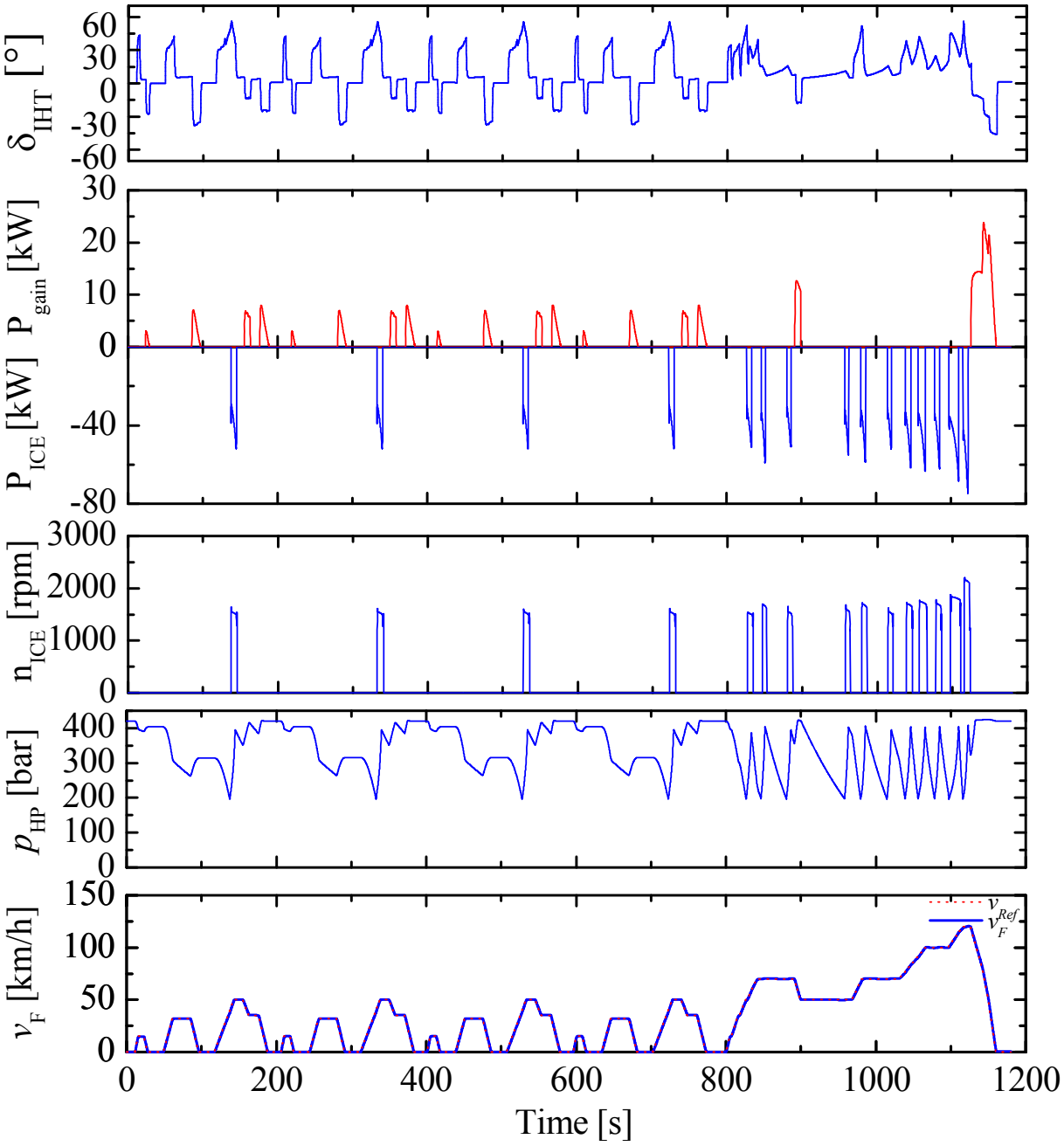

Figure 7.19-a: The Hydrid drivetrain performance curves during the NEDC cycle

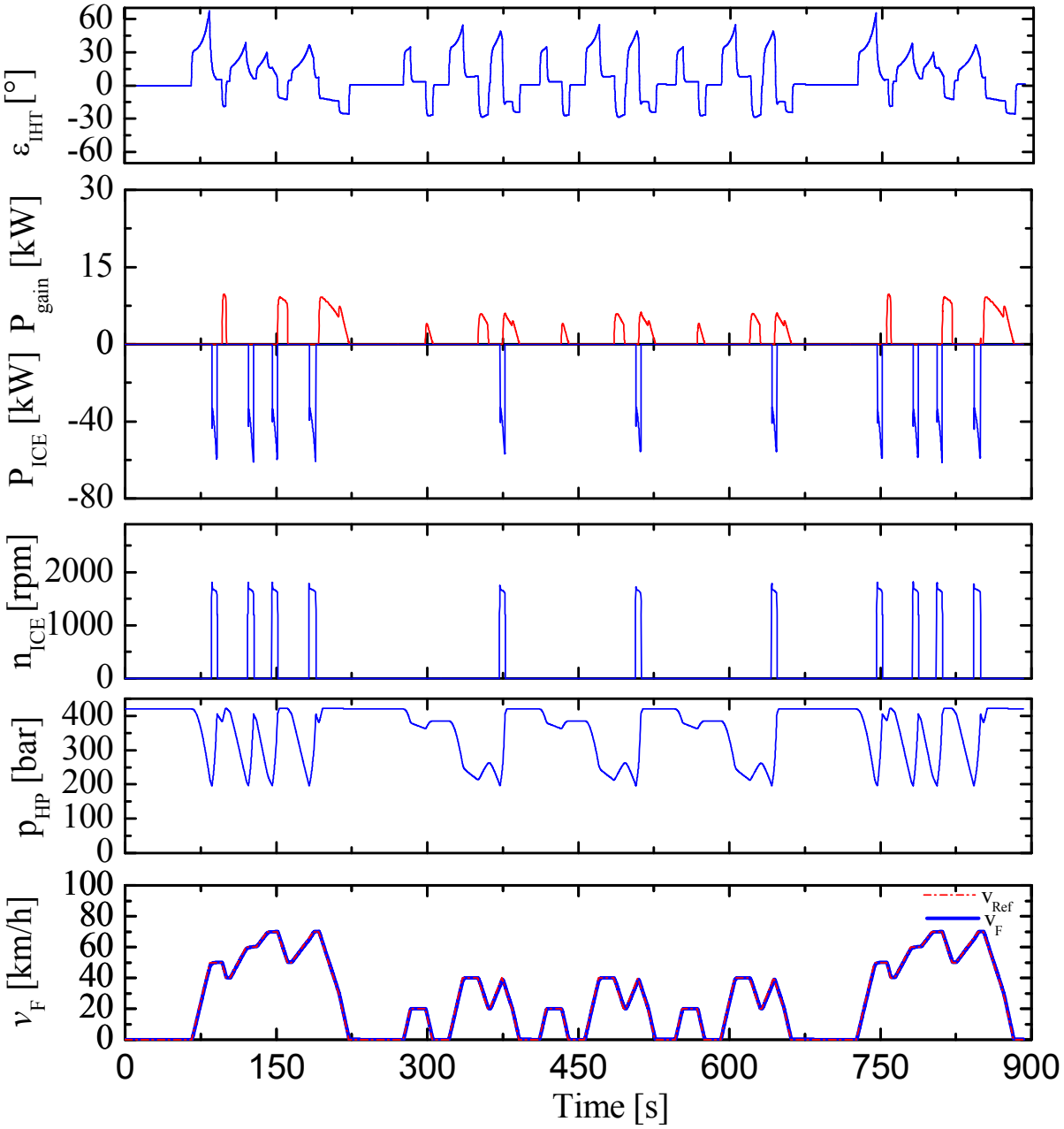

Figure 7.19-b: The Hydrid drivetrain performance curves during the10/15-mode cycle

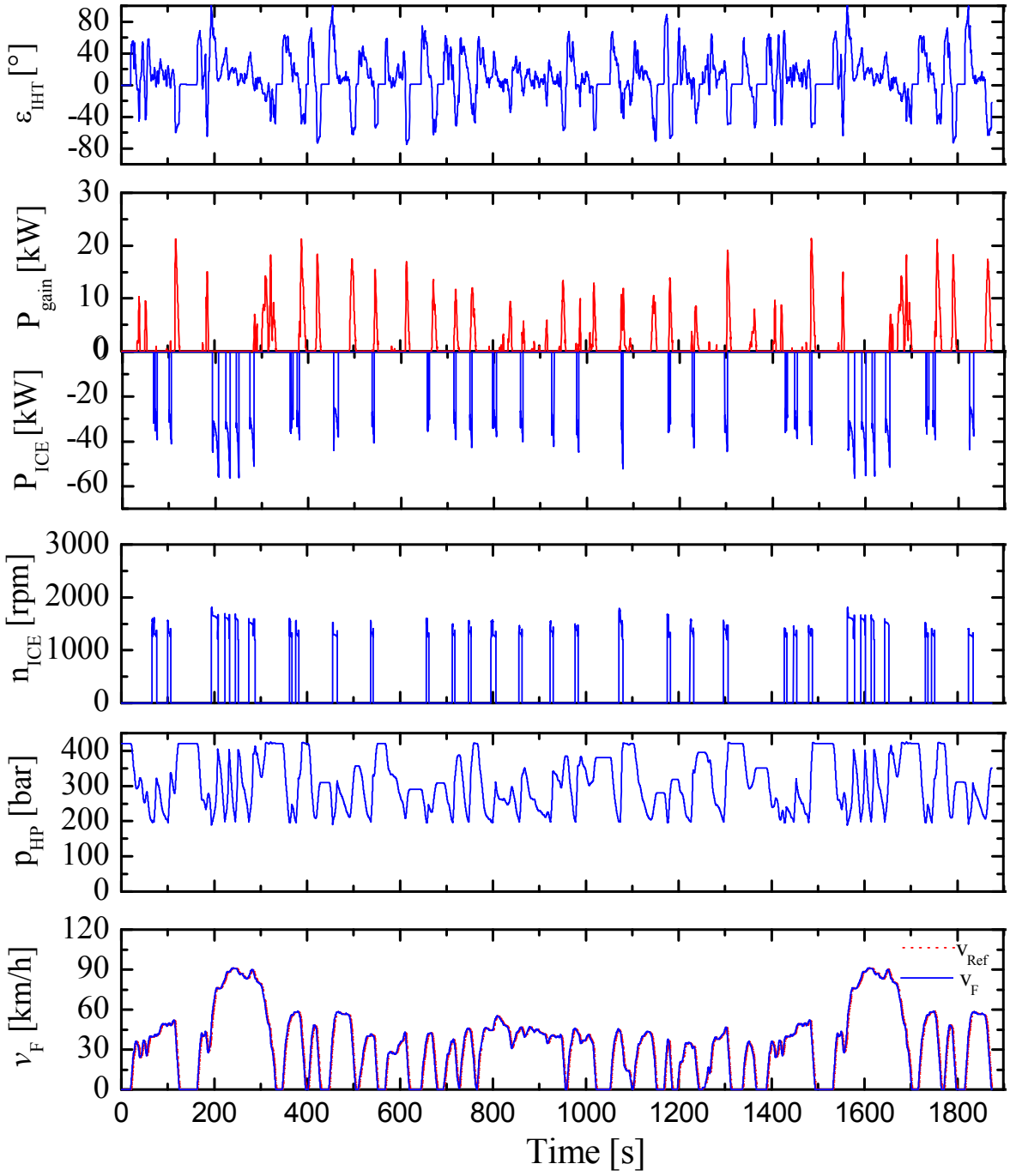

Figure 7.19-c: The Hydrid drivetrain performance curves during the FTP-75 cycle

The simulation shows that the hydraulic energy required by the in-wheel hydro-motors is supplied exclusively by the accumulator. When the speed of the vehicle increases; the engine does not start operation until the working pressure of the common pressure rail CPR becomes smaller than the minimum value, which is pre-adjusted in the dead zone of the pressure control loop. The working pressure of the CPR consequently decreases while the vehicle speed increases; the pressure does not necessarily have to be constant, as the hydraulic transformer is used as a control device

to compensate the gap in pressure between the hydro-motors pressure and the accumulator pressure.

The speed controller causes the displacement of the IHT to become negative in order to produce negative pressure/torque as the load decelerates. The transformer subsequently pumps oil from the low pressure line depending on the pressure level. This in turn also causes the working pressure of the CPR to become higher than the set pressure. However, the logic in the pressure controller restricts the torque and consequently the speed of the engine to be zero. The oil pumped by the in wheel hydro-motors therefore cannot be discharged via the pump and will be stored in the accumulator.

7.6.2 Components operating points on efficiency maps

In this section a detailed description of components efficiency will be discussed for the NEDC cycle which considers enough to show the operating points for each component of the drivetrain on their efficiency maps.

As presented in chapter 4, the installed engine in the conventional vehicle is running at partial loads results in engine efficiency around 28 %. The strongly reduced engine efficiency at these operating conditions is the most important reason for a vehicle having high fuel consumption while driving in the city. Contrary, the Hy*d*rid aims to improve the fuel economy of the vehicle at partial loads. The pressure p-controller in the Hy*d*rid always forces the engine to run at high loads above 200 Nm as shown in the right diagram of Figure 7.20 which results in average engine efficiency around 37 %.

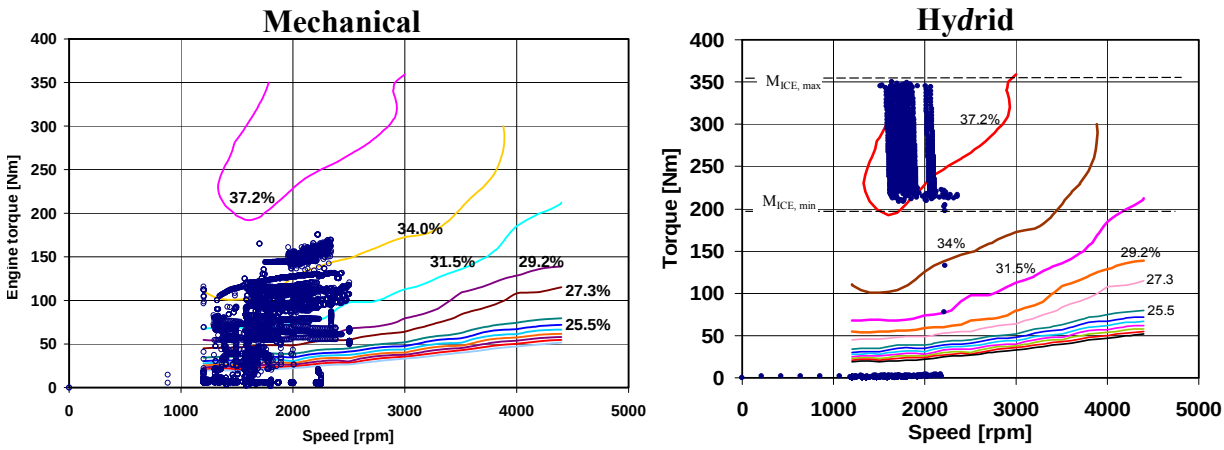

Figure 7.20: Engine operating points of mechanical and Hydrid drivetrains for the NEDC

The fixed displacement floating cup pump is directly coupled to the engine shaft and subjected to the same controller which forces the engine to run in high torque according to the SOC of the accumulator. Therefore, the pump operating points exhibit the same behavior as the engine, running in the region of high efficiency on the contour line of the efficiency map, as shown in Figure 7.21 The average efficiency of the pump cover the NEDC cycle is about 94 %.

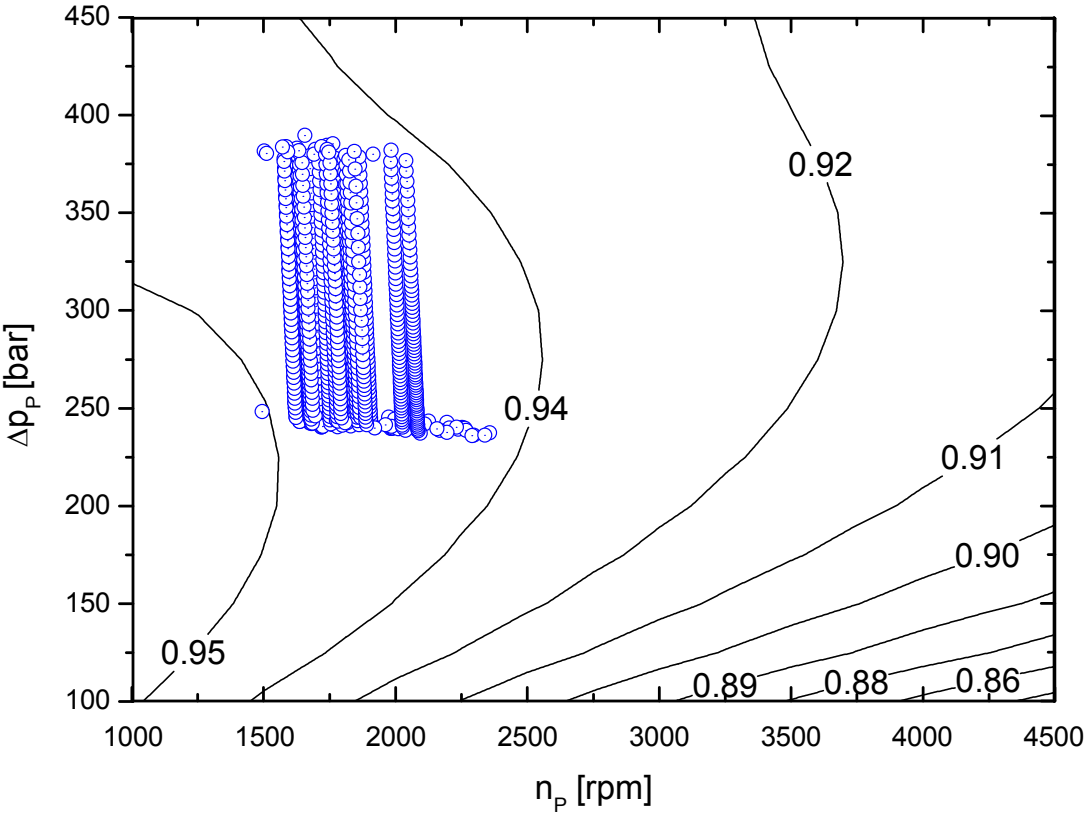

Figure 7.21: operating points of FC-Pump during the NEDC cycle

Like the engine, the pump is only in operation when it is needed for charging the accumulator, i.e. it runs only when the engine is turned-on. This is not the case for the hydraulic transformer and the in-wheel motors. Both IHT and hydro-motors are in operation throughout the propulsion and braking modes of the cycle. Figure 7.22 and 7.23 indicate the operation point of the IHT in the two quadrants of operation. The average efficiency of the IHT during propulsion is about 91 % and in braking mode reaches about 93 %.

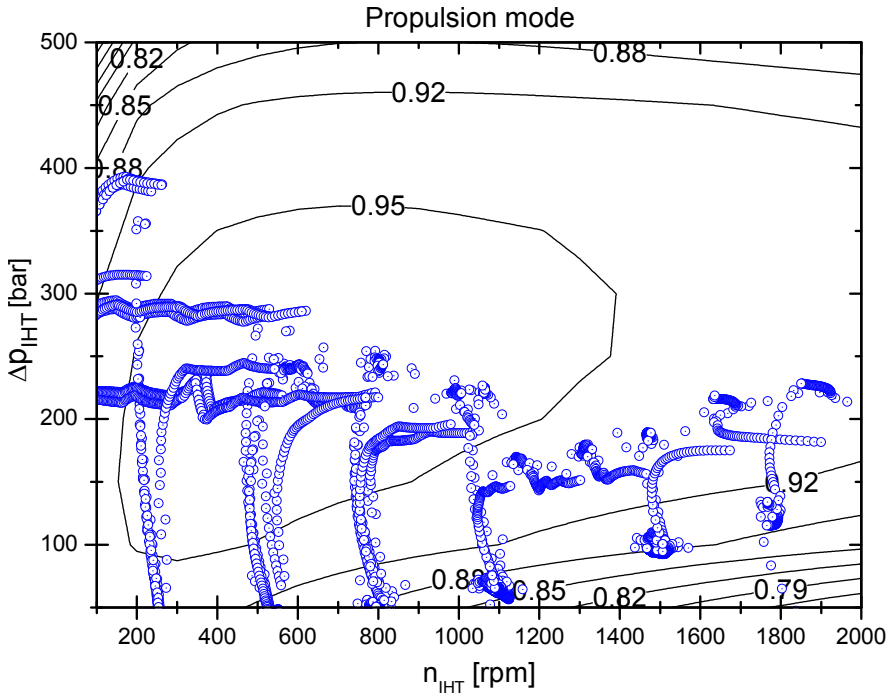

Figure 7.22: IHT operating point during propulsion mode during the NEDC cycle

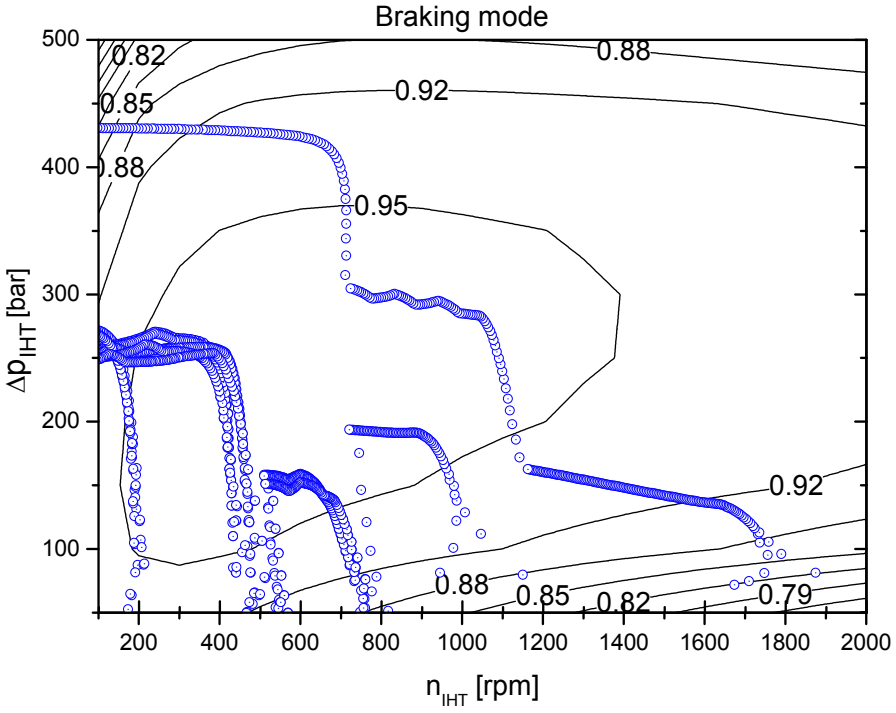

Figure 7.23: IHT operating point during braking mode during the NEDC cycle

One important benefit of the transformer is that it permits for a smaller motor size because it can amplify the pressure level on the motor side up to 500 bar, even when the pressure level in the accumulator is only 200 bar.

The operating points of the constant displacement floating cup hydro-motors are depicted in Figure 7.24. The in-wheel hydro-motor as used in the Hy*d*rid will operate at average efficiencies about 96 % during propulsion mode and average of 94 % during braking mode.

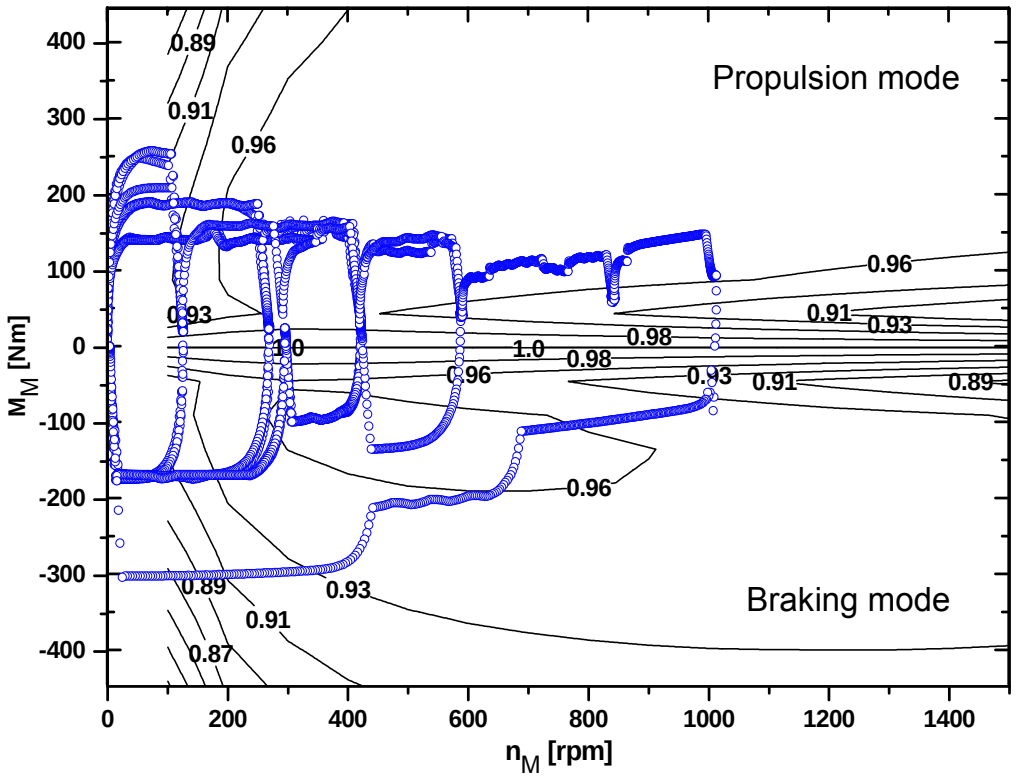

Figure 7.24: Operating points of the in-wheel Hydro-motors during the NEDC

7.6.3 Transmission efficiency

The required energy of a mid-sized Sedan during driving can be obtained by integration of the required power during the NEDC cycle time. This amount to 1164 Wh of energy must be supplied to the vehicle. The grater part of this energy is required to overcome the aerodynamic drag, especially when driving at high speeds i.e. during the highway part of the cycle, and the rest to overcome rolling resistance. The same amount of aerodynamic energy is needed for the Hy*d*rid drivetrain, but the brake energy is not dissipated during braking. Instead, it is supplied back to the common pressure rail in order to be stored in the accumulator.

The efficiency of the hydraulic components that constitute the hydrostatic transmission alone don't show higher efficiency than the mechanical transmission of the baseline vehicle, because they have more losses due to series configuration, but

these losses are compensated by the energy recuperated during breaking mode as shown in Figure 7.25. By considering the recuperated brake energy, the total transmission efficiency of the Hy*d*rid vehicle at the end is somewhat better than mechanical transmission efficiency.

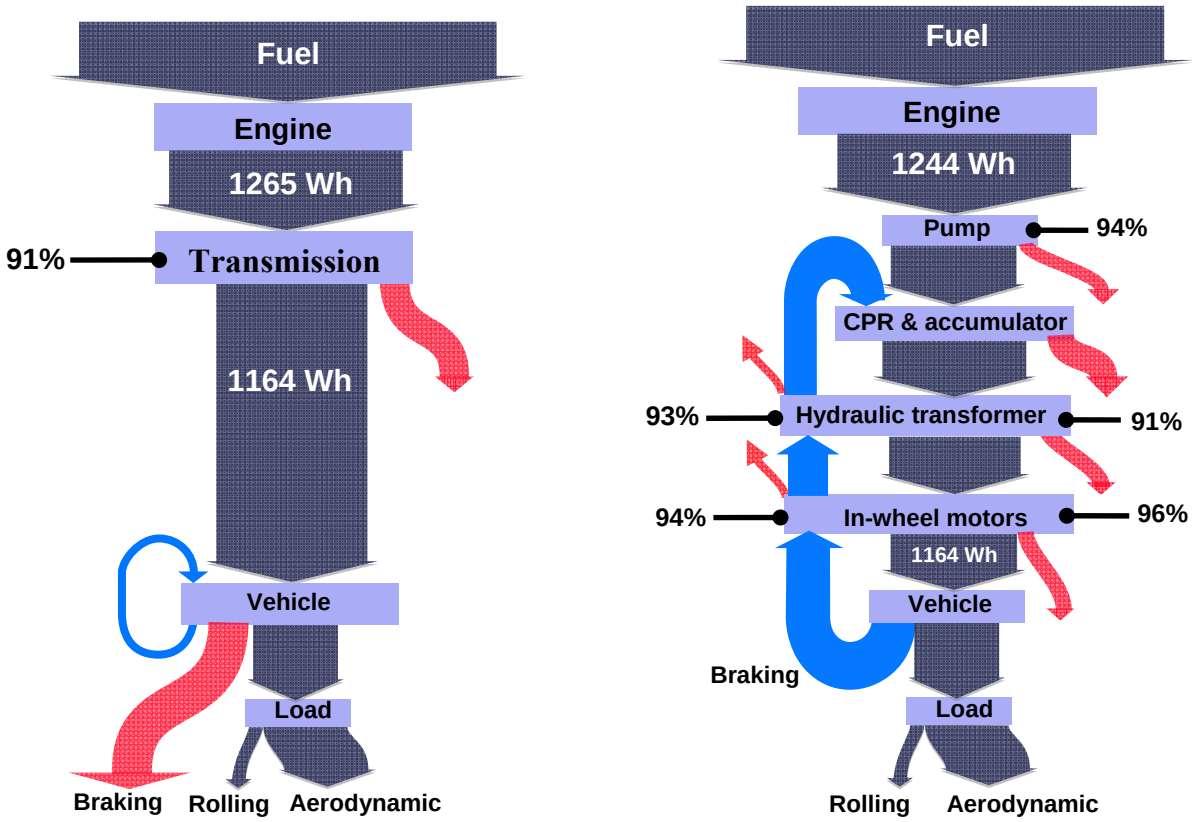

Mechanical drivetrain ($\eta_{T,mech} = 92\ \%$) **The Hy*d*rid drivetrain** ($\eta_{T,mech} = 93.5\ \%$)

Figure 7.25: Transmission efficiencies of mechanical and Hydrid drivetrains

The transmission efficiency can be expressed as the ratio of the consumed energy at the vehicle wheels to the supplied energy from the primary power source i.e. ICE as indicated by the following formula.

$$\eta_T = \frac{\int_0^{t_{cycle}} P_{out}(t)\,dt}{\int_0^{t_{cycle}} P_{in}(t)\,dt} = \frac{\int_0^{t_{cycle}} P_{Wheel}(t)\,dt}{\int_0^{t_{cycle}} P_{ICE}(t)\,dt} \qquad (7\text{-}4)$$

During propulsion, the total average transmission efficiency including pump, transformer and motors is about 83.6 %. During braking, the combined average efficiency of the motors and transformers is 88.3 %. During braking 15 % of the

energy delivered by the engine is recuperated in the high-pressure accumulator via the in-wheel motors. Theoretically, this amount could be increased if more energy could be stored in the accumulator.

7.6.4 Fuel consumption and CO_2 emissions

The question must now be raised concerning the value of fuel economy and emission benefits gained by the Hy*d*rid. The fuel consumption and CO_2 emissions have been calculated during three introduced cycles, based on a mid-sized Passat sedan. Figure 7.26 shows the Hy*d*rid's fuel consumption advantage over conventional vehicles and how it depends on driving cycle.

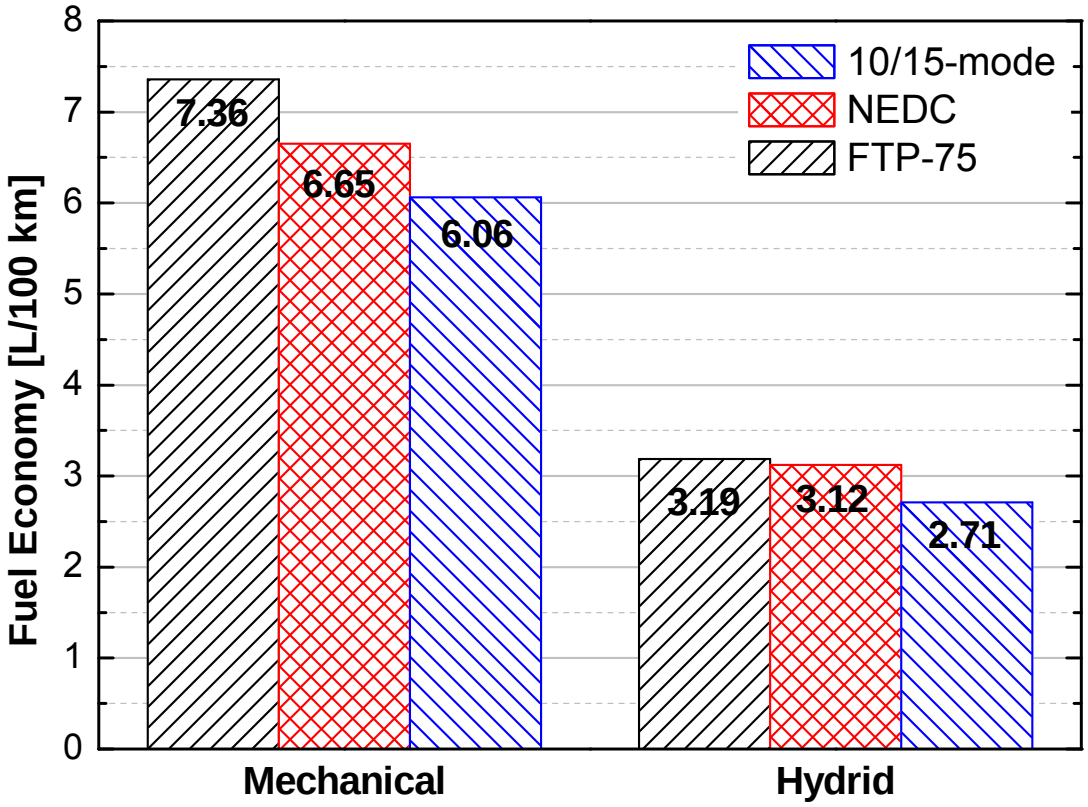

Figure 7.25: Fuel consumption of the Hydrid compared to the mechanical drivetrain

It is evident from the figure that the Hy*d*rid appears does best on slow cycles with a great deal of stop-and-go drive as found in the Japanese cycle.

Specifically, for the European NEDC the Hy*d*rid vehicle has a total fuel consumption of approximately one third (0.344) liters, at a total travelled distance of 11.02 km. This amounts to an average specific fuel consumption of 3.12 Liter/100 km and CO_2 emissions to 82.11 g/km.

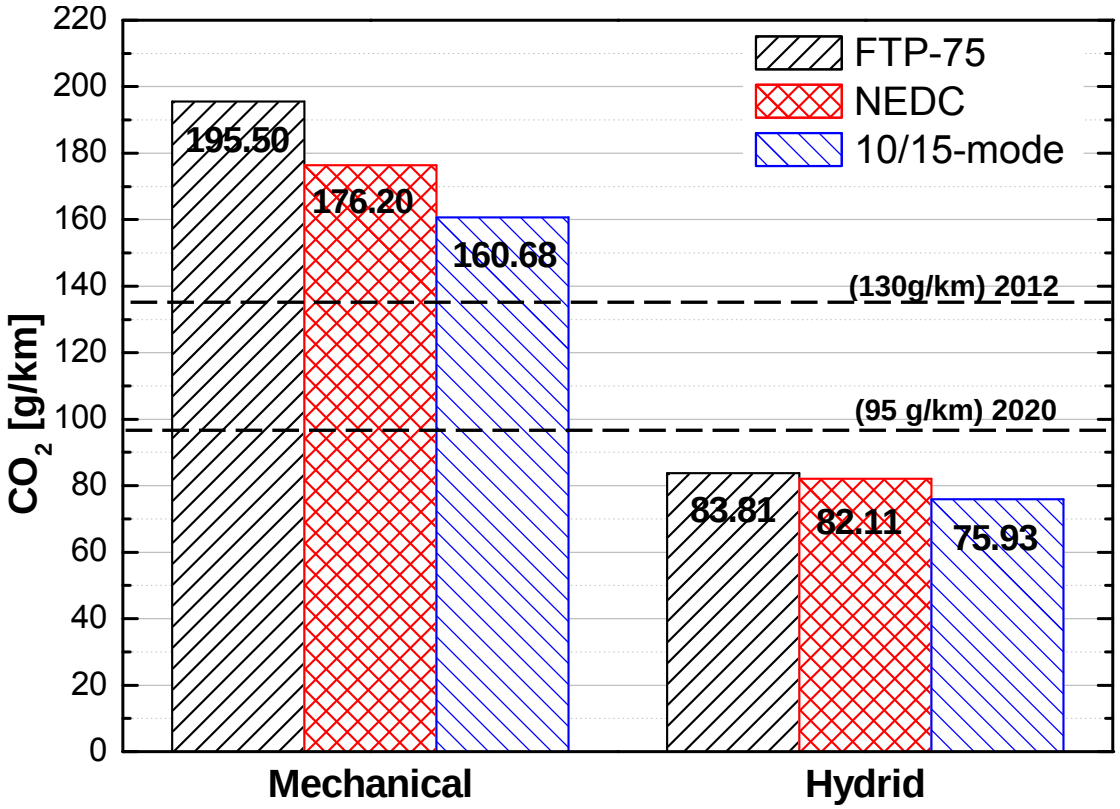

Figure 7.26: CO_2 emissions of the Hydrid compared to the mechanical drivetrain

The reduction of CO_2 emissions of the Hy*d*rid drivetrain over the conventional vehicle is shown in Figure 7.26. The best relative fuel saving value is about 57.0 % for the FTP-75 cycle compared to 54.3 % for the 10/15-mode cycle and 53.1 % for the NEDC which is directly related to the percentage of braking time of the cycles.

The European Commission has recently announced CO_2-emission limits for new passenger cars. The proposal sets mandatory targets from 2012 onwards to an average maximum level of 130 g/km. The European Parliament also insisted on a second step to be taken in view of the longer-term target: the average new car should reach 95 g CO_2/km by 2020 and possibly 70 g CO_2/km by 2025, subject to confirmation or review by the Commission no later than 2016.

The CO_2 emissions of the Hy*d*rid are reduced far below the limits set by the European Commission of 130 g/km for 2012, and even below the long term target of 95 g/km as a limit for 2020. For instance CO_2 emissions during the NEDC cycle is equal to 82.11 g/km.

The results show that the fuel consumption and consequently the CO_2 emissions are reduced during the city part as well as during the highway part of the driving cycles by more than 50 %.

Contrary to conventional drivetrains, the city cycle does not result in higher fuel consumption per 100 km than the highway driving, which makes an efficient drivetrain.

The good fuel economy of the Hy*d*rid is achieved due to:

- The reduction of vehicle weight due to the elimination of mechanical drivetrain and the low weight of the hydraulic components characterized by its high torque and power density.
- Shutting the engine off during approximately 84 % of the cycle time.
- Recuperated brake energy (about half of the energy that can be recuperated during the cycle is stored in the high-pressure accumulator).
- The high efficiency of the hydraulic components (pump, accumulators, transformers and in-wheel motors).
- Forcing the engine to run at high efficiency.

It can be concluded that, with modern hydraulic components, a very efficient serial hybrid drivetrain for on-road vehicles can be achieved.

7.7 Conclusions

This chapter assesses the potential fuel savings and emissions reductions associated with the Hy*d*rid drivetrain for mid-sized passenger cars such as VW Sedan Passat vehicle for three real driving cycles.

The performance of the Hy*d*rid drivetrain under rule based power management strategy is presented. The control strategy enables recovery and reuse of energy normally lost in conventional vehicle during braking mode. It also eliminates idling losses by shutting off the engine during braking or stopped periods as the vehicle can still be operated and driven with the engine turned off. Reducing engine operation time results in a significant fuel consumption improvement. This in turn will reduce vehicle maintenance, particularly for the brakes. The Hy*d*rid technology also provides a cleaner and more efficient operation when engine speed is independent of vehicle speed.

The results reveal that the Hy*d*rid vehicle's fuel economy is highly dependant upon accumulator SOC, and the Hy*d*rid drivetrain achieves the largest percentage gain in fuel economy over the baseline conventional vehicle on the slowest driving cycles. This is due to the inefficiencies of slow stop-and-go driving, high idling losses, high braking losses and highly inefficient engine operation being overcome by the Hy*d*rid control system, where the engine is forced to run only under high loads due to the controlled effective range of accumulator pressure (200 ~ 400 bar).

Based on the recently developed component technology used in the Hy*d*rid, such as the floating cup units and the IHT, as well as the particular Hy*d*rid drivetrain configuration applied, fuel saving ranging from 48 ~ 53 % over the baseline vehicle can be obtained. Thus the Hy*d*rid introduces a highly efficient alternative drivetrain has the potential to reduce fuel consumption and consequently CO_2.

The key to the good efficiency of the Hy*d*rid drivetrain is the recuperated energy in the accumulator and the improved operation of the engine which enables the engine to operate at its peak efficiency in short times.

The Hy*d*rid is able to compete with the electric hybrid vehicles due to the remarkable efficiency of the IHT and the new floating cup units, robust control and high power density. CO_2 emissions are reduced to 82.1 g/km, far below the limits set by the European commission of 130 g/km at year 2012. The results are encouraging enough to recommend the Hy*d*rid drivetrain for automobile industry with the benefits of conserving fuel and preserving the environment. The Hydrid has the potential to become a market leader.

Chapter 8

Summary and Outlook

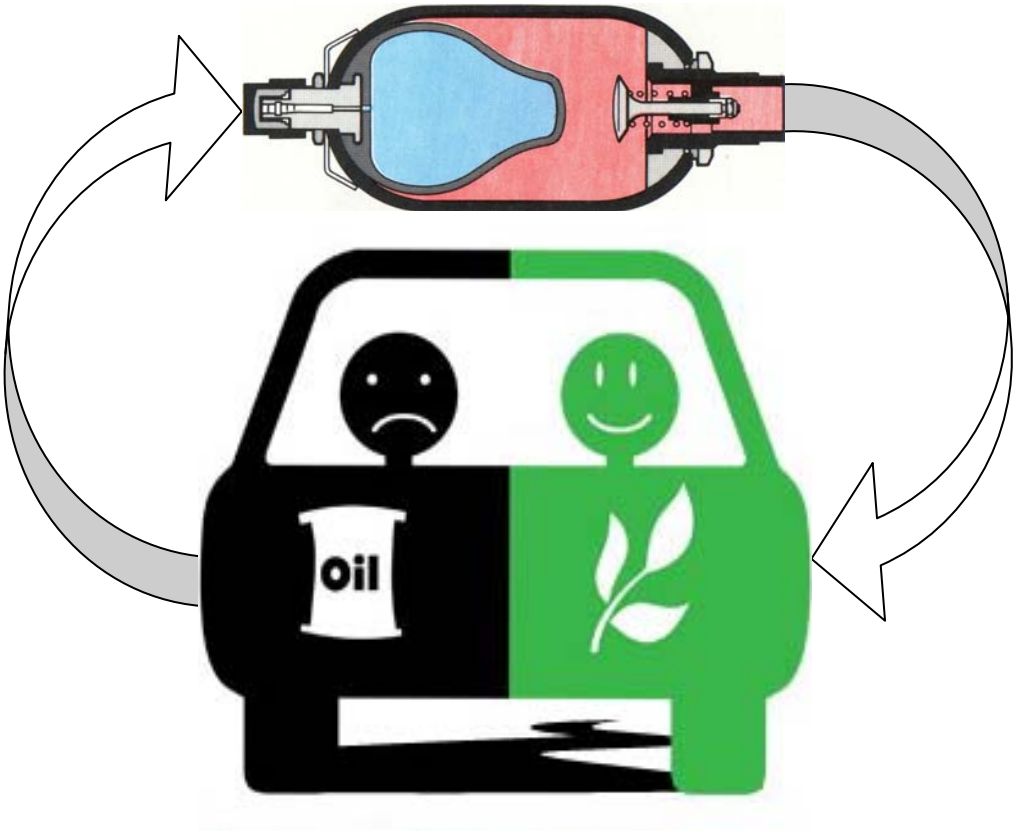

Summary

In order to develop a hydrostatic transmission that can be applied to medium sized passenger cars, some key problems need to be solved such as how to design displacement units to satisfy size and noise constraints; how to recuperate braking energy; how to design a hydrostatic drivetrain configuration that reduces power loss.

Three alternative drivetrains using hydraulic power were evaluated by simulation modeling in order to determine the potential of different hydrostatic drivetrain configurations to be applied in mid-sized vehicles. The well-known continuously variable hydrostatic transmission (CV-HST), integrated with a controlled engine to operate at minimum fuel consumption points is discussed and evaluated. An algorithm based on engine specific fuel consumption is implemented to set an Ideal Operating Line (IOL) for the engine. This allows the engine, being connected to the input shaft of the transmission, to operate mostly in efficient operating points.

The results show that CV-HST has the potential to provide such desirable attributes especially in city drive as: a wide range ratio, good fuel economy, shifting ratio continuously and smoothly, but it is not suitable to passenger application due to high losses at high driving speeds as well as the large size and consequently weight and cost of the transmission. The simulation shows that this system has almost no fuel saving compared to the gear-shift transmission because the gain in IOL operation will be lost by low component efficiency.

Next, a pressure coupling secondary controlled hydrostatic transmission (SC-HST) is simulated. With the SC-HST where the engine is forced to run at medium to high torque loads only, the fuel consumption is reduced to approximately by 30 % but it still has the problem of size, noise and low efficiency at low motor displacements during low loads. Current hydrostatic components cannot comply with the ambitious aspirant of fluid power engineers to design fully hydraulic hybrid passenger cars.

Utilizing the innovative distinct configuration of series hydraulic hybrid referred to as “the Hy*d*rid”, together with high efficiency floating cup hydrostatic units in addition to on/off control strategy leads to better fuel economy and further emission reduction compared to the SC-HST using traditional units.

The performance of the Hy*d*rid drivetrain under rule based power management strategy is presented. The control strategy of using on/off control through three real driving cycles exhibits a fuel saving, ranging from 48-53 % over the baseline vehicle. Contrary to the gear-shift transmission, the Hy*d*rid allows optimum operation for the engine in the region of maximum efficiency. The Hy*d*rid drivetrain offers a means of improving the engine efficiency by letting the engine run only at medium to high load with brief peaks avoiding partial load operation. The strategy implemented reduces the engine run time by shutting it off or idle during 69 % of the cycle time, which is depends mainly on the state of charge (SOC) of the accumulator.

The lower fuel consumption of the Hy*d*rid does not result solely from the energy recovery system by shutting off the engine in most of the drive cycle, but also form the optimized control concept, that permits running the hydrostatic units under optimum operating conditions with respect to their losses, which consequently leads to higher overall transmission efficiency .

The results are encouraging enough to recommend the Hy*d*rid drivetrain for automobile purposes with the aim to save fuel and preserve the environment by reducing emitted carbon dioxide, as well as to satisfy future European regulation for passenger cars. The results reveal that the Hy*d*rid vehicle's fuel economy is highly dependant upon accumulator SOC and the Hy*d*rid drivetrain achieves the largest percentage gain in fuel economy over the baseline conventional vehicle on the slowest driving cycles. This is due to the fact that the inefficiencies of slow stop-and-go driving, high idling losses, high braking losses and highly inefficient engine operation is excluded by the Hy*d*rid control system.

It is estimated that the Hy*d*rid has a good potential to conquer the market as the efficiency of the new floating cup units is remarkably high. Moreover, the price of the hydraulic components is compare favorably to the electric solution and the life-time of the hydraulic accumulator is longer than electric batteries. The CO_2 emissions are reduced to 82.1 g/km, far below the limits set by the European Commission of 130 g/km in 2012, and even below the long term target of 95 g/km as a limit for 2020.

Outlook

Collecting accurate data on the production units of the different components necessary in driveline configurations including the engine is mandatory. Further improvement of control strategy for the driveline, an adaptive learning method while driving by intelligent control could be an avenue to take. Further investigation of the Hy*d*rid under different conditions in different driving cycles containing road slope will be necessary.

Downsizing the engine in the Hy*d*rid is not dealt within this study and needs investigation. This is relatively more important in engine-on strategy than with engine-off strategy, since with the latter the engine is already operating at or near its peak efficiency point most of time.

A prototype vehicle, designed on the distinct configuration of the Hy*d*rid, is required to validate the proposed system. As the engine in the Hy*d*rid is controlled by an on/off strategy, some aspects should be considered during validation, such as finding a means to drive the power steering pump as well as the alternator to maintain battery charge.

The high pressure hydraulic oil available in the high pressure side of the common pressure rail of the Hy*d*rid can be used to provide power steering and also to operate the alternator hydraulically. In addition, more frequent engine starting, if accomplished using a conventional starter, would require a larger battery to handle the increased usage. Starting the engine from the pressure stored in the accumulator is another consideration. The need for drive modifications depends on the exact system configuration, with some requiring no change at all from the conventional system.

References

[1] K. Petter, New system solutions for working hydraulics to achieve energy efficiency improvement, *Presentation at IFS 2010 meeting*, 27-28 January 2010, Norrköping, Sweden

[2] K.-E. Rydberg, Energy Efficient Hydraulic Hybrid Drives, *Proceedings of the 11th Scandinavian International Conference on Fluid Power*, SICFP'09 June 2-4 2009, Linköping, Sweden

[3] G. Wagner, Application of Transmission Systems for Different Driveline Configurations in Passenger Cars, *SAE Technical Paper 2001*, No. 2001-01-0882

[4] H. Ortwig, Numerical Optimization of Hydrostatic Transmission performance calculation, *6th world congress of structural and Multidisciplinary Optimization*, Rio de Janeiro, Brazil, 30 May- 03 June 2005

[5] Hybrid vehicles, *http://en.wikipedia.org/wiki/Hybrid_vehicle,* 2010

[6] C. R. Burrows, Fluid power systems-some research issues, Proceedings of the Institution of Mechanical Engineers, Part C: *Journal of Mechanical Engineering Science* Vol. 214, No. 06399, 2000, Prof. Eng Publ. Ltd London Engl., pp. 203-220

[7] H. Murrenhoff, *Grundlagen der Fluidtechnik, Teil 1:Hydraulik*, Aufgabe 2005, Shaker Verlag, ISBN 3826594460, 2005, Aachen, Germany

[8] A. Akers, M. Gassman, R. Smith, *Hydraulic Power system Analysis*, Published 16 April 2006 by CPC press © 2006 by Taylor & Francis Group, LLC, ISBN: 978-0-8247-9956-4

[9] R. Kordak, *Hydrostatic drives with control of the secondary unit*, volume 6 of Hydraulic Trainer-Mannesmann Rexroth, Lohr am Main, 1996

[10] *Progress report on clean and efficient automobile technologies under developments at EPA*- Interim Technical Report EPA420R04

[11] Y. Ito, Analysis of characteristic performance of Hydrostatic transmission for vehicles, *Bulletin of JASME*, Vol. 19, No. 138, December 1976

[12] R. Kordak, Praktische Auslegung Sekundär-Geregelter Antriebsystem, *Hydraulic Kolloquium*, 13 May 1982, Hamburg, Germany

[13] E. A. Prasetiawan, *Modeling,* Simulation and Control of an Earthmoving Vehicle, *Master thesis, University of Illinois at Urbana-Champaign*, USA, 2001

[14] M. A. Holland, K. Harmeyer, J. H. Lumkes, Electrically Controlled Fixed-Displacement pump, variable displacement motor hydrostatic transmission, *SAE technical paper*, 2006-01-3469

[15] K.-E. Rydberg, On performance optimization and digital control of hydrostatic drives for vehicle applications, *Ph.D. dissertation, Linköping studies and Technology*, No. 569, Linköping, Sweden, 1983

[16] J. Lennevi, K.-E. Rydberg and J.O. Palmberg, *Microprocessor* control of hydrostatic transmission adapting to driving conditions, *11th Aachner Fluidtechnisches Kolloquim*, 1994, Aachen, Germany

[17] M. Sanelius, On Complex Hydrostatic Transmission, *Ph.D. dissertation, Linköping studies and technology*, No. 569, 1999, Linköping, Sweden

[18] K. Huhtala, Modelling of Hydrostatic Transmissions–Steady State, Linear and Nonlinear Models, *Ph.D. Dissertation, Acta Polytechnica Scandinavica, Mechanical Engineering Series* No. 123, 1996, Tampere, Finland

[19] H. Murrenhoff, Systematic approach to the control of Hydrostatic Drives, *Proceedings of the Institute of Mech. Engrs*. Vol 213, Part I, IMechE 1999

[20] N. D. Manring, and G. R. Lueke, Modeling and Designing a Hydrostatic Transmission with a fixed-Displacement Motor, *ASME Journal of Dynamic Systems, Measurement and Control*, Vol. 120, March 1998, pp. 45-49

[21] A. Kuge, et. al., Modeling and Simulation of hydrostatic transmission with variable displacement pump, *Journal of Mathematics and computers Simulation* 2000, Vol. 53, Elsevier Science Ltd Exeter Engl., pp. 409-414

[22] I. A. Njabeleke, R.F. Pannett, P.K. Chawdhry, C.R. Burrows, Design of H_∞ loop-shaping controllers for fluid power systems, Proceedings of the Institution of Mechanical Engineers, Part C: *Journal of Mechanical Engineering Science,* Vol. 214 , No. 3, 2000, Prof. Eng. Publ. Ltd, London, Engl., pp 483-500

[23] J. Lennevi, K-E. Rydberg, J-O Palmberg, Digital Control of Hydrostatic Drives, *Fifth Bath international fluid power workshop on Circuit, Component & Systems Design*, Sep. 1992

[24] J. Lennevi, K-E. Rydberg and J. Palmberg, Modelling, Simulation and Measurements of Hydrostatic Drives with Varied System Dynamics, *Third Scandinavian International Conference on Fluid Power*, Linköping, Sweden, 1993, pp 247-270

[25] M. Ibrahim-Sokar, Robust control of hydrostatic transmission system, *Master thesis, Benha University*, Cairo, Egypt, 2003

[26] S. P. Hampson, P. K. Chawdhry, C.R. Burrows, Design of a robust controller for hydrostatic transmissions, *FPST Fluid Power Systems and Technology Proceedings of the 1996 ASME International Mechanical Engineering Congress and Exposition* Nov. 1996, Vol. 3, 1996, Atlanta, GA, USA, Sponsored by: ASME IEEE Los Alamitos CA USA, pp. 107-112

[27] K. Wu, Q. Zhang and A. Hansen, Modelling and identification of a hydrostatic transmission hardware-in-the-loop simulator, *International Journal of Vehicle Design*, Vol. 34, No. 1, 2004, pp 52-64

[28] J. Ossyra, Control Concepts for Vehicle Drive Line to Reduce Fuel Consumption, *Ph.D. dissertation, Hamburg-Harburg University,* VDI Verlag GmbH Düsseldorf 2005, Germany

[29] A. Macor, and M. Tramontan, Hydrostatic Hybrid system: System definition and application, *International Journal of Fluid power*, V8, 2007, Nr2, pp. 47-62

[30] D. Sung, S. Hwang, H. Kim, 2005, Design of Hydromechanical Transmission Using Network Analysis, *Proc. IMechE, Part D, Journal of Automobile Engineering*, Vol. 219, No. 1, pp 53-63

[31] G. Berger, Automatisches, stufenlos wirkendes hydrostatisch-mechanische für Kraftfahrzeuge, *Ph.D. dissertation, 1986, Bochum University, Germany*

[32] U. Blumenthal, Beurteilungskenngrößen für stufenlos wirkende hydrostatisch-mechanische Lastschaltgetriebe in Pkw, *Ph.D dissertation, Bochum University, 1989*

[33] B. Carl, K. Williams, M. Ivantysynova, Comparison of Operational Characteristics in Power Split Continuously Variable Transmissions, *SAE 2006, Commercial Vehicle Congress Exhibition*, October 2006, Chicago, IL, USA, SAE 2006-01-3468

[34] T. Kohmäscher, Modelbildung, Analyse und Auslegung hydrostatischer Antriebsstrangkonzepte, *Ph.D. dissertation, RWTH Aachen,* Germany, 2008

[35] K. Stelson, et al., Optimization of a passenger hydraulic Hybrid vehicle to Improve Fuel Economy, *Proceedings of the 7th JFPS International Symposium on fluid Power*, Toyota 2008, September 15-18, 2008, pp173-148

[36] J. Meyer, K. Stelson, B. Hencey, A. Alleyne , Optimization of the power management strategy for a hydraulic hybrid vehicle, 5th *FPNI PHD symposium Krakaow*, 2008, 1-5 July, Poland, pp 371-378

[37] C. Hugosson, Cumulo Hydrostatic Drive – a Vehicle Drive with Secondary Control, *Proc. of the 3rd Scandinavian International Conference on Fluid Power,* May 1995, Linköping Sweden

[38] B. Wu , C. Lin, Z. Filipi, H. P. Peng, D. Dennis, *Optimal Power Management for a Hydraulic Hybrid Delivery Truck*, Vehicle System Dynamics, Volume 42, Issue 1, 2 December 2004, pp. 23 – 40

[39] R. Kumar, M. Inantysynova, An optimal power Management strategy for hydraulic hybrid output coupled power split transmission, *Proceedings of the ASME 2009, Dynamic System and control Conference DSCC2009*, October 12-14 2009, Hollywood, California, USA

[40] Eaton Corporation, Unveils Breakthrough Fuel Savings Technology, at 2002 *North America international Auto show, Eaton Corporation press release*, January 7, 2002.

[41] V. Duray, C. Arneson, R. Isaacs, M. Stoner, Advantages of Parallel hydraulic Systems*, Proc. of the 7th Inter. Fluid Power Conf.*, 22-24 March 2010, Aachen, Germany

[42] T. Verkoyen, et al., Retrofittable Hydraulic Hybrid system for road Vehicles, *Proc. of the 7th Inter. Fluid Power Conf.*, 22-24 March 2010, Aachen, Germany

[43] T. P. Sim, P. Y. Li, Analysis and Control Design of A Hydro-Mechanical Hydraulic Hybrid Passenger Vehicle, *ASME-Dynamic System and Control Conference (DSC C2009)*, October 12-14 2009, Hollywood, California, USA

[44] F. B. Mensing, A Hierarchical Control Strategy for Hybrid Vehicles, *Master thesis, University of Minnesota, USA, July 2010*

[45] E. Wassenberg, Vergleich Primär- und Sekundär-Geregelter Antriebe in Sonderfahrzeugen, *Hydraulic Kolloquium*, 13 May 1982, Hamburg, Germany

[46] H.-J. Fahl, Hydrostatischer Fahr- und Lenkantriebe an einem Fahrzeug mit Radseitenlenkung, *Hydraulic Kolloquium*, 13 May 1982, Hamburg, Germany

[47] G. Wu, The intelligent control for the hydrostatic drive system of secondary regulation using neural networks, *SAE Special Publications, New Fluid Power Applications, Components, and Testing, Proc. of the Int. Off-Highway & Power plant Congress & Exposition*, Aug 1996, Vol 1192, Indianapolis, IN, USA, SAE

[48] T. Sosnowski, et al., Pump/Motor Displacement control using high-speed on-off valves, SAE Special Publications New Fluid Power Applications, Components, and Testing. P*roceedings of the 1998 International Off-Highway & Power plant Congress & Exposition*, September 1996, Vol. 1380 Milwaukee, Wisconsin, USA, SAE pp1-9

[49] H.-W. Wu, C.-B. Lee, Self-tuning adaptive speed control of a pump/inverter-controlled hydraulic motor system, *ASME Proceedings of the Institution of Mechanical Engineers. Part I, Journal of Systems & Control Engineering*, Vol. 209, No. 2, 1995 MEP Edmunds Engl., pp 101-114

[50] Y. M. Jen, C.B. Lee, Influence of an accumulator on the performance of a hydrostatic drive with control of the secondary unit, *ASME Proceedings of the Institution of Mechanical Engineers. Part I, Journal of Systems & Control Engineering*, Vol. 207, No. 3, 1993, pp 173-184

[51] A. Johansson A., J.-C. Ossyra, Hydraulic Hybrid Transmission Design Considerations for Optimal Customer Satisfaction, *Proc. of the 7th International Fluid Power Conference*, 22-24 March, 2010 Aachen, Germany.

[52] *Clean Automotive Technology Program, Developing Cleaner and More Efficient Vehicles and Engines for Tomorrow*, EPA 2005 Annual report

[53] M. Ivantysynova, et al., Continuously Variable Transmissions for Truck Applications - Secondary Control versus Power Split, *Proc. of the 5th International Fluid Power Conference, 5th IFK*, 2006, Aachen, Germany, Vol. 1, pp 25-44

[54] Freightliner Custom Chassis Introduces Series Hydraulic Hybrid Unit, 2009, http://www.greencarcongress.com/2009/03/freightliner-cu.html

[55] HT2 media release 2008 05_V2 Artemis, http://www.artemis.com

[56] W. Rampen, Hydraulic Transmission for Hybrid vehicles, Artemis Intelligent power LTD., *Presentation at IFS meeting in Eskilstuna*, 5th November, 2008

[57] EPA (2006), World's first full hydraulic hybrid in a delivery truck, http://www.epa.gov/otaq/technology/ 420f06054.pdf

[58] P. Achten, Z. Fu., G. Vael, Transforming future hydraulics: a new design of a hydraulic transformer, *proceedings of the 5th Scandinavian Int. Conf. on Fluid Power*, SICFP'05, 1997, Part 3, IKP Linköping University, Sweden

[59] G. Vael, P.Achten, Z. Fa, The Innas Forklift truck - working under constant pressure, *1st Int. Fluid power Conf.- 1. IFK*, Vol.1, 17-18 March 1998, Dresden, Germany

[60] G.Vael, P. Achten, Z. Fa, The Innas Hydraulic Transformer, The Key to the hydrostatic Common Pressure rail, *SAE technical paper* 2000, 2000-01-2561

[61] P. Achten, Changing the paradigm, *Proc. of the 10th Scandinavian Int. Conf. on Fluid Power*, SICFP'07, May 21-23, 2007, Tampere, Finland

[62] P. Achten, The Hydrid Transmission, *Proc. SAE 2007 Commercial Vehicle Engineering Congress & Exhibition*, SAE 2007-01-4152, October 2007, USA

[63] S. Digeser, et al., The New Mercedes-Benz 3-Cylinder Diesel Engine for Smart and Mitsubishi, *MTZ*, Vol. 66, Jan. 2005

[64] E. Tzirakis, et al.,Vehicle Emissions and Driving Cycles: Comparison of The Athens Driving Cycle (ADC) With Ece-15 And European Driving, Cycle (EDC), *Global NEST Journal,* Vol 8, No 3, 2006 pp 282-290

[65] G. Lechner, et. al., *Automotive Transmissions, Fundamentals, Selection, Design and Application*, Springer-Verlag, Berlin Heidelberg, Printed in Germany, 1999

[66] Wikipedia, History of automobile, http://wikipedia.org/wiki/History_of_the_automobile

[67] *Technische Daten der Testfahrzeuge für der Volkswagen passet*, 2007

[68] H. Wallentowitz, *Longitudinal dynamics of vehicles*, 4th., 2004, Automotive engineering, IKA, RWTH Aachen, Germany

[69] S. Zetina, Optimal Control with Kane Mechanics Applied to a Hybrid Power Split Transmission, *PhD thesis, , 2009, RWTH Aachen, Germany*

[70] T. D. Gillespie, *Fundamentals of Vehic1e Dynamics*, Published by Society 0f Automotive Engineers, SAE, (1992-03), ISBN-10: 1560911999

[71] International Organization of Motor Vehicle Manufacturers, *World Forum for Harmonization of Vehicle Regulations (WP.29)*, Informal document No. GRPE-48-5, 48th GRPE, 1-4 June 2004, agenda item 5.3

[72] C. Breitfeld, The Efficiency–Optimised Drive- a Vision?, *Proc. 6th Int. CTI Symposium, Innovative Automotive Transmission*, Berlin, 3-7 December 2007

[73] T. Ze-yang, Hydaulic motors and vehicle Hydrostatic transmission system of wheel motor type, *patent no*. 4903792, 1990

[74] Triet Hung HO and Kyoung Kwan AHN, Modeling and simulation of hydrostatic transmission system with energy regeneration using hydraulic accumulator, *Journal of Mech. Science and Technology*, ISSN 1738494x, 2010, Vol. 24, no 5, pp 1163

[75] M. J. Pinches and J. G. Ashby, *Power Hydraulics*, Prentice Hall, 1989

[76] Bosch Rexroth AG, Elchingen. *Product Catalog Mobile Hydraulics,* RE 90005-01/07.06, 2007

[77] M. Ibrahim-sokar, Research on Series Hydraulic Hybrid Drivetrain for Using in Automobile, *14th International Conference on Applied Mechanics and Mechanical Engineering*, AMME-14, May 2010, Cairo, Egypt

[78] H. W. Nikolaus, Antriebskonzept Hydrostatischer Systeme mit Energiespeicherung, *Hydraulik-Kolloquium*, 13. Mai 1982, Hamburg, Germany

[79] P. Wüsthof, Secondary control technology applications, *16th conference of hydraulics and Pneumatics* 98, pp104-115, 30.9-2.10.1998, Brno, Czech Republic.

[80] H. Yen, Feature benefits of Secondary control, *ASME Proceedings of the Institution of Mechanical Engineers. Part I, Journal of Systems & Control Engineering*, Vol. 207 No. 2, 1993

[81] R. Rahmfeld, Development and control of energy saving hydraulic servo drives for mobile systems, *Als Ms. gedr. - Düsseldorf*: VDI-Verl., 2002. - XI, 127 S.: Ill., graph. Darst. - (Fortschrittberichte VDI: Reihe 12. Verkehrstechnik, Fahrzeugtechnik ; 527) Zugl., Duisburg, Univ., Diss., 2002, ISBN 3-18-352712-X

[82] K. Pettersson, Secondary Controlled Swing Drive, *Master Thesis, Fluid and Mechanical Engineering Systems,* Department of Management and Engineering, LIU-IEI-TEK-A-09/00549SE, Linköping University, 02.10.2009

[83] T. Kohmäscher, H. Murrenhoff, Efficient recuperation of kinetic energy – hybrid versus hydrostatic approach, *Technical report*, *Institute for Fluid Power Drives and Controls*, 2007, Aachen, Germany

[84] *Hydrostatic_Regenerative_Braking_Brochure.pdf, www.boschrexroth-us.com/*

[85] A. Bandivadekar, et al., on the road in 2035*, interim Report,* No. LFEE 2008-05 RP, MIT, 2008, Bosten, USA

[86] S. Rogers, *Advanced power electronics and electric machines*, report of APEE M, R&D, 2008

[87] P. Achten, G. Vael, T. Kohmäscher, M. Ibrahim-Sokar, Energy efficiency of the Hydrid, *Proc. Int. Fluid Power Conference 6th IFK*, 2008

[88] Baseley, S., et al., Hydraulic Hybrid Systems for Commercial Vehicles, SAE technical paper, 2007

[89] A. Palmen, et al., Wirkungsgraduntersuchung an einer Floating Cup-Axialkolbenpumpe*,* Technical report, *IFAS of RWTH Aachen*, 2007

[90] P. Achten, G. Vael, T. Kohmäscher, M. Ibrahim-Sokar, Design and Fuel Economy Of A Series Hydraulic Hybrid Vehicle, Proceedings of the 7th JFPS International, Symposium on Fluid Power, September 2008, TOYAMA, Japan

[91] M. Ibrahim-Sokar, H. Murrenhof, Simulation Modeling, Assessment and Energy Management of the Innovative Concept of Series Hydraulic Hybrid for Passenger Cars, *International Congress on Automotive and Transport Engineering* CONAT2010, October 27-29, 2010, Brasov, Romania

Curriculum Vitae

Personal Data

Name	Mohamed Saber Ahmed Ibrahim-Sokar
Gender	Male
Date of birth	13th December 1971
Place of birth	Cairo, Egypt
Citizenship	Egyptian
E-Mail	moh_sokar@gmx.net
Address	Benha University, faculty of engineering, mechanical engineering Dept., 108 Shubra Str., Postal code 11241, Cairo, Egypt

Education

1977-1983	Primary school in Cairo, Egypt
1983-1986	Preparatory (middle) school in Cairo, Egypt
1986-1991	Galal Fahmy Secondary advanced high technical school in Cairo, Egypt
1991-1996	Bachelor of science in mechanical engineering (power and Energy), faculty of engineering at Shubra, Benha University, Egypt
1996-1998	Military service
1998-2000	Preliminary Master courses
2000-2003	Master of science in mechanical engineering (Power and Energy), M.Sc. thesis title, "***Robust control of hydrostatic transmission system***", faculty of engineering at Shubra, Benha University, Egypt
2006-2007	Germany language courses, Goethe Institute, Cairo, Egypt
2007-2011	Doctoral students and guest research assistant at the Institute of Fluid Power Drives and control (IFAS), RWTH Aachen University, Germany

Specialization

Major:	Mechanical Engineering (Power and Energy)
Minor:	Automatic control, fluid power drives and Mechatronics

Professional experience

03.1998-03.2003	Teaching assistant, Faculty of Engineering at Shubra, Benha University, Cairo, Egypt
04.2003-12.2006	Assistant Lecturer, Faculty of Engineering at Shubra, Benha University, Cairo, Egypt
01.2007-02.2011	Guest scientists at Institute for Fluid Power Drives and Controls (IFAS) of RWTH Aachen University